Master Thesis Project

Chrysanthi Anastasiou

December 2015 – July 2016

Delft University of Technology

Thermal Breakage of Glass

Comparison and Validation of thermal shock calculation methods

Date	December 2015 - July 2016
Course	MSc Thesis
University	**Delft University of Technology (TU Delft)**
TU Delft Supervision – Chair Assessment Committee	Prof. ir. Rob Nijsse Dr. ir. Fred Veer Dr. Oğuzhan Çopuroğlu Ir. Telesilla Bristogianni
Company	**ABT**
Company supervision	Kars Haarhuis
Address	
Telephone number	
Fax number	
Website	https://www.abt.eu
Student	**Chrysanthi Anastasiou**
Master	Civil Engineering - Building Engineering - Building Technology and Physics
Student number	4412354
Telephone number	+31 61 7271 681
University email address	C.Anastasiou-1@student.tudelft.nl
Personal email address	ch_anastasiou@hotmail.com
Address	Oostplantsoen 20, 2611 PH, Delft, the Netherlands

This page is intentionally left blank

Brief Introductory Note

Glass is known for its optical transparency and brittle behavior. The use of glass surfaces in buildings -windows, facades, roofs- requires a profound understanding on its failure mechanisms. When glass is exposed to significant temperature differences across its surface, thermal fracture poses a threat. Thermal fracture might occur as a result of solar heating.

The hereby MSc thesis explains the principle of thermal fracture and gives an awareness toward recognizing this type of failure and preventing its occurrence. In order to reduce the risk factor in thermal calculation methods, standards and software used in the industry were examined as part of a literature review. The focus of the study is on analyzing the glass behavior under solar radiation with experimental procedures, examine and compare with previous numerical investigations and estimate the magnitude of thermal stresses calculated with different methods.

The relevance of this MCs thesis lies on the fact that to date, very little industry guidance is available to assess thermal stresses on glass, despite it's widely acknowledged risk. Even though glass products with improved resistance to thermal stresses do exist; such as heat-strengthened glass, toughened glass, borosilicate glass and glass ceramics, their use increases significantly the project budget. For that reason, as well as for its optical flatness its fracture pattern and its considerably shorter lead-in times, the use of annealed glass is often desired. The increasing use of glass in temperate climates leads to higher risk of thermal fracture of glass.

Acknowledgements

I must express my very profound gratitude to the people who made this thesis possible. I wish to thank all the participants of the Chair Assessment Committee of my MSc thesis in TU Delft, Prof. ir. Rob Nijsse for his valuable advices and share of experience as well as Dr. ir. Fred Veer whose guidance was indispensable. It is a pleasure to thank Dr. Oğuzhan Çopuroğlu and Mrs. Ir. Telesilla Bristogianni for teaching and inspiring me throughout this project. I had a chance to collaborate with Mr. Ir. Kars Haarhuis (ABT) who provided me with ideas, answers and motivation. I want to express my thanks to Dr. ir. Kenneth Zammit (Buro Happold) who inspired me on the road finding my research topic and mentored me through it. I would like to acknowledge the help of Dr. Marc Vandebroek, for his practical advice on his field of expertise.

I am grateful to my dear family and friends, who participated in this experience with their encouragement and invaluable support.

Chrysanthi Anastasiou,
Delft, 1 July 2016

SUMMARY

Glass has become one of the most popular and complex building materials used today, because of virtually unlimited aesthetic options, combined with outstanding performance. The growing interest of contemporary architecture to use glass in large façade surfaces raises technical issues. In order to propose reliable engineering solutions in glass constructions, understanding the failure mechanisms is vital. The vast majority of the occasional failures of glass panes in facades are caused by other factors than the loads allowed for in design codes. Thermal breakage is one of these reasons.

Glass in the vision and non-vision areas of a façade expands in response to the heat of the sun. Internal thermal stresses are developed when glass is subjected to variations in temperature across its area. The edges of the glass are encased within the rebate of the frame and are therefore protected from the direct heat of the sun, they heat up more slowly and expand less.

If the temperature difference between the main area of the glass and the edges causes the development of stresses that exceed the glass strength, the glass may crack. This is referred to as thermal breakage.

Thermal actions are simplified in literature and the standards and fatigue of a glass is not accounted for. Only simple façade configurations are taken into account, while they are non-applicable to double skin facades. Current literature is not detailed enough, finite element software studies need to be used to examine the temperature difference in glass façades and the induced stresses.

The hereby MSc thesis explains the principle of thermal fracture and gives an awareness toward recognizing this type of failure and preventing its occurrence. In order to reduce the risk factor in thermal calculation methods, standards and software used in the industry were examined as part of a literature review. The practice of

different calculation methods is elaborated for French, British, Belgian and European standard.

The focus of the study is on analyzing the glass behavior under solar radiation with experimental procedures, examine and compare with previous numerical investigations and estimate the magnitude of thermal stresses calculated with different methods.

The largest temperature difference by radiating with 1000W/m² on an annealed glass pane was recorded 17.3ºC. This was achieved with the dark coating on a glass spacimen with 59% absorption value.

The developed temperature magnitude was confirmed by numerical analysis ([Balcaen 2013], [Vansteenbrugge 2012], [Feryn 2012]). Based on these, and aiming to compare and validate temperature and thermal stress results, the graph below was created, compairing dtress values resulting from different ways of thermal risk assessment and different input climatic data:

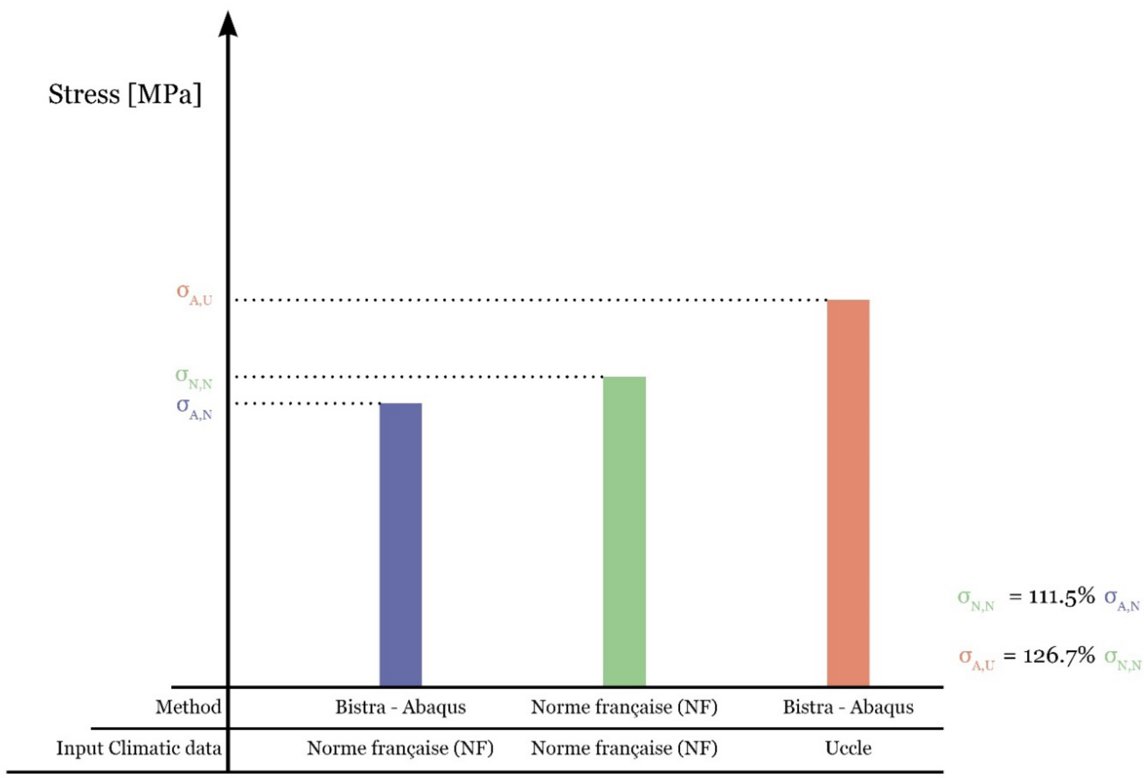

In the graph, the higher thermal stresses are given with real climatic data as input and numerical methods of calculation, then the stresses calculated by French standard are 26.7% lower than these, and finally stresses calculated with numerical methods, with NF input climate data are 11.5% lower than the later.

List of Figures

List of Tables

TABLE OF CONTENTS

This page is intentionally left blank

1. Introduction

1.1. Background and motivation

Glass has been in our everyday lives for hundredths of years. People recognize glass items from their transparency and their brittle nature. In architecture, the beginning of a new era was defined by the entry of glass in roofs, canopies and facades. Crystal Palace, a cast-iron and glass building erected in London by Joseph Paxton to house the Great Exhibition of 1851 (*Figure 1.1*) was only the beginning of the continuous search for the ideal structure: invisible yet protective against the weather (Schipper 2011). Glass in building facades provides efficient floor areas, accessible to the natural full spectrum lighting, creating desirable living and working environment. There have been multiple studies supporting that connection to nature increases human productivity and benefits our health by decreasing stress levels. Glass constructions are ideal for achieving that connection while sheltering users in a controllable indoor environment.

Figure 1.1. Crystal Palace by Joseph Paxton, 1851 Great Exhibition, Hyde Park, **(The Telegraph 2013)**.

Apart from functional purposes, glass in architecture serves for prestige and recognizability. Hardwick Hall in England, 1597 (*Figure 1.2*) is a perfect early example of this. Despite the energy loss disadvantage of the single glazing (cold in the winter and worm in the summer), the expensive –at that time- glass projects perfectly the social class of the residents. Looking at a present-day example, the entrance of the

Apple Center in Fifth Avenue, New York (by Bohlin Cywinski Jackson 2006, reconstructed 2011) is the modern symbol of the luxury of simplicity (*Figure 1.3*).

Figure 1.2. Hardwick Hall, England 1597, **(National Trust Filming Locations 2013)**.

Figure 1.3. Apple Store, Fifth Avenu, **(Bohlin Cywinski Jackson 2011)**.

Glass in contemporary architecture has been used in double facades for enhancing building physics aspects: energy conservation and noise reduction. The demanding design of glass structures requires skills and material knowledge. The research on structural application of glass has only just begun.

1.2. Problem statement

The growing interest among the contemporary architectural community to design buildings with glazed single or double skin facades has raise technical issues. In order to propose reliable engineering solutions in glass constructions, understanding the failure mechanisms is vital. The vast majority of the occasional failures of glass panes in facades are caused by other factors than the loads allowed for in design codes. These factors include thermal stresses and exceptional deteriorations in strength caused by defects or mishandling during manufacture, design, mounting or use of a glass structure (Vuolio 2003).

Solar radiation causes a considerable increase of temperature to the central part of the glazing unit in comparison with the part concealed with the framing that remains colder. Uneven heating due to direct sunlight makes glass expand and contract at different rates. This temperature difference lead to high tensile stresses at the cold part (usually the edge of the pain), since the warm part is trying to expand and the cold part is trying to withstand this expansion. Glass fracture will occur if these stresses exceed the local glass edge strength. Glass temperature might be raised also as a result of space heating devices (CWCT 2010).

Thermal breakage starts at the edge and is perpendicular to the glass edge. Breakage may be single or multiple depending on the built up stress. Several cracks indicate high thermal stresses across the glass pane. A fully tempered glass has significantly higher edge strength to withstand chances of thermal breakage (Glazette n.d.).

In many cases where thermal breakage is suspected the use of the building has changed in some way. Schools have a tendency to stick posters on the glass of children’s art work. Offices can add blinds where none were predicted or films for solar control or blast resistance have been added as an afterthought. Most installations of glass are well within the operating tolerance but in some cases the unexpected changes can put the stress beyond the limits (Pilkington n.d.).

There are many different ways to deal with this problem today. Traditional methods for avoiding the thermal fracture risk in practice result in very conservative design solutions, since enhancement of material strength is being applied. In many cases a more efficient use of materials could be succeeded, even avoiding completely the use of Heat Strengthened Glass (HSG) or Fully Tempered Glass (FTG). A similar effect may occur also if supporting conditions do not adequately allow for thermal expansion (CWCT 2010).

To sum up, the engineering problem can be summarised in the following:

- Solar Radiation and radiation from heaters on exposed glass leads to uneven heating of the glass surfaces.

- The prediction of these temperatures is a complex problem involving radiation, conduction and convective heat transfer depending on the problem being tackled.

- Significant temperature differences occur between the centre of a glass pane and its edges which are often sheltered by the frame keeping the glass in place.

- Temperature differences can be aggravated when solar control glass and shading devices are used.

- Glass used in different applications is often straightforward from a purely structural point of view, such as full height glazing and glass spandrel panels. However thermal stresses in such cases may be significantly affected by the placement of furniture in full height glazing and very high temperatures reached in closed, opaque glass panels.

(Zammit 2015)

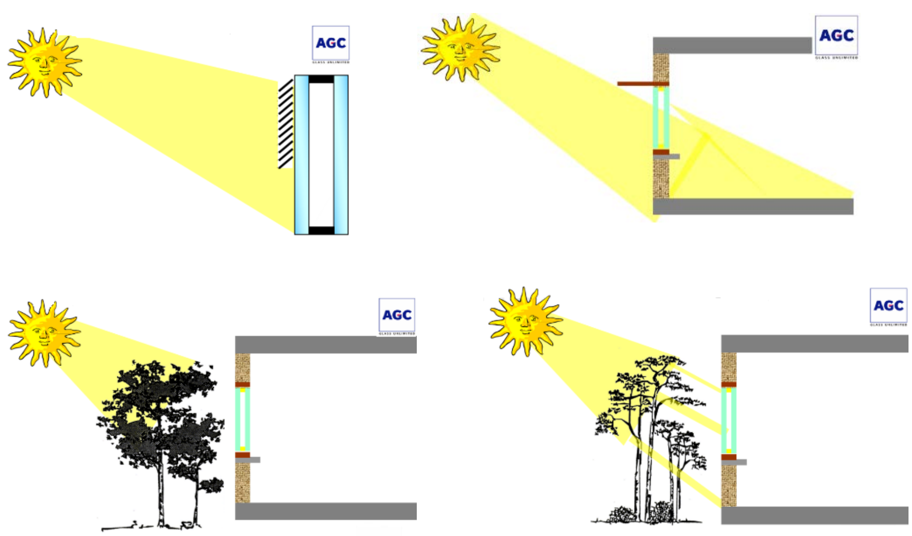

Figure 1.4. Outside "architectural" parameters –accidental shadow on glazing, **(AGC 2008)**.

Validity: Why is it important?

Usual design proposals today use Tempered or Heat Strengthened, Laminated glass for various applications, even though this is not always a structural demand. This is a conservative approach in order to reduce the risk of failure because of thermal differences. This approach leads to inefficient use of material. To emphasize on the importance of this material wastage problem, two of its aspects are summarized below: aesthetic demands and cost of a project.

Aesthetics

When thinking of some of the world's most dramatic, visually breathtaking buildings, they most likely involve large expanses of glass. Before these architectural masterpieces are created, the glass usually gets heat-treated. With both heat strengthening and tempering of the glass, optical distortion of the view behind it is a strong possibility. Optical image distortion occurs in glass for many reasons, including glazing pressure, wind load, temperature and barometric pressure changes – or even changes in altitude between where a glass is made and where it is installed. Because of its fluidity at higher temperatures, glass also is susceptible to roller wave, bow and warp while it is being heat-treated (PPG Glass Education Center n.d.).

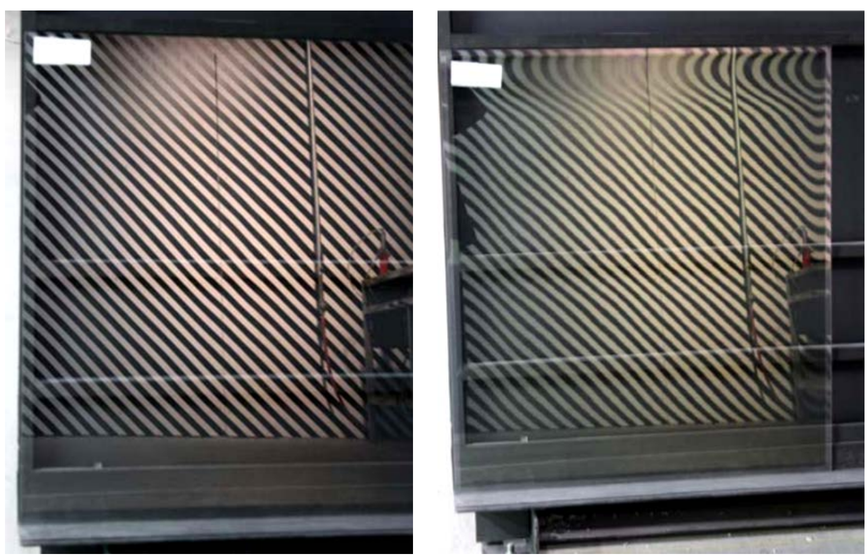

(a) *(b)*

Figure 1.5. Visual distortion in (a) Annealed Glass and (b) Low-E Tempered Glass, **(Viwinco 2012)**.

The optical distortion risk that heat strengthening and tempering glass hold, often requires the built of a full-scale mock-up under job-site conditions, especially for large scale developments (PPG Glass Education Center n.d.). It is only until optical aesthetics are evaluated that the production and construction process can be continued.

In order to minimize the potential impact of glass visual distortion in thermal tempered glass the use of thicker panels is often proposed, as they less prone to distortion.

To summarise, the use of glass material in contemporary constructions is inefficient. This is inapt to a society progressing towards a more sustainable future.

Cost

Design proposals are usually based on laminated glass panels in buildings. This type of safety glass holds the glass together when shattered. As a result, should a fracture occur, the glass breakage poses no immediate threat to the public. Increased glass thickness is a design solution used against thermal fracture, but it cannot solely resist surface stresses induced by temperature difference. Traditional methods for evaluating thermal loading on building structures are based on the 50-year-return period of the annual temperature highest and lowest peaks (Vanderbroek, Belis and Louter 2013), as described in EN 1991-1-5:2003. Results are therefore very conservative, considering that these conditions are highly unlikely (Baldini, Lenk and Rammig 2015). All the above could lead to the conclusion that more cost effective and less conservative design solutions are necessary.

I like to believe that this research could be interesting for designers, by pointing out the thermal breakage risk and explaining its mechanism, for engineers, by explaining and validating thermal breakage risk assessment methods and giving recommendations to avoid it, and also for building owners, to inform them on the parameters triggering this phenomenon.

1.3. Main objectives

The hereby study aims to reduce the risk factor in thermal calculation methods existing today: standards and software used in the industry. A thorough review of the existing standards was part of the research as well as experimental investigations. The experiments conducted provide a better understanding of the glass behavior under extreme thermal loads. The numerical analysis examine the impact of the parameters of influence with and make comparisons with the standard.

The content of this research could be important for designers, by pointing out the thermal breakage risk and explaining its mechanism, for engineers, by explaining and validating thermal breakage risk assessment methods and giving recommendations to avoid it, and also for building owners, to inform them on the parameters triggering this phenomenon.

1.4. Methods

In the herby study, multiple glass samples were experimentally investigated, applying a stochastic approach. The results were analyzed statistically in order to provide a better insight in the mechanisms of glass failure caused by thermal stresses.

Parameters whose effect on the thermal cracking was to date not quantified were examined. Numerous experiments addressed the effect of different glass edge finishes and nominal thicknesses for diverse glass types under various thermal regimes. Support/boundary conditions were considered as well as the way thermal differences were developed in the glass panes. The small-scale specimens were soda-lime silicate glass, which contains machining flaws at the edge.

2. State of the Art

2.1. Introduction

In order to analyze the behavior of glass under temperature differences, it is important to first examine and understand the physical properties of glass material. The state-of-the-art knowledge concerning glass production, glass strength and thermal failure actions are presented in this chapter, with the aim to provide the fundamental aspects of glass as a building material.

2.2. Glass: the material

In order to analyze the behavior of glass under temperature differences, it is important to first examine and understand the physical properties of glass material.

2.2.1. Glass Composition

Glass is a non-crystalline inorganic solid material, optically transparent as a result of the ordination of the electrically charged elements within the molecules. Glass material used in construction is usually soda-lime, consisting of about 75% silica (better known as sand), plus sodium carbonate (soda ash), calcium oxide (lime) and other additives. The percentage of each ingredient added, has an influence on the melting point during the manufacture process and the mechanical and optical characteristics of the final product. By melting the ingredients and cooling them down rapidly the translucent property of glass is achieved (Schipper 2011). Actual composition of the glass varies between suppliers in order to change physical and chemical properties and the color according to the needs of the client.

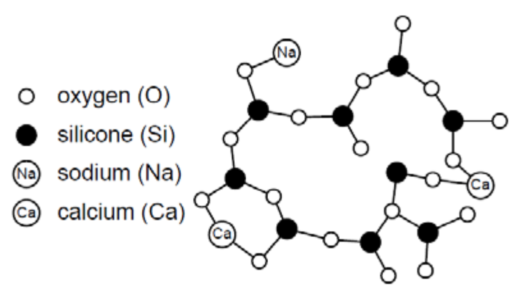

Figure 2.1. Schematic view of the irregular network of a soda lime **(Haldimann, Fracture strength of structural glass elements – Analytical and numerical modelling, testing and design 2006)**

Glass material composition is standardized in European norm (EN 572-1 2004). The standardized material composition is presented in *Table 2.1.*

Table 2.1. Soda-lime glass composition according to European standard **(EN 572-1 2004)**.

Oxide		Range %
Silicon dioxide	(SiO_2)	69-74
Calcium oxide	(CaO)	5-14
Natrium oxide	(Na_2)	10-16
Magnesium oxide	(MgO)	0-6
Aluminum oxide	(Al_2O_3)	0-3
Others		0-5

Molecular structure differences between the three different states of glass, solid, liquid and gas, affect the strength, density and volume of the material. In the transition from liquid to solid state, a lattice structure is formed, which causes decrease of volume (crystallization). The solid is formed amorphously, without crystallization, during the controlled cooling down process in manufacturing. This disordered crystal structure (comparable to liquid and molten materials) makes glass behavior so difficult to study. It is also the reason why glass does not have a fixed melting point (around 600^{o}C) and does not have any direction-dependent properties (Schittich, et al. 1999).

Glass is known to be an inert substance (chemical non-reactive), able to remain unchanged over time. Indeed, glass is used in laboratories and pharmaceutical sectors to protect their products against chemical or biological contamination. Glass is considered to be the healthiest packaging material since it does not react with foreign substances or absorb them and is also virtually impermeable to oxygen (FEVE n.d.). On the other hand, regular float glass in facades is vulnerable to acid and alkaline fluids. In buildings windows are sometimes etched by cement water that is flowing from the façade. That risk is controlled with the addition of coatings or the use of a modified glass composition (Schipper 2011).

2.2.2. Glass Production

Brief historical review

In 1832, Chance Brothers became the first company to adopt the cylinder method to produce sheet glass *(Figure 2.2)*. The glass was taken from the furnace in large iron ladles and thrown upon a cast-iron bed of a rolling-table, where it is rolled into a sheet with an iron roller. The sheet, still soft, was pushed into the open mouth of an annealing tunnel or a lehr, down which it was carried by a system of rollers (Cable 2008). Henry Bessemer in 1843 introduced an early form of "Float Glass", which involved pouring glass onto liquid tin. The mass production of glass was developed in 1887 by the firm Ashley (Buch Polak 1975). Chance Brothers also introduced the machine rolled patterned glass method in 1888 (Chance Brothers and Co n.d.). Between 1953 and 1957, Pilkington Brothers developed the first successful commercial application for forming a continuous ribbon of glass using a molten tin bath on which the molten glass flows unhindered under the influence of gravity. The success of this process lay in the careful balance of the volume of glass fed onto the bath, where it was flattened by its own weight. Full scale profitable sales of float glass were first achieved in 1960 (Schipper 2011).

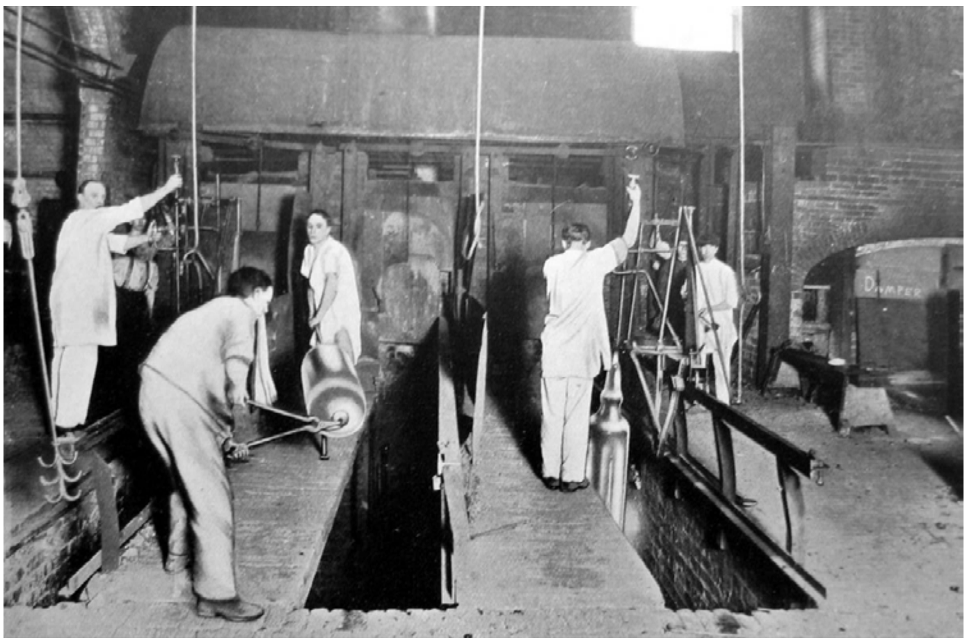

Figure 2.2. Making the cylinders from which the sheet glass was produced **(US Lighthouse Society - The Fresnel Lens Makers n.d.).**

Float glass manufacture today

The raw ingredients of glass are mixed in a batch mixing process and fed together with suitable recycled waste glass -in a controlled ratio- into a furnace where it is heated to approximately 1500°C. Once molten, the temperature of the glass is stabilized to approximately 1200°C for a homogeneous specific gravity. The molten glass is poured into a "tin bath". Tin is suitable for the float glass process because it has a high specific gravity, is cohesive, and is immiscible into the molten glass. Subsequently, the glass flows onto the tin surface forming a floating ribbon with perfectly smooth surfaces on both sides and an even thickness. As the glass flows along the tin bath, the temperature is gradually reduced from 1100°C until the sheet can be lifted from the tin onto rollers at approximately 600°C. The glass ribbon is pulled off the bath by rollers. Once off the bath, the glass sheet passes through an annealing lehr kiln for approximately 100 m, where it is further cooled gradually so that it anneals without strain and does not crack from the change in temperature. On exiting the "cold end" of the kiln, the glass is cut by machines (Wikipedia n.d.) *(Figure 2.3)*.

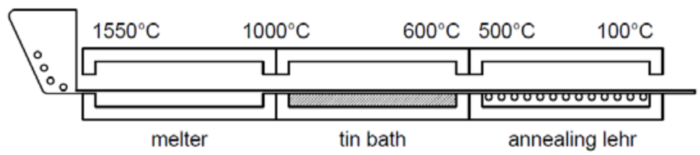

Figure 2.3. Production process for float **(Haldimann, Fracture strength of structural glass elements – Analytical and numerical modelling, testing and design 2006)**.

After the production of float glass further processes are usually performed in order for the glass to reach the characteristics required by the client. The most common of these processes are: cutting, coating, laminating, thermal/chemical treatment. In *Table 2.2* below, a summarizing overview of the most common glass production processes, processing methods and glass products is presented.

Table 2.2. Glass production processes and products overview **(Haldimann, Fracture strength of structural glass elements – Analytical and numerical modelling, testing and design 2006)**.

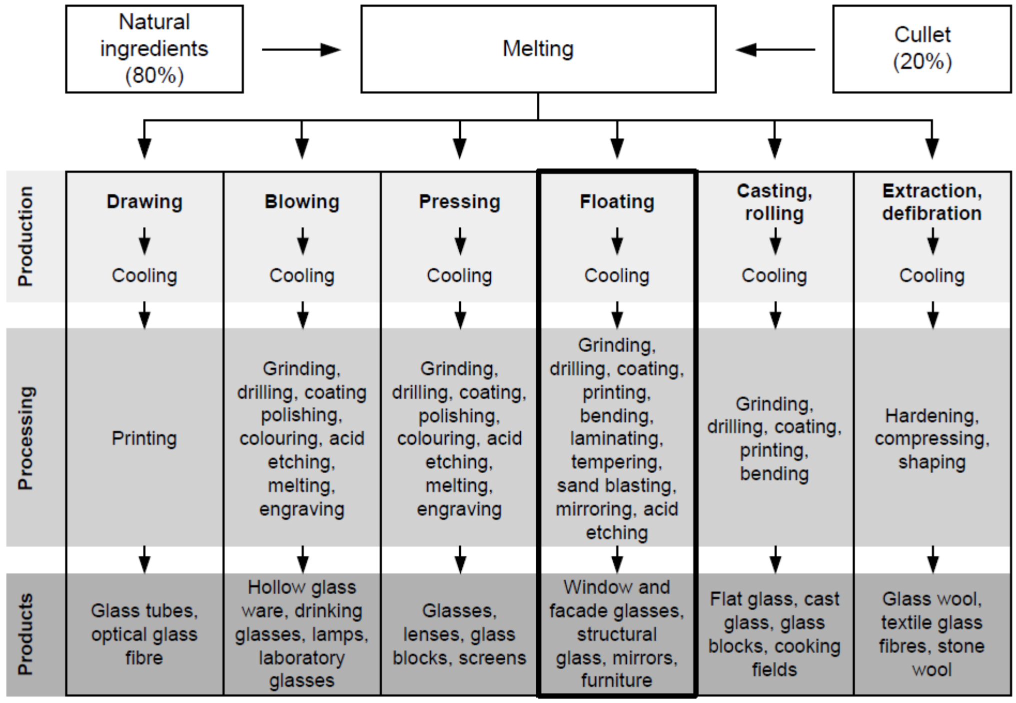

2.2.3. Glass & Sustainability

Glass is a fully recyclable material which can be recycled in close loop over and over again. That is a great benefit to the environment and the saving of natural resources. In addition, recycling glass benefits public health, because of the reduced carbon dioxide emissions. In many of its application glass can contribute to energy saving (e.g. it allows the manufacturing of light-weight transport modes and therefore decrease of fuel consumption). Glass recycling also saves energy as cullets melt at a lower temperature than raw materials. Consequently, less energy is required for the melting process. Glass can also be used to generate renewable energy through solar-thermal and photovoltaic applications (Glass Alliance Europe n.d.).

2.3. Glass strength

2.3.1. Introduction

The widespread use of glass in modern architecture dictates the importance to understand the engineering properties of glass accurately. One of the most unpredicted glass failures is due to thermal differences developed in the pane. A lot of research has been done to evaluate the initiation and the influence factors of this type of failure, but there are still many questions to be answered.

Basic structural properties
Glass specific weight = 2350 to 2500 kg/m^3
Young's Modulus E_g = 70000 to 740000 N/mm^2

Strength
The almost perfectly elastic, isotropic behavior observed in glass and its inability to yield plastically explains the brittle behavior of the material. Glass cannot redistribute local stress concentrations by local yielding and is, therefore, extremely susceptible to failure that occurs without warning *(Figure 2.4 a)*. The theoretical tensile strength (based on molecular forces) of glass is exceptionally high *(q.v. 2.3.2)*. It is however of no practical relevance for structural applications. The actual tensile strength, the relevant property for engineering, is much lower. The reason is that the surface of glass panes contains a large number of mechanical flaws of varying severity which are not necessarily visible to the naked eye. As with all brittle materials, the tensile strength of glass depends very much on these surface flaws. A glass element fails as soon as the stress intensity due to tensile stress at the tip of one flaw reaches its critical value. Flaws grow with time when loaded, the crack velocity being a function of several parameters and extremely variable.

The tensile strength of glass is not a material constant, but it depends on many aspects, in particular on the condition of the surface, the size of the glass element, the action history (intensity and duration), the residual stress and the environmental conditions. The higher the stress, the longer the load duration, the deeper the initial surface flaw and the lower the effective tensile strength.

As surface flaws do not grow or fail when in compression, the compressive strength of glass is much larger than the tensile strength. It is, however, irrelevant for virtually all structural applications. In the case of stability problems, tensile stresses develop due to buckling. At load introduction points, the Poisson's ratio effect causes tensile stresses. An element's tensile strength is, therefore, exceeded long before the critical compressive stresses are reached (Haldimann, Fracture strength of structural glass elements – Analytical and numerical modelling, testing and design 2006).

The behavior described above explains the lack of a single accurate value for the design strength of glass and why the maximum stress approach is unsuited for designing structural glass elements. In order to avoid unexpected stress concentrations, the design glass model must account for all relevant aspects and be analyzed thoroughly. A technically sound structural model of a glass structure should account for conventional actions due to load, imposed deformations as well as temperature differences.

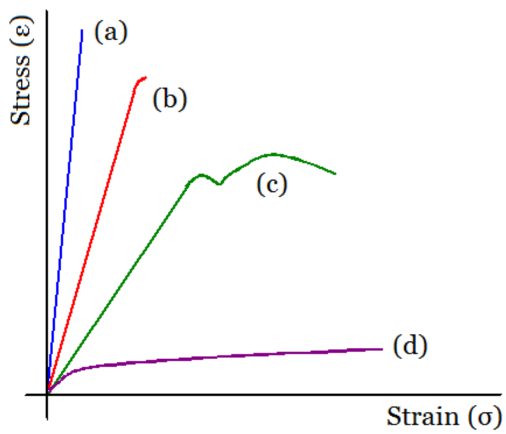

Figure 2.4. Stress-strain graphs of materials: (a) brittle (b) non-ductile (c) ductile (d) plastic **(Antonine n.d.)**

The following paragraphs are summarizing the basic mechanical characteristics of glass material and its failure behavior, necessary engineering knowledge in order to develop a sensible detailing of a glass design.

2.3.2. Fracture Mechanics

Soda-lime glass is a brittle material with an almost perfectly linear elastic behavior. The maximum elongation is in the area of 0.1%. After the slightly extension out of the boundaries of elastic deformation glass is led to abrupt failure. There is no plastic behavior zone and therefore it is not possible to anticipate its failure. Therefore linear elastic fracture mechanics (LEFM) is an ideal theory to model the behavior of glass. In fact, glass was the material used for the development of the basis of LEFM. In LEFM, mechanical material behavior is modeled by looking at cracks. The theory describes the relation between the tensile strength and the flaw parameters, i.e. the flaw geometry and the flaw depth. A crack is an idealized model of a flaw having a defined geometry and lying in a plane. It may either be located on the surface (surface crack) or embedded within the material (volume crack) (Haldimann, Fracture strength of structural glass elements – Analytical and numerical modelling, testing and design 2006).

Theoretical failure stress of glass can be determined from the strength of the atomic bonds between the individual atoms. The highest failure tensile stress σ_m amounts to 32 GPa (Haldimann, Luible and Overend, Structural Engineering Document 10: Structural use of glass 2008), but the strength of ordinary annealed glass is smaller than this theoretical value.

The *theoretical failure stress* can be calculated with:

$$\sigma_{\mathrm{m}} = \sqrt{\frac{E \cdot \gamma}{r_0}} \tag{2.1}$$

where:
E = 70 young's modulus [GPa]
γ = 3 fracture surface energy [Jm^{-2}]
r_0 = 0.2 equilibrium spacing of the atoms [nm]
(Jacob 1999)

The reason why the practical and theoretical strength of glass differ is the surface cracking of the material. When the tensile stress in a glass edge exceeds 14 to 21 MPa, the probability of breakage becomes significant. The actual edge strength depends on the cut edge quality ... .

Table 3.12: Characteristic and design strength values for different edge finishings.

edge finishing	LSM (Weibull distribution)		LSM (normal distribution)	
	$f'_{eg,k}$ [MPa]	$f'_{eg,d}$ [MPa]	$f'_{eg,k}$ [MPa]	$f'_{eg,d}$ [MPa]
smooth ground	47.0	26.1	50.6	28.1
ground	33.7	18.7	37.2	20.7
arrissed	43.0	23.9	44.3	24.6
cut	35.9	19.9	36.7	20.4

Fracture mechanics examines the crack, the length of which increases upon loading, until this crack becomes critical. The length of the crack defines the point where crack propagation changes from stable to unstable. Griffith's solids theory (Griffith 1920) was modified by Irwin (Irwin 1957), introducing a term called stress intensity factor (SIF). This concept allows the basic rule of glass failure to be expressed in simple terms: *A glass element fails, if the stress intensity factor K_I due to tensile stress at the tip of one crack reaches its critical value K_{Ic}.*

Crack propagation can happen in three different ways, as illustrated in *Figure 2.5*. Mode I is caused by a force normal to the crack plane due to tensile stresses. Mode II is linked to a shear stress acting parallel to the plane of the crack; in-plane crack shearing or sliding. Mode III acts in out-of-plane shear; anti-plane crack shearing or tearing. K_{Ic} is the form of stress intensity factor for plain-strain fracture toughness (Mode I).

The crack propagation due to thermal fracture follows Mode I failure, since a tensile stress is acting on the crack opening. The stress field induced by thermal or mechanical loading is uniaxial in this study. According to (Lawn 1993) the action of the imposed shear deflects the crack away from plane geometry and moreover, tends toward the orientation of minimum shear.

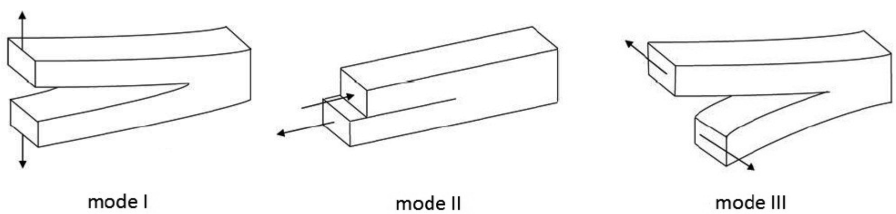

Figure 2.5. Schematic illustration of failure Modes, according to Irwin **(Lawn 1993)**.

Irwin defines stress intensity factor for Mode I according to:

$$K_I = Y \cdot \sigma_n \cdot \sqrt{\pi \cdot a} \tag{2.2}$$

where:
K_I stress intensity factor
σ_n the tensile stress normal to the flaw's plane [MPa] (*Figure 2.6*)
Y geometry factor which depends mainly on the crack geometry [-]
a crack depth; measured perpendicularly to the edge and contains the longest crack length, in case the flaw spreads over two edges (*Figure 2.6*)

Hertzberg stated: "Stress is to strength as stress intensity factor is to fracture toughness" (Hertzberg 1996).

K_{Ic} is a material property. For glass, failure occurs when the stress intensity factor reaches a critical value. The fracture toughness of soda lime glass is K_{Ic}=0.75 MPa$\sqrt{m}$ (Porter n.d.).

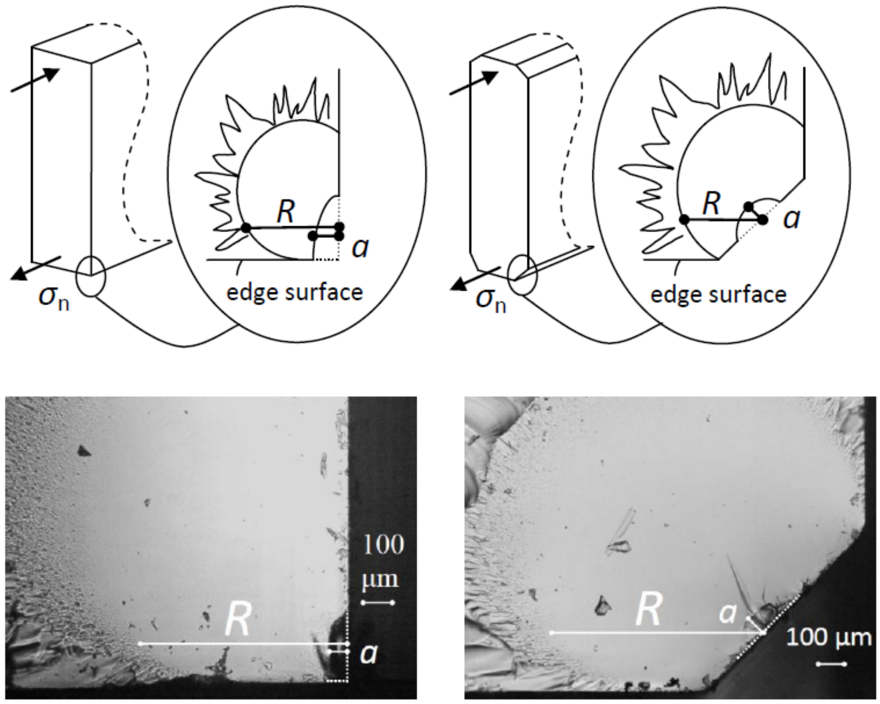

Cut Edge Arrised/Smooth Ground Edge

Figure 2.6. Schematic (above) and microscopic (below) view of edge flaws, σ_n denotes the tensile stress normal to the flaws plane, a the flaw depth perpendicular to the surface and R the mirror zone depth **(Vandebroek 2015)**.

2.4. Glass thermal properties

Glass has a thermal expansion coefficient a_T = 9 10^{-6} (1/K) (at 20°C), which is a really low value compared to that of steel a_T = 12 10^{-5} (1/K) (Schittich, 1999). This difference contributes in local stress concentration in glass at contact points between steel and glass.

2.4.1. Resistance against thermal fracture

The strength of glass against thermal stress failure is usually given as an allowable maximum temperature difference. If the calculated temperature difference is less than the allowable temperature difference ΔT_{adm} the panel can be considered thermally safe. Of course there are many different calculation methods that can predict more accurately the initiation temperature of the thermal fracture (*q.v. 3.6 Thermal fracture calculation methods*). The following *Table 2.3* lists allowable temperature differences for different glass types and edge qualities. These values are based on tests carries out by Pilkington in a cooling frame and are derived for assumed load duration of 3.5 hours per day (Colvin 2005).

Table 2.3. Maximum allowable temperature difference ΔT_{adm} **(Haldimann, Luible and Overend, Structural Engineering Document 10: Structural use of glass 2008).**

	As-cut or arrised (°C)	Smooth glass (°C)	Polished (°C)
Float or sheet glass, h<12 mm	35	40	45
Float glass, h=15 mm or 19 mm	30	35	40
Float glass, h=25 mm	26	30	35
Patterned glass	26	26	26
Wired glass	22	22	22
Heat strengthened glass (all types)	100	100	100
Fully tempered glass (all types)	200	200	200
Laminated glass	Smallest value of the component panes		

According to French standard (NF P 78-201-1/A1(DTU39) 1998), tempered glazing, borosilicate glass, glass-ceramics, alkaline and alkaline-earth silicate glasses are by nature very high thermal shock resistant, and do not require verification.

3. Thermal Breakage of Glass

3.1. Introduction

Thermal breakage or fracture of glass can occur between two zones of the glass, as a result of large temperature difference between them. Under the influence of solar radiation, the temperature rises in the central part of the glazing, in contrast with the shaded glass parts. Since glass is a poor conductor of heat, the heat is slowly dispersed over the entire window area. The glass inside the frame remains colder and tensile stresses occur. In this chapter the general principles of the thermal fracture are explained. In addition, the various factors that can cause this phenomenon are listed.

There is a number of well-known methods around the word providing risk assessment for thermal fracture in glass. In this chapter the most important calculation methods are described.

3.2. General principles

3.2.1. Thermal breakage in façades

Window glass is heated and cooled by visible and invisible (infra-red) radiation from the sun and other heat sources; by natural and forced convection from wind; by air from HVAC vents, etc.; and by conduction from contact with framing and other materials. The small differential expansions and contractions of the hot and cold areas create stresses which, if they are excessive, can cause breakage of ordinary annealed glass (Pilkington n.d.).

New, high performance products developed by the glass industry nowadays can be an additional threat against thermal breakage. For example coatings (like low), decrease the thermal transmittance of insulating glass unit but, on the other hand, they increase the thermal shock breakage risk because their high thermal absorptance. Also the use of multi-cavity in insulated glazing units increases this risk (Mognato and Barbieri 2013).

The glass fracture in modern curtain wall systems can be generated on days with typically clear sky conditions with strong sun irradiation and high daily ambient air temperature differences. The difference in the thermal expansion coefficient between glass and steel, mentioned in *2.4*, contributes in local stress caused by solar radiation or by artificial heating or cooling. In either case, a thermal stress break is possible to occur. The central glass area is heated rather quickly, while shaded areas or particularly the glass edge area, protected and shaded by the profile, remains relatively cool. Due to this temperature difference on the glass volume a linear zone of tension stress can be generated between hot and cold areas, particularly on calm days when there is no cooling breeze, as explained in *1.2 (Figure 3.1).*

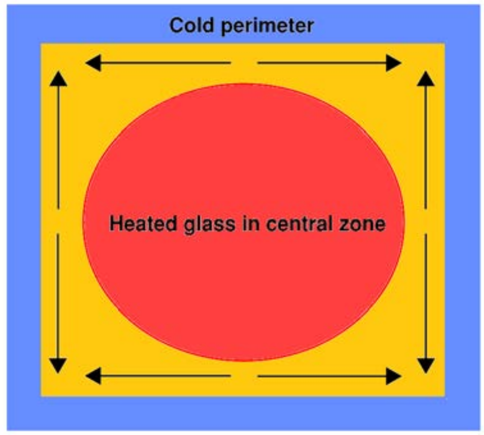

(a)

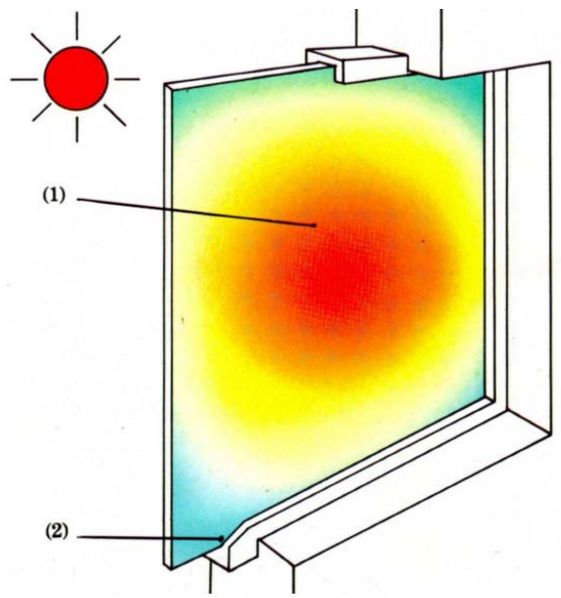

(b)

Figure 3.1. Visualization of temperature differences that cause thermal fracture **((a) image by author, (b) (AGC 2008)).**

The expansion of ordinary window glass with heat is small but can be of considerable consequence. In usual industrial practice, when a thermal stress problem occurs the first step of the analysis is to calculate for every glass configuration (which includes shading, blinds or backups) the resulting temperature difference on the glass, i.e. the temperature difference between heated glass central zone and the cooler shaded glass and glass edge areas. This allows a decision to be made as to whether the glass requires an additional treatment, either additional edge grinding or further heat treatment such as strengthening or tempering, to guarantee its integrity.

The characteristic crack caused in glass by thermal shock always starts at the edge of the glass, perpendicular to the edge and the face of the glass and results in a "lazy/meandering" crack *(Figure 3.2)*. This typical thermal stress crack has a high energy straight leg of about 75-100mm, which then extends over time with a meandering low energy crack which often bifurcates along its path (Stevens 2013). It is important to consider that the edge strength can be lower than the surface one because of edge working and the concentration of tension induced by the frame boundaries (Mognato and Barbieri 2013).

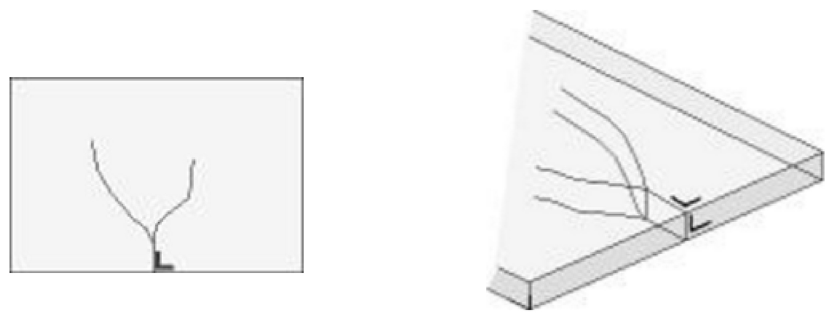

Figure 3.2. Glass cracking caused by thermal shock **(AGC 2008)**.

The breakage can be single or multiple *(Figure 3.3)*.

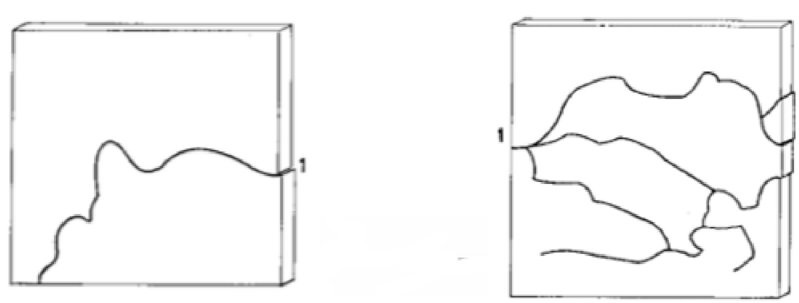

Figure 3.3. Single and multiple glass thermal fracture **(AGC 2008)**.

3.2.2. Parameters of influence

There are many factors that could lead to thermal breakage of a glass pane. Some of the most important parameters of influence of the thermal shock / generation of temperature differences between two points of the same glass pane are:

- Climate conditions
  - Geographic location
  - Daily difference of temperature
  - Intensity of the incident solar radiation
  - Time of day
  - Wind
  - Altitude

- Parameters depending on the glazing itself and its settings
  - The nature of glazing
  - Thermal inertia (dependent upon its absorptivity, its specific heat, its thermal conductivity and its dimensions)
  - The type of setting and colour of the frame (structural glazing, aluminum with/without thermal break, wood/PVC frame, dark steel, concrete/masonry etc.)
  - State of the glass edges: damaged edges or presenting chips increase the risk of thermal breaking, since the latter is initiating from these weak points
  - Use of toughened or heat strengthened glass or sliding frame with low E

- Outside “architectural” parameters
  - Orientation of the façade
  - Eventual shadows on the glazing (eaves of a building, blinds) letting only one part of the glazing in the shadow *(q.v. 1.2, Figure 1.4, page 4), (Figure 3.4) from AGC and (Figure 3.5)* form Viracon.
  - …Size of building overhang, if present
  - Size of mullion and transom caps, if present
  - Details of any external louvres

  Since outdoor shading is seasonal, it one of the most dynamic factors that can affect glass (PPG Glass Education Center n.d.).

- Inside “architectural” parameters

  - Presence of blinds *(Figure 3.6 a)*
  - Proximity of heating appliances
  - Proximity of the inside aeration forcing air system (hot or cold) on the glazing

- Details of internal heating systems
- Inside ceiling *(Figure 3.6 b)*
- Proximity of a dark object behind the glazing
- Nature of the walls in the vicinity of the glazing
- Air circulation behind the glazing

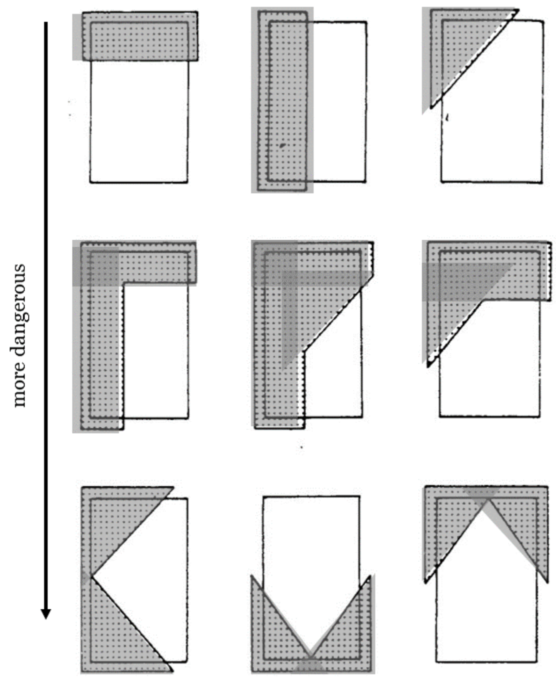

Figure 3.4. Critical, "dangerous" for thermal fracture, shading areas on a window **(AGC 2008)**.

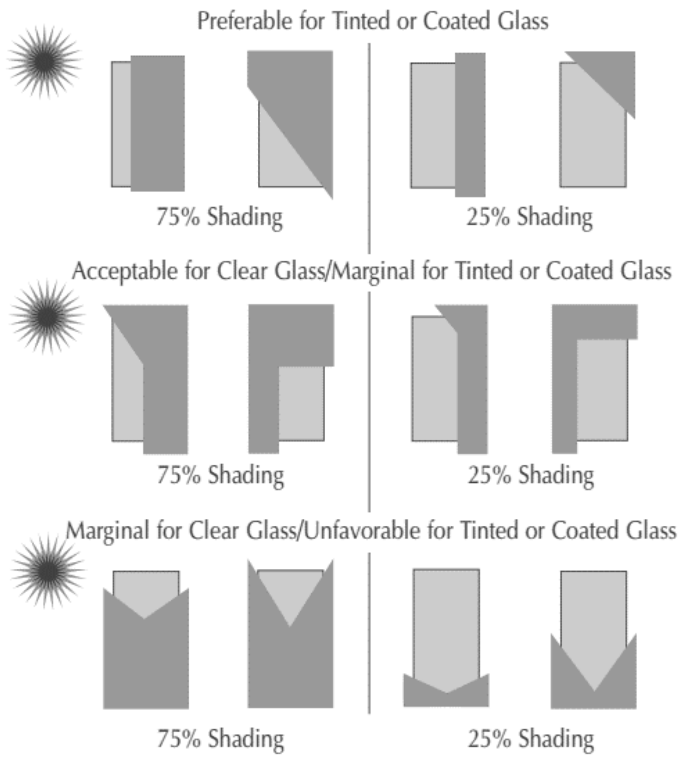

Figure 3.5. Critical, "dangerous" for thermal fracture, shading areas on a window **(Viracon n.d.)**

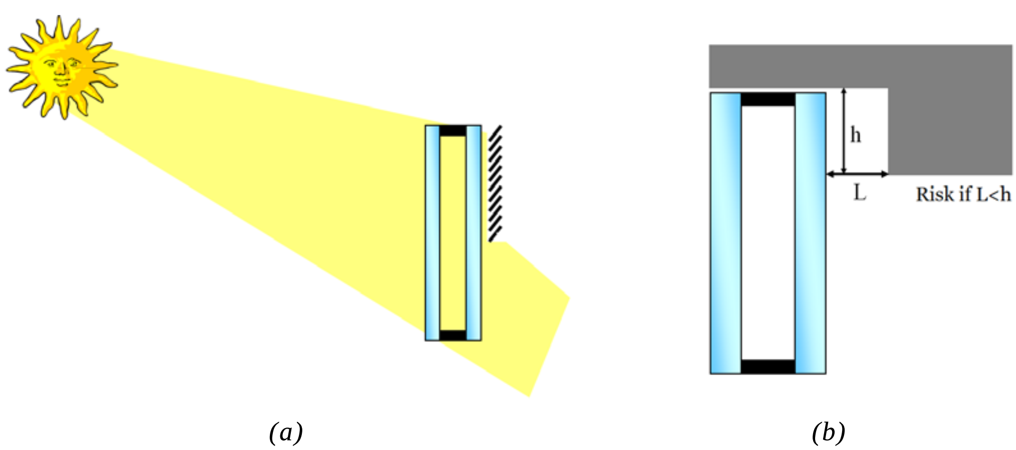

Figure 3.6. Inside "architectural" parameters of influence for thermal fracture **(AGC 2008)**.

Sometimes unique conditions should be taken into account when designing against thermal fracture. Snow accumulation is a good example of that, and can be predicted based on the climate, wind direction and velocity and geometrical characteristics of the window. In this case the exposed part of the glass absorbs sunlight and a large temperature difference can easily develop between the exposed area and the portion of the glass shaded and cooled by the snow (*Figure 3.7*).

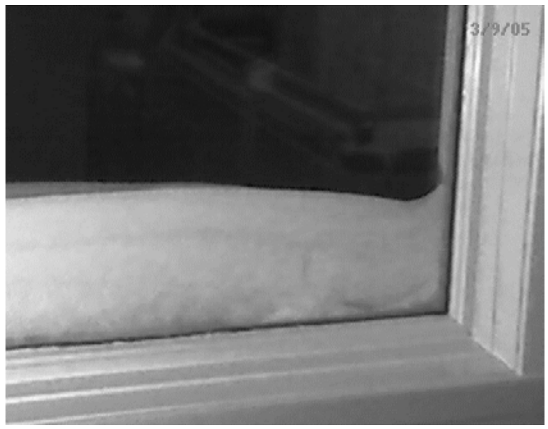

Figure 3.7. Snow accumulation against wndow **(Pilkington n.d.)**.

Another example is a corner where two curtain walls meet. Reflections from one glass pane orientation to another cause increased temperature differences in glass. When the heat from the grazing solar reflection of an adjacent glazing is added to the direct solar radiation, the thermal fracture risk is increased.

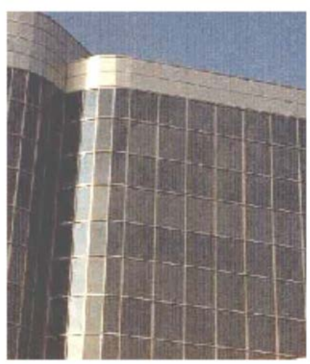

Figure 3.8. Point where two curtain walls meet **(Pilkington n.d.)**.

According to the European standard, the effect of heating and cooling system shall be considered only in the case in which the air is blown directly to the glass surface. A heating radiation intensity value (I_h) is indicated to be calculated by an appropriate method without specifying which the method is.

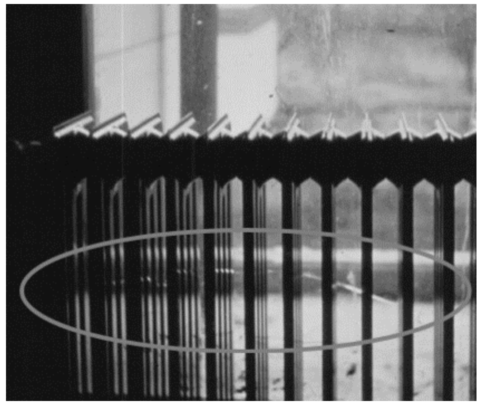

Figure 3.9. Thermal breakage fracture in front of heater **(AGC 2008)**.

None of the standard accessing thermal breakage risk quantifies the contribution of these situations to thermal fracture.

Construction

During construction thermal stress breakage can occur as a result of jobsite conditions. Exterior scaffolding can create large shade patterns on the glass and elevate thermal stresses. Before a building is heated, it is subjected to large diurnal temperature fluctuations. Since the framing can cool down dramatically overnight, the glass edges remain cooler for longer periods. These high stresses can cause significant breakage. Materials used to protect the glass on-site may also increase the risk against thermal stress in a pane. Welding, painting and concrete work are sometimes not performed prior to installation, which also increases the danger against this type of failure (Viracon n.d.).

3.2.3. Occurrence

In general, the *stress level* at which the glass will break is governed by several factors. Toughened glass is very resilient and not prone to failing due to thermal stress. Laminated glass and annealed glass behave in a similar way. Thicker glasses are less tolerant. Glass containing wire is more vulnerable. The edge quality of the glass can play a part. Glass with damaged edges will take less stress than clean cut glass. A good clean cut edge is the best finish along with fully polished edges. Ground edges and arrised edges may not be as good. A ground or arrised edge is a series of small defects around the glass. The effect brings all the defects to an average level and may at best be only more predictable than a glass with more random damage (Pilkington n.d.). Nowadays, due to energy efficient demands for building that follow the Zero-Energy principle, glazing products such as triple glazing, vacuum glazing and high efficiency glass have been developed. The high insulating behavior of these materials often leads to greater temperature differences, associated with the risk of thermal fracture (Feryn 2012). Experiments were conducted in the context of this thesis confirm some of these facts *(q.v. chapter 4)*.

As the hotter exposed area is usually much larger than the cooler edge area, the edges are stretched into a state of tensile stress of about 0.62 MPa for every degree °C (50 psi for every degree °F) difference between the center and the edge. On a calm day, sunlit heat-absorbing glass can easily reach 4.5°C above the ambient air temperature. The covered glass edge temperature will be somewhere between that of the ambient air and the exposed glass. The frame detail determines how much heat reaches the edges. A typical case of high stresses causing thermal fracture is that of insulation behind an annealed, heat absorbing glass and the shadow from an overhang, on a clean cut edge *(Figure 3.7)*.

Figure 3.10. Thermal fracture on glass shaded by the overhang **(Pilkington n.d.)**.

Low energy mechanism thermal breakage could be reduced if the following actions are taken. Obviously and most importantly, the damage of the edges of the glass panes should be avoided. Air circulation between the glass panes should be ensured. Additionally, glass panes must be entirely covered. Partial covering might cause temperature difference and breakage. Anything glued on the surface of untoughened glass could pose a risk for thermal fracture. To reduce this risk, insulating glass units, reflective and wired glass panes may not be stored in the direct sunlight before glazing.

Quality control is very important: a check on delivered material and inspection of panes both when manufactured and before glazed into frame is crucial. Only if absolutely necessary, glass panes should be toughened.

3.3. Thermal breakage types

Thermal breakage of glass can be identified in two types: low and high energy release. In both cases the start of crack is at 90° to both the edge and the surface of the glass, as already mentioned. The type of breakage depends on the magnitude of stress involved at the moment of fracture. The two types are:

Low energy release, the most common because it is related to edge damage. In fact the presence of edge imperfection, associated to micro cracks, request a low value of tensile stress to increase the crack dimension up to the critical one. Generally this phenomenon is characterized by a single crack *(Figure 3.9)*.

High energy release (Figure 3.8) is more rare because it requests very high thermal stress. Generally this phenomenon is characterized by an initial crack branching off into a number of separated cracks at a short distance from its origin (Mognato and Barbieri 2013).

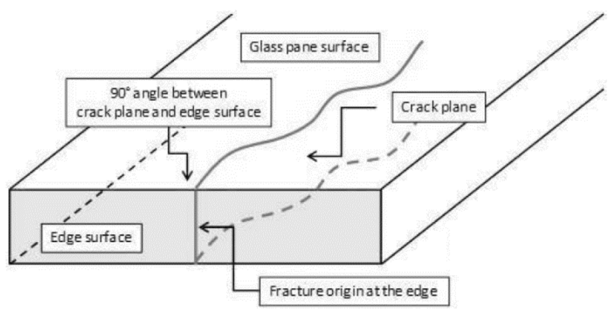

Figure 3.12. Low energy release thermal breakage **(Mognato and Barbieri 2013)**.

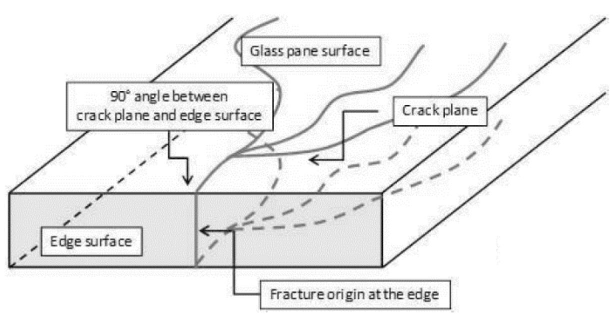

Figure 3.11. High energy release thermal breakage **(Mognato and Barbieri 2013)**.

3.4. Thermal breakage patterns

Thermally-initiated fractures caused by high tensile stresses that possibly result from edge damage can identifies by characteristic breakage patterns. The crack in thermally broken glass is initially perpendicular to the edge and glass for 20-50mm and then branches out into one or more directions. The number of branches or secondary cracks is dependent on the amount of stress in the glass.

Center – 2/3 of edge

Low stress <10MPa

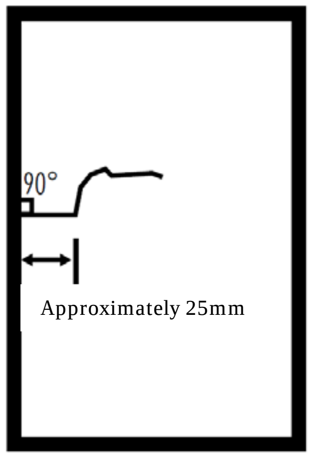

Figure 3.13. Glass break starts perpendicular to edge and does not finish **(Viracon n.d.)**.

Center – 2/3 of edge

Low stress ≃10MPa

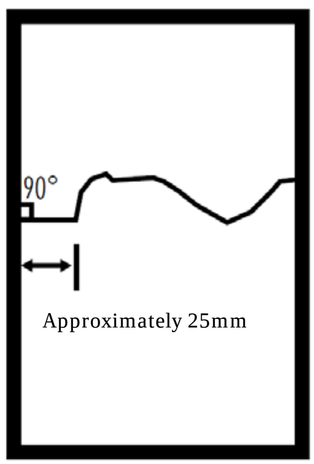

Figure 3.14. Glass break starts perpendicular to glass edge and finishes at another edge **(Viracon n.d.)**.

Center – 2/3 of edge

High stress
Initial fracture ≃10MPa
Each branch ≃7MPa
Total stress ≃24MPa

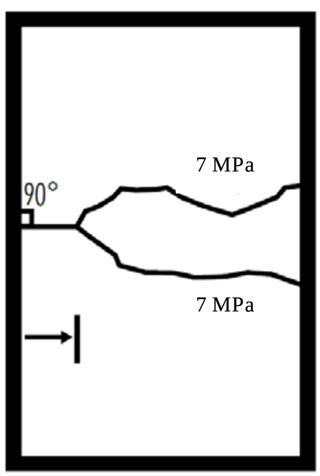

Figure 3.15. Glass break starts perpendicular to glass edge and branches into two breaks within 51mm of original break **(Viracon n.d.)**.

Figure 3.16. Thermal Breakage Pattern **(Glazette n.d.)**.

Figure 3.17. Thermal Breakage Pattern **(Pella n.d.)**.

3.5. Thermal shock and nickel sulfide NiS

There is a breakage phenomenon of glass that that often appears in a similarly to the thermal shock. That is called "spontaneous" breakage. Attention should be paid for these two phenomena are not correlated. In both of them the main actor is solar irradiation, but thermal shock breakage is generally referred to annealed float glass, whereas the breakage due to NiS (nickel sulfide) inclusion is specific of thermally toughened glass. Spontaneous breakage depends by batch contamination, in contrast with thermal shock breakage that is related to design mistakes (Mognato and Barbieri 2013).

Figure 3.18. NiS (Nickel Sulphide) inclusions cause "spontaneous" glass breakage **(Ian Weekes - Nickel Sulphide Inclusions 2015).**

3.6. Thermal fracture calculation methods

In this section the practice of different calculation methods according to different regulation and principles will be elaborated. Each of these practices are different form each other, in the introduction of parameters of influence, precision and application domains.

3.6.1. Common principles of calculation methods

3.6.2. French standard
(NF P 78-201-1/A1(DTU39) 1998); (NF P 78-201-3/(DTU 39) 2006)

There are three methods of thermal stress assessment in French standard. The first two are simpler, and are using tables:

(a) The first method *provides tables with solutions for annealed glazing* which need no further investigation against thermal fracture

(b) The second method is *based on tables that indicate the energy absorption coefficient* which may not be exceeded in a glazing unit

Both methods are meant to be used or a quick verification of the third, most accurate method. The following method proposed by the French standard is also the most widespread, and consists of:

(c) *Calculating the temperature difference between different areas* of the glazing unit; described in annex E of the standard (NF P 78-201-1/A1(DTU39) 1998)

The later method sets three different levels of calculation:

(c.1) The general method

(c.2) The simple method

(c.3) The simple manual method

Each level provides a calculation of the temperature difference occurring at a different level of complexity and precision. The general method delivers the most accurate approximation of the actual conditions, but it is also the most complex method. In addition to a difference in the complexity between these three methods, there is also a difference in the considered parameters and the applications used (*Table 3.1*).

Table 3.1. Levels of calculation according to French standard – application domain **(VandenPoel 2010)**.

	Transient or steady conditions?	Application domain
general method	Transient	All types of glass and window frames
simple method	Stationary	Window frames with weak thermal inertia
simple manual method	Stationary	Window frames with weak thermal inertia

As explained in the table above, the calculation of the temperature differences can be carried out in steady-state regime, and is only applicable on frames with a low thermal inertia. For other frames, these temperature differences must be calculated transient over a period of one day (depending on the season and the orientation of the glazing). The maximum temperature difference between two parts of the glazing unit is used to compute the stress which has to stay below an allowable stress. The calculated stress depends on the inertia of the frame and the shadow on the glazing. The allowable stress depends on the type of glass, the sensibility of the edge to thermal fracture, the inclination and the support conditions of the glazing. “Vitrages decision” software is available to help perform the calculations based on French standard. This program is developed by CEBTP and performs heat calculations in order to dimensionalise a glass element and verify its performance (VandenPoel 2010).

The methods used in French standard are deterministic. Stresses are calculated but no safety coefficients are introduced. Again, the unknown safety margin is identical for structural elements, secondary elements or infill panels. This method takes into account the influence of the latitude and the altitude of the site, the orientation and the slope of the glazing as well as the period of year by calculating during one day per season. However, only an instantaneous stress is considered, a maximum stress value, which is determinative for the complete lifetime of the glazing unit (modified form (Vandebroek 2015)). The scope of the French standard is limited to windows, possibly equipped with shading devices and are not directly exposed to an artificial heat source (VandenPoel 2010).

To sum up, the French standard thermal stress assessment (NF P 78-201-3/(DTU 39) 2006) propose the following approach: The stress generated by temperature difference on the edges of glass sheets has to be lower than the maximum allowable glass stress:

$$\sigma_{\mathrm{th}} < \sigma_{\mathrm{adm}} \tag{3.1}$$

σ_{th} = thermal induced glass stress
σ_{adm} = maximum allowable glass stress

with:

$$\sigma_{\mathrm{th}} = K_{\mathrm{t}} \cdot E \cdot \alpha \cdot \delta\theta \tag{3.2}$$

where:
E = 70 young's modulus of glass [GPa]
$\delta\theta_{max}$ maximum temperature difference [°C]
$\alpha = 9\ 10^{-6}$ expansion coefficient of glass [1/K]
K_t thermal stress coefficients:

$K_t = K_f\ K_o$
Frame systems with low heat capacity, no shades: 0.8
Frame systems with low heat capacity +shades: 0.9
Frame systems with mean heat capacity +shades: 1.0
Frame systems with high heat capacity +shades: 1.1
K_f depends on heat capacity of frame
K_0 depends on presence of external shading
(the exact shape of the outer shadow is usually not known)

and:

$$\sigma_{adm} = K_{\mathrm{v}} \cdot K_{\mathrm{a}} \cdot \sigma_{vm} \tag{3.3}$$

where:

K_a inclination & support coefficient

Vertical (<60°): 1.0 (Circumferential support), 0.8 (other support type)
Inclined (≥60°): 0.9 (Circumferential support), 0.65 (other support type)
Horizontal (<30°): 0.8 (Circumferential support), 0.5 (other support type)

K_v sensibility coefficient of glass to thermal fracture

Laminated annealed glass, sawed from big sheets: 0.85
Monolithic annealed float glass/laminated annealed, normally clean cut: 1.0
Monolithic annealed glass/laminated annealed glass with machine smooth ground: 1.2
Monolithic thermally treated glass; tempered or heat strengthened: 2.5

σ_{vm} allowable basic stress on glass [MPa]

Annealed/laminated glass: 20
Heat strengthened clear/toughened with ceramic frit also laminated: 35
Toughened clear monolithic/laminated glass: 50
Wire glass: 16
Thermally toughened patterned glass: 40

The formulae (3.1), (3.2) and (3.3) of the French standard evident the influence of the *type of window frame*, *outer shadow* (factor K_t), the *glass finish* (factor K_v), as well as the *slope* of the window and its *supports* (factor K_a).

Note: the effect of the *inclination of the window* will be charged twice: on the one hand from the peak of the global solar radiation (during the temperature difference calculation, as is explained in the following paragraph), and on the other hand via an influence factor of the tensile strength of the glass.

The maximum temperature difference $\delta\theta_{max}$

In order to determine the maximum temperature difference value $\delta\theta_{max}$ mentioned above the window is divided into three zones by the French standard:

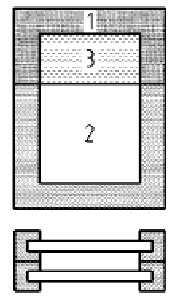

Figure 3.19. Zones of glazing according to French standards **(NF P 78-201-3/(DTU 39) 2006).**

- The temperature of the glass trapped in the window frame $\theta 1$ [°C]
- The temperature of the glass subject to solar radiation $\theta 2$ [°C]
- The temperature of the glass that is shaded $\theta 3$ [°C]

These temperatures are determined for a typical day per season, to which the global solar radiation, diffuse solar radiation and outside temperature are given.

The acting temperature difference is equal to:

$$\Delta T = \max(\theta_1 - \theta_2,\ \theta_2 - \theta_3,\ \theta_1 - \theta_3) \qquad (3.4)$$

General method

Each of the graphs illustrated in *Figure 3.17* corresponds to a season and shows the outside temperature over one day.

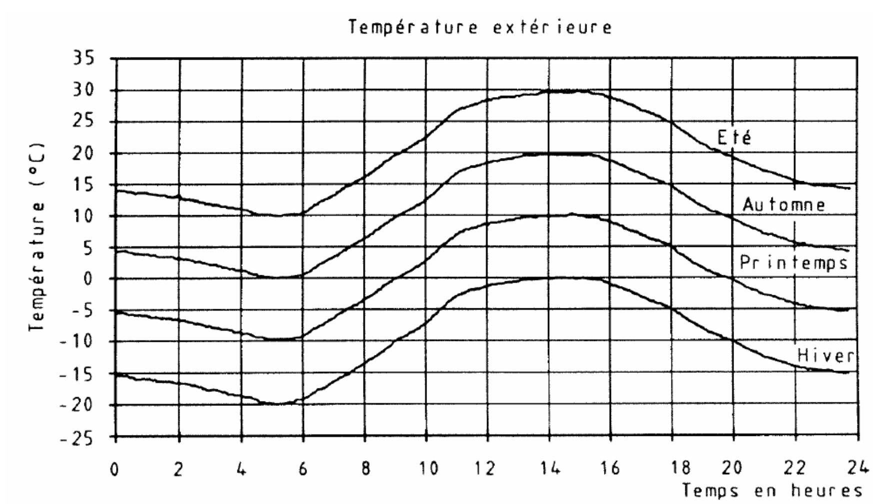

Figure 3.20. Outside temperature depending on the season **(NF P 78-201-3/(DTU 39) 2006).**

In the same way, the diffuse solar radiation graphs, depending on the season, are presented in *Figure 3.18*.

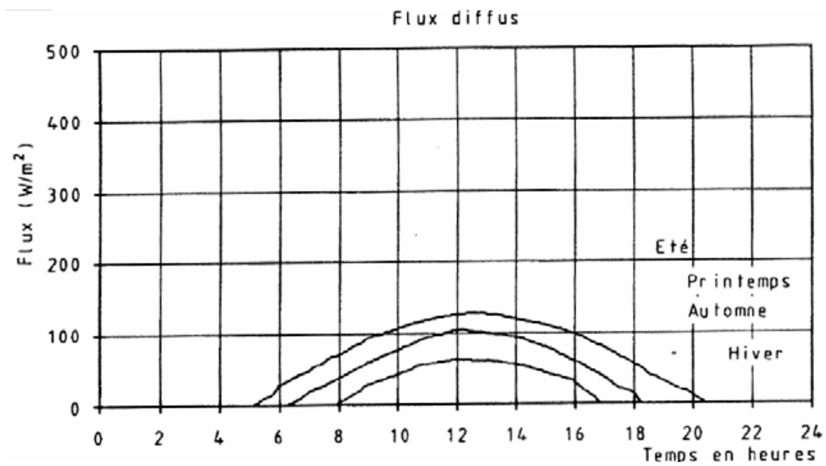

Figure 3.21. Diffuse solar radiation depending on the season **(NF P 78-201-3/(DTU 39) 2006)**.

The *global solar radiation* dependents on the considered season and orientation of the facade. The following graphs refer to vertical façade applications. The global solar radiation is the sum of *direct* and *diffuse* solar radiation.

This means that only *the direct portion of the global solar radiation which is dependent on the façade orientation*, as the *diffuse component is only dependent on the considered season*.

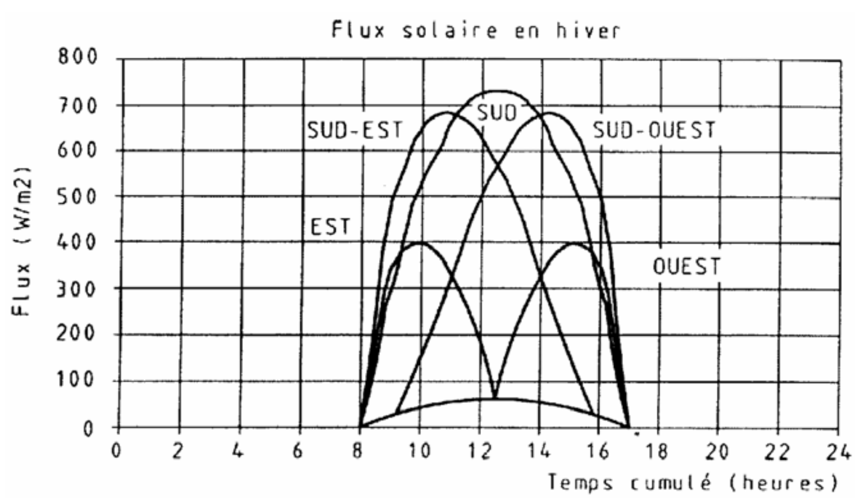

Figure 3.22. Global solar radiation in the winter, depending on the facade orientation **(NF P 78-201-3/(DTU 39) 2006)**.

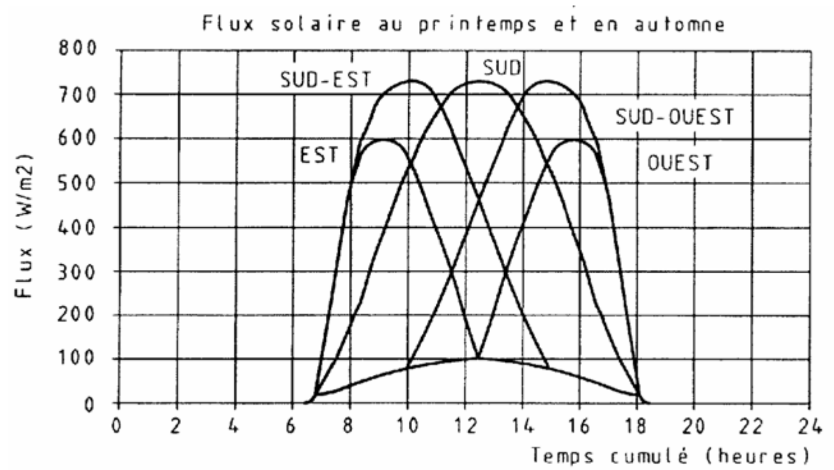

Figure 3.23. Global solar radiation in the spring and fall depending on façade orientation **(NF P 78-201-3/(DTU 39) 2006)**.

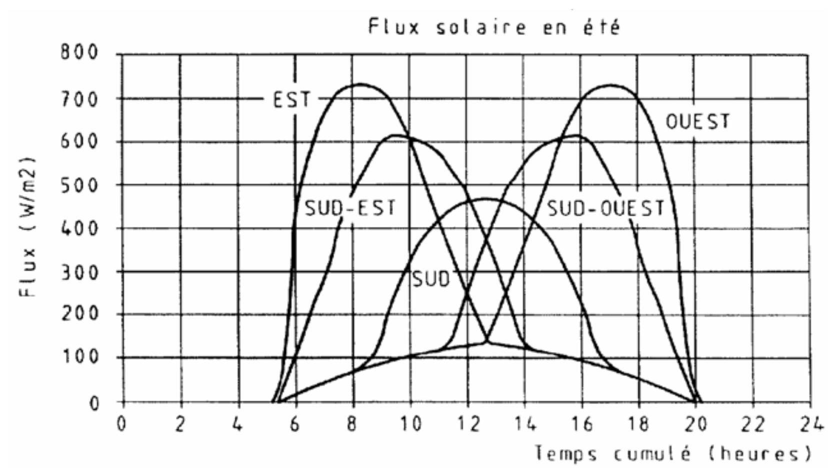

Figure 3.24. Global solar radiation in the summer, depending on facade orientation **(NF P 78-201-3/(DTU 39) 2006)**.

The diagrams of the previous figures correspond to a maximum solar radiation of 750 W/m^2 on vertical façades. If the inclination of the window is not vertical the amount of the incident solar radiation should be increased.

To summarize, the *outside temperature* and the *diffuse solar radiation* are dependent on the season, the time of day and the *global solar radiation*. The later depends on the season, the time of the day, the facade orientation and the inclination of the facade.

The calculation of the temperatures θ_1, θ_2 and θ_3 of the various zones of the glazing are based on finite element method.

Simple method

This method is only applicable for window frames with weak thermal inertia (wood, PVC, aluminum), as indicated in *Table 3.1*. According to the simple method, the outside temperature is no longer found in a function, as in the general method, but by constant values depending on the geographical position and the season. *Figure 3.22* illustrates the maximum temperature values that should be used in the summer and *Figure 3.23* the maximum temperature values to be used during winter. These values should be increased by 5°C if the calculated temperature corresponds to a zone directly exposed to solar radiation.

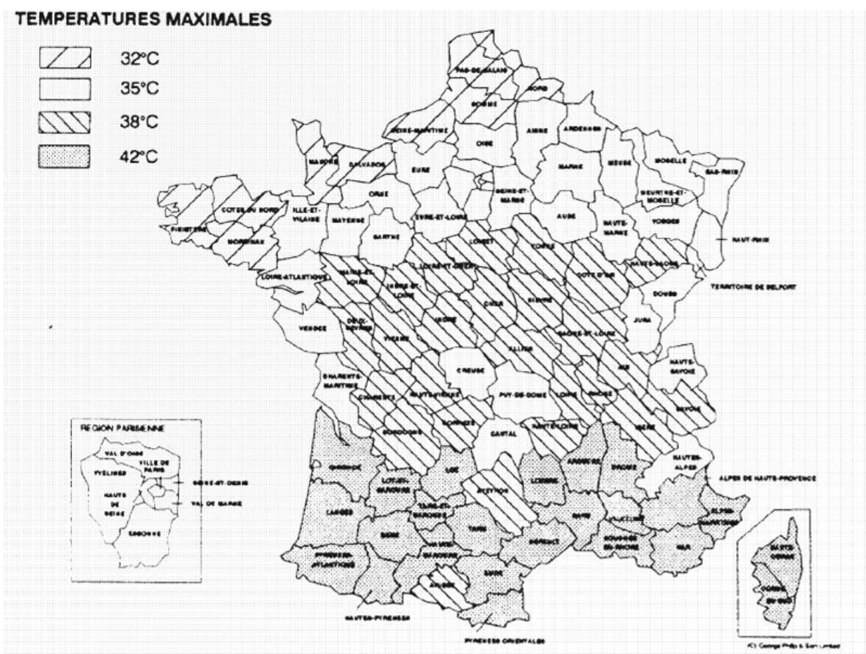

Figure 3.25. Outside summer temperatures according to the simple method **(NF P 78-201-3/(DTU 39) 2006)**.

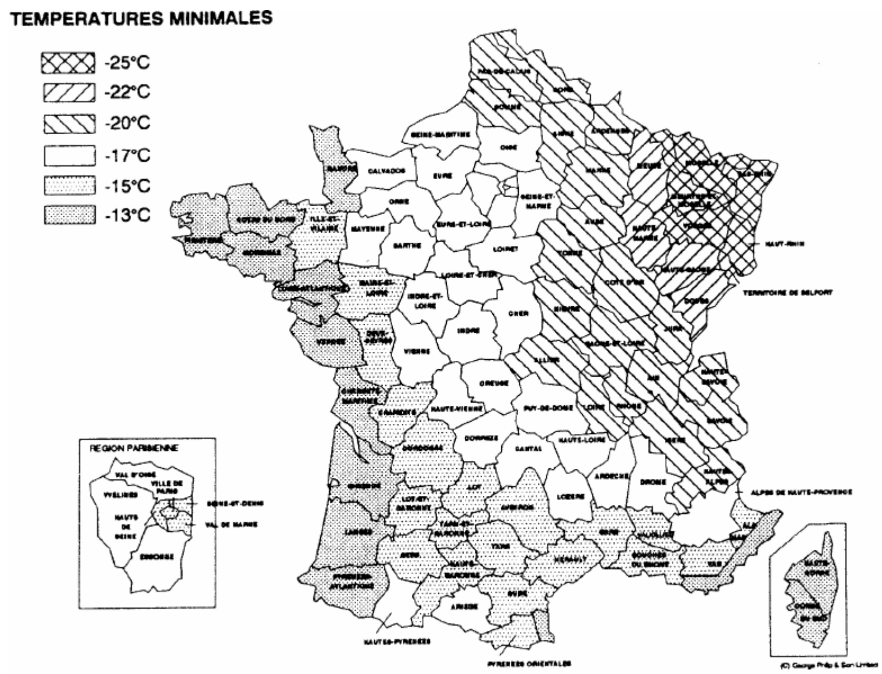

Figure 3.26. Outside winter temperatures according to the simple method **(NF P 78-201-3/(DTU 39) 2006)**.

The maximum global solar radiation is defined in the standard taking into account the altitude and type of area. A correction factor might be necessary to introduce the effect of the season, and of the slope of the façade (relative to the horizontal) (NF P 78-201-1/A1(DTU39) 1998).

To summarize, the outside temperature depends on the season, the geographical position and the altitude. The maximum global solar radiation depends on the altitude, type of area, season and inclination of the facade -with respect to the horizontal.

The calculation of the temperatures θ_1, θ_2 and θ_3 of the various zones of the glazing can be done on the basis of the thermal balance of each part of the frame (VandenPoel 2010).

Simple manual method

This method, like the previous one, is only applicable for window frames with weak thermal inertia (wood, PVC, aluminum), as indicated in *Table 3.1*.

The outdoor temperatures are defined in the same way as the simple method, as well as global solar radiation. The difference between the two methods lie on the calculation method of the temperatures θ_1, θ_2 and θ_3 of the different zones of the glazing, which is now performed manually, as the name indicates.

- For the calculation of the temperature of the glass trapped in the window frame θ_1:

$$\theta_1 = \frac{h_i \cdot \theta_i + h_e \cdot \theta_e}{h_i + h_e} \tag{3.5}$$

- For the calculation of the temperature of the glass subject to solar radiation θ_2:

$$\theta_2 = \frac{h_i \cdot \theta_i + h_e \cdot \theta_e + \mathrm{A} \cdot \mathrm{I}}{h_i + h_e} \tag{3.6}$$

with I the maximum global solar radiation

- For the calculation of the temperature of the glass that is shaded θ_3:

$$\theta_3 = \frac{h_i \cdot \theta_i + h_e \cdot \theta_e + \mathrm{A} \cdot \mathrm{I}}{h_i + h_e} \tag{3.7}$$

with I equal to 10% of the maximum global solar radiation

Vitrages Decision calculation software

Vitrages Decision is a special French software developed by the public company C.E.B.T.P. It is used for computing the temperature differences on glass, officially based on the newest edition of the norm; (NF P 78-201-3/(DTU 39) 2006). This method serves nowadays as reference model for thermal stress analysis for the most important European façade engineering companies or leading manufacturers.

Vitrages Decision calculates in 15min. time steps, using finite difference method, the resulting transitory temperatures on the unshaded and shaded glass center, and shaded glass edge areas in function of external course of the air temperature, sun position and intensity. No heat conductivity is assumed between glass edge and center.

For all orientations, first the most critical season is determined. Then the maximum resulting temperature difference, $\delta\theta_{max}$, is indicated for further evaluation on maximum allowable stress. For the spandrel or ventilated applications, the steady state approach is applied. Vitrages Decision performs the calculations based on the third, and more precise method of the French standard. That requires calculation of the temperature difference between three different areas of the glazing (this method is described in annex E of the standard; (NF P 78-201-1/A1(DTU39) 1998).

If a blind is applied, the calculations are done for blind up and blind down. The zones with/without sun and with/without blind are considered. Then the maximum temperature difference is determined.

3.6.3. British standard (CEN/TC129/WG8-N180E 2004)

The calculation against thermal fracture according to UK standard is a simplistic one. A very important note is that these rules only apply to windows produced by the company Pilkington.

According to the British standard, the maximum occurring temperature difference is not calculated with an equation, but from tables. The temperature difference is defined by the glass type, the amount of solar radiation and the amplitude of daily temperature. The latter two can be read from the United Kingdom detailed map or from a world map (VandenPoel 2010).

The glass breaking resistance is linked to the permissible temperature difference: there is no risk of thermal breakage as the temperature difference is smaller than the permissible temperature difference. The maximum ΔT for float glass is 30°C according to the British standard. *Table 3.2* illustrates the different limits for temperature difference based on glass type and edge finish.

Table 3.2. Maximum temperature differences according to UK standards **(Feryn 2012)**.

	Cut or beveled glass [°C]	Cut glass [°C]	Polished glass [°C]
Float glass, t <12 mm	35	40	45
Float glass, t = 15 mm or 19 mm	30	35	40
Float glass, t = 25 mm	26	30	35
Heat strengthened glass	100	100	100
Thermally toughened glass	200	200	200

The acting temperature difference found above is corrected by the effect of:

- Internal shading devices
- Material of the window frame
- Outside shade

3.6.4. Belgian standard

(FIV (Fédération de l'Industrie du Verre), Belgian Glass 01 1997)

The Belgian rules FIV 01 were published in 1997 by the Association of the lass industry (VIG) or La Fédération de l'industrie du Verre (FIV) (VandenPoel 2010). The thermal risk assessment is based on a simplistic calculation, similar to the British standard.

The maximum allowable temperature differences are identical to the ones of the British standard, and there is no risk of thermal breakage occurring with a lower ΔT. The following equation applies to single glazing:

$$\Delta T = \frac{I \cdot a}{h_e + h_i} + \frac{A \cdot h_e}{h_e + h_i} \qquad (3.8)$$

where:

I = Intensity of solar radiation [W/m^2]

a = Absorption coefficient of the single glass [-]

A = Maximum amplitude of the average daily temperature over at least 10 years

(This is a constant value depending on the geographical position)

he = Heat transfer coefficient to the outer surface [W/m^{2}K]

hi = Heat transfer coefficient to the inner surface [W/m^{2}K]

Thus, it is clear that the temperature difference is affected by the amount of solar radiation (first part of the equation) as well as (the influence of the daily temperature variations (second part of equation).

The acting temperature difference calculated is then adjusted and influenced by the effect of:

- Internal shading devices and ventilation space
- Material of the window frame
- Outside shade

Influence of the inside blinds:

$$\Delta T_1 = \Delta T + \Delta T' \qquad (3.9)$$

Where the ΔT values are summarized on the following *Table 3.3 and Table 3.4:*

Table 3.3. Temperature influence of the inside blinds, simple glazing **(AGC 2008)**.

Simple glazing	Ventilated space	Non ventilated space
Open weave	3 ^{o}C	6 ^{o}C
Closed weave	4 ^{o}C	7 ^{o}C
Venetian blinds	5 ^{o}C	8 ^{o}C

Table 3.4. Temperature influence of the inside blinds, simple glazing **(AGC 2008)**.

Double glazing	Outside glazing		Inside glazing	
	Ventilated space	Non ventilated space	Ventilated space	Non ventilated space
Open weave	2^{o}C	4^{o}C	4^{o}C	8^{o}C
Closed weave	3^{o}C	5^{o}C	5^{o}C	9^{o}C
Venetian blinds	4^{o}C	6^{o}C	6^{o}C	10^{o}C

Influence of the frame:

$$\Delta T_2 = \Delta T_1 \cdot f_1 \tag{3.10}$$

Where the f_1 values are summarized on the following *Table 3.5*:

Table 3.5. Influence coefficient of the type of frame **(AGC 2008)**.

Type of frame	**f1**
Concrete	1.0
Clear steel	0.9
Dark steel	0.8
Steel with thermal break	0.8
Clear aluminum without thermal break	0.8
Wood/PVC	0.75
Dark aluminum without thermal break	0.7
Aluminum with thermal break	0.7
Structural glazing	0.5

Influence of the outside shadows:

$$\Delta T_3 = \Delta T_2 \cdot f_2 \tag{3.11}$$

Where the f_2 values are summarized on the following *Table 3.6:*

Table 3.6. Influence coefficient of the outside shadows **(AGC 2008)**.

Sort of shadow	SV and outside glass of double glazing	Inside glass of double glazing
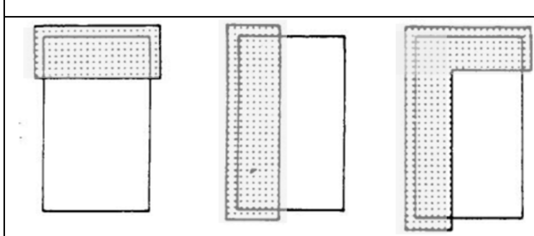	1.2	1.1

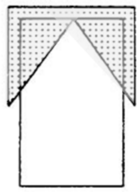	1.5	1.2

According to the Belgian standard, a glass pane does not need to be checked against thermal fracture in its orientation is not on the gray zone, *Figure 3.18*. These glass panes are considered safe against thermal breakage.

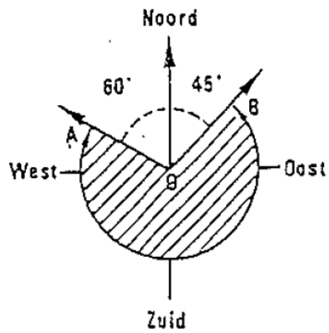

Figure 3.27. Thermal breakage risk: only in the shaded area **(VandenPoel 2010)**.

The stress in the glass is calculated from:

$$\sigma = E \cdot \varepsilon = E \cdot \alpha \cdot \Delta T_3 = 0.63 \cdot \Delta T_3 \tag{3.12}$$

Criteria for acceptability against the risk of thermal fracture according to AGC are:

$\Delta T_3 < 30°C$: Acceptable

$\Delta T_3 > 30°C$: Thermal treatment (toughened or heat strengthened) is suggested

In addition, according to the 3.5.4. Belgian standard, the edge treatment is not considered as a good solution to prevent of the risk of thermal shock. Also, the spandrels must always be tempered.

3.6.5. European standard (prEN thstr 2004)

The calculation method used in the European standards first calculates the basic temperature difference for the glass subject to the environment at the place of use. The basic temperature difference is then modified, to take into account construction and other details which have an effect on the stress in the glass, to give a calculated temperature difference. The calculated temperature difference is then compared with the allowable temperature difference for the glass product to assess whether the glass is thermally safe (prEN thstr 2004).

- The *basic temperature difference* depends on the solar energy absorption of glass, the solar radiation intensity, the heat transfer coefficients, the possible heating from radiant heaters, the diurnal temperature range and the internal temperature rise, which can be caused by the air in the vicinity of the window not being ventilated, and thus being different from the ambient room temperature.

- The *calculated temperature difference* additionally accounts for the influence of blinds, backups, possible shadow on a part of the pane (static -present for more than 3 hours- or transient) and the frame factors and coefficients. The color of the blinds is important, as well as the ventilation between the blinds and the glazing. Also, backup walls or ceilings can cause an accumulation of hot air and thus influence the glass temperature (prEN thstr 2004).

The method used in the European standard is still under development. This method is based on the "Belgian Glass" document; "Evaluation des contraintes thermiques dans les Vitrages" (Belgian Glass 1997, a document of the "Fédération de l'industrie du Verre"). Both methods are deterministic (stresses or safety coefficients are not mentioned). Moreover, the unknown safety margin is identical for structural elements, secondary elements and infill panels. Concerning the influence of solar radiation, the altitude of the site and the orientation of the glazing, the influence of haze and ground reflectance and the time of the year are important. These methods simplify these influences by assuming a maximum intensity which has to be taken into account during the lifetime of the glazing, regardless of the aforementioned influences on the solar radiation. Thus, only an instantaneous temperature difference is considered, assuming this maximum difference to be determinative for the complete lifetime of the glazing unit. In addition, stress corrosion is not considered (modified from: (Vandebroek 2015)).

3.7. Glass edge conditions

Glass edge condition is the most important parameter of influence in a thermal breakage of annealed glass. Therefore in this paragraph we will emphasize on its effects. As indicated by the standard used to access thermal breakage risk, the condition of the glass edge is crucial against high tensile stresses developed close to the pane edges. It is important to consider that the edge strength can be lower than the surface one because of edge handling and the concentration of tension induced by the frame boundaries (Mognato and Barbieri 2013).

Glass with clean cut edges has the greatest resistance to thermal breakage. However, annealed glass edges that have been damaged in handling or during installation have greater risk of thermal breakage and sometimes edge worked glass is advisable (Metro n.d.).

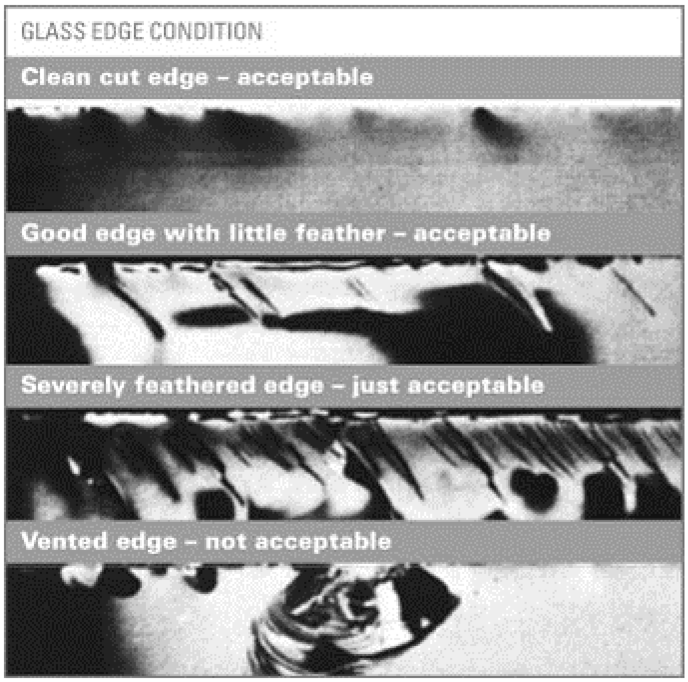

Figure 3.28. Acceptable Edge of Glass Conditions **(Metro n.d.)**.

3.8. Chapter Highlights

The context of this chapter clarifies the failure mechanism of thermal fracture, a phenomenon generally referred to annealed glass. Parameters that influence this phenomenon can be summarized in the categories: Climate conditions, gazing characteristics, inside and outside "architectural" parameters. Thermal breakage occurs in high stress levels that will trigger often pre-existing microcracks into fracturing the pane. There are two types of thermal breakage that depend on the magnitude of these stress. Based on the pattern of fracture, a high or low energy release breaking can be recognized.

In most of the codes and standards around the word there is no prediction against thermal fracture. There is a limited number of methods to estimate risk assessment for this glass failure. Each of these practices are different form each other, in the introduction of parameters of influence, precision and application domains. In this chapter the most widespread calculation methods against thermal breakage risk are analysed. These methods only consider simple façade configurations. The fatigue of a glass pane exposed to weather conditions is not taken into account.

4. Laboratory Experiments

4.1. Introduction

In this chapter, the different laboratory experiments are described. The experiments were conducted aiming to simulate as realistic as possible the actual conditions of a glass application. These experiments were done on as-received glass samples. Further possible damage from environmental conditions (humidity etc.) on exposed glass, transportation, handling and further incidental flaws are not considered.

4.2. Specimens

Annealed glass with raw cut edges has the lowest resistance to thermal stress fracture, although it might be perfectly adequate if used for a façade with no interactions with localized heating, like a north oriented façade (Stevens 2013). The samples tested in the context of my research were glass panes of annealed glass and cut edges, of different coatings and dimensions.

4.3. Equipment

4.3.1. Introduction

Temperature tests are often time consuming and difficult to control in comparison to external loading tests. In the contents of my research, the application of thermal loads was necessary to simulate thermal fracture in practice.

In order to access characteristics to the glass specimens and investigate their behavior under intense solar radiation, two different types of solar simulators were used. Surface temperature measurements were possible by using thermo-couples. With the use of a spectrophotometer the absolute reflectance of the surface and the light transition could be measures, and as a result the absorption could be calculated.

The characteristics of the state-of-the-art technology equipment used are described in the following paragraphs.

4.3.2. Large area solar simulator, EternalSun®

In order to simulate as realistic as possible the situation in which a glass panel is heated with solar radiation, a “large area solar simulator”; developed and tested at Delft University of Technology (Figure 4.1) was used in the experimental procedures.

Figure 4.1. Large area solar simulator **(Eternal Sun n.d.)**.

The artificial sunlight produced by our solar simulation systems is mostly applied to carry out performance testing. These performance tests vary according to the application of the tested product.

- In the **solar energy industry (Solar PV)**, performance testing with artificial sunlight is done to determine the useful output of a solar powered system. The efficiency is calculated by dividing this maximum power output by the power of the solar irradiance received by the panel.

- The performance of a **solar thermal collector** is assessed differently. It is determined by measuring the difference in water temperature of the in- and outlets of the thermal collector, at a certain flow rate and ambient temperature.

- **Accelerated life tests** are applied in order to detect product failure in early stages of the development or as quality control during production. Solar simulation for testing with sunlight is a usual setup of an ALT test.

In the hereby study, the experimental procedure aimed on assessing the performance of a glass pane, heated up under solar radiation and therefore experiencing temperature differences along its thickness and between the center and the edges of the pane. This performance assessment demanded the recording of temperatures in different parts of the glass panes for a relatively short period of time. This was until the equilibrium of temperatures, so the stabilization of temperature difference, or the temperature difference was equal to zero.

The “large area solar simulator” (Eternal Sun®) produces AAA-accuracy, steady-state and long pulse sunlight. Its operation was easy since positioning is flexible, under different angles.

The simulator could easily be adjusted and used for the large glass panels required for the experiment.

4.3.3. Super Solar simulator, Wacom®

4.3.4. Research Arc Lamp, Newport®

Arc lamp light sources have high ultraviolet and visible output with some prominent lines in the near infrared. The small, bright arcs have significant advantages for collimation and intense irradiation.

4.3.5. LAMBDA 950 UV/Vis/NIR Spectrophotometer, PerkinElmer®

When solar radiation strikes glass, it is partly reflected, partly absorbed in the thickness of the glass and partly transmitted. The ratio of each of these 3 parts to the incident solar radiation defines the reflectance factor, the absorptance factor and the transmittance factor of the glazing. If these ratios are plotted for the electromagnetic spectrum, they form the spectral curve of the glazing. Factors that affect these ratios for a given incidence are the tint of the glass, its thickness and, in the case of a coated glass, the nature of the coating.

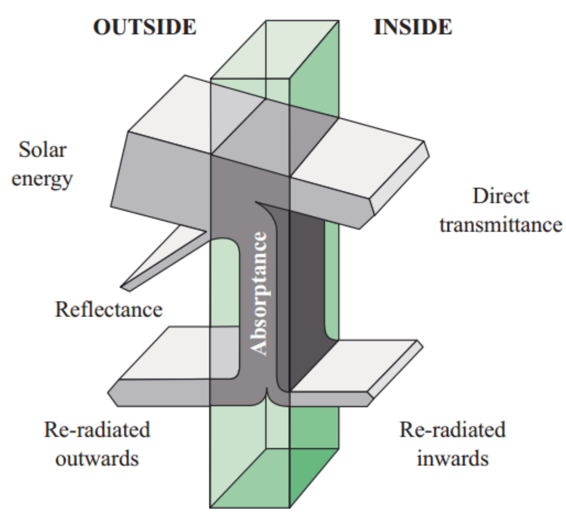

Figure 4.2. Total solar energy transmittance **(Pilkington n.d.)**

LAMBDA 950 UV/Vis/NIR it the spectrophotometer type used to measure the absolute reflectance and light transmittance of the glass samples. This way high performance testing across the spectral range up to 3300 nm was possible. The UV/Vis resolution reaches 0.05 nm, while the NIR resolution reaches up to 0.20 nm.

4.3.6. Temperature measurements with Thermo-couples

Thermo-couples are industrial temperature contact sensors. Temperature is the measure of average molecular kinetic energy; as the kinetic energy of the substance increases so does the temperature. Temperature measurements rely on the transfer of heat energy from the material to the measuring device. Contact temperature sensors are the most common and widely used form of temperature measurement.

A thermo-couple consists of two wires of dissimilar metals that are electrically connected to one end. Applied heat produces voltage between the wires (electromotive force E.M.F.) proportional to temperature. The relationship between two temperatures and E.M.F. is described in the equation ... :

$$\mathbf{e = a\ (T_1 - T_2) + \beta(T_1^2 - T_2^2)}$$

where:
e: E.M.F.
a & b: constants for thermocouple
T1 & T2: temperatures
A schematic for a thermo-couple connection is shown in the diagram below *(Figure 4.3)*. The thermo-couples used in this research are fusion-welded on the tip to form a pure joint, which maintains the integrity of the circuit and provides high accuracy.

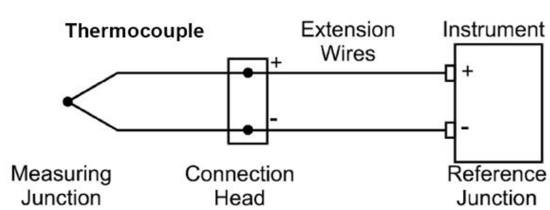

Figure 4.3. Schematic for thermo-couple connection **(Instrumentation Toolbox n.d.).**

Thermo-couples were used as a mean of temperature measurement because of their accuracy for large temperatures and their fast response. Their small size and reasonable stability made them appropriate for this application.

Fluke 54 II B Dual Input Digital Thermometer, Fluke®

Fluke 54 II B dual input digital thermometer *(Figure 4.4, Figure 4.5)* with data logging is the measuring device used to list the surface temperatures developed during the experiments. Its laboratory accuracy is (0.05% + 0.3°C).

Figure 4.4. Fluke 54 II B dual input digital thermometer **(Fluke n.d.)**.

Figure 4.5. Fluke 54 II B dual input digital thermometer **(Image by author).**

4.4. Set-ups and Results

4.4.1. Introduction

The generated tensile stresses developed on the glass might be sufficient to activate pre-existing micro-cracks and lead to fracture. Therefore, to evaluate the performance of the glass sample under peak temperature fluctuations, specimens were exposed to solar radiation intensity (1000w/m^2).

In order to have a better understanding of the glass behavior under thermal load, the set-ups described below were executed as part of the experimental investigation of the MSc thesis.

When the glass pane is uniformly heated, the adsorbed radiation causes expansion. When this expansion is free, there is no stress development. In the following set-ups the edges are not trapped in a frame, so expansion is not restrained.

4.4.2. 1st Set-up

In the first clear floating glass was used. The temperature was measured for 18 minutes, until the temperature difference was equal to zero. Part of the glass was trapped in an aluminum frame and shaded by it *(Figure 4.6)*. *Figure 4.7* and *Figure 4.8* illustrate the temperature difference and surface temperatures measured with thermo-couples during this experiment.

Solar simulator:	Large area solar simulator
Glass sample:	6mm thickness, 25x15cm
Coatings:	Clear glass
Shading method:	Aluminum frame
Temp. Measurement:	Thermo-couples

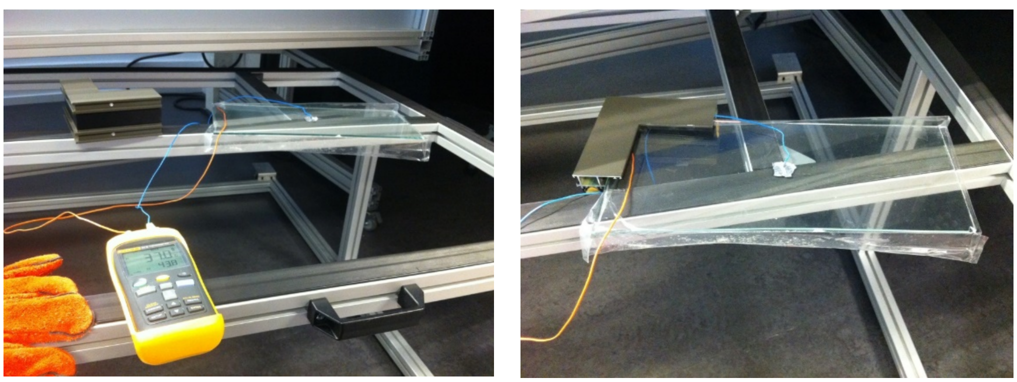

(a) *(b)*

Figure 4.6. (a) & (b): 1st Set-up.

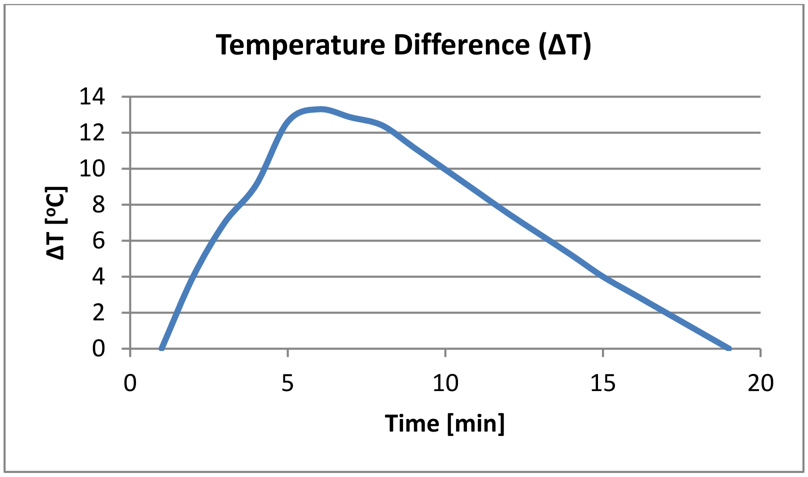

Figure 4.7. 1st Set-up - Temperature difference diagram.

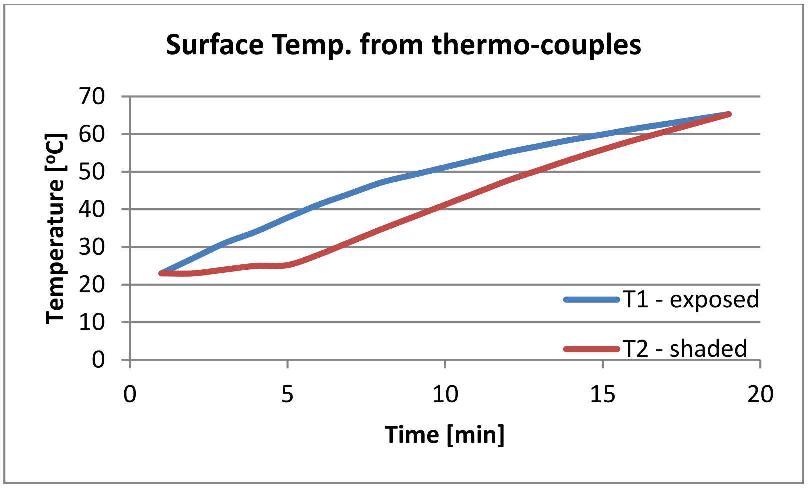

Figure 4.8. 1st Set-up - Surface temperature diagram.

4.4.3. 2nd Set-up

The second set-up used a shading shape that is the most risky against thermal breakage *(Figure 4.9)*. The temperature was measured for almost an hour, until the temperature difference was stabilized to 15 degrees. *Figure 4.10* and *Figure 4.11* illustrate the temperature difference and surface temperatures measured with thermo-couples.

Solar simulator:	Large area solar simulator
Glass sample:	6mm thickness, 25x15cm
Coatings:	Protective transparent film
Shading method:	Critical shading shape with created with reflective tape
Temp. Measurement:	Thermo-couples

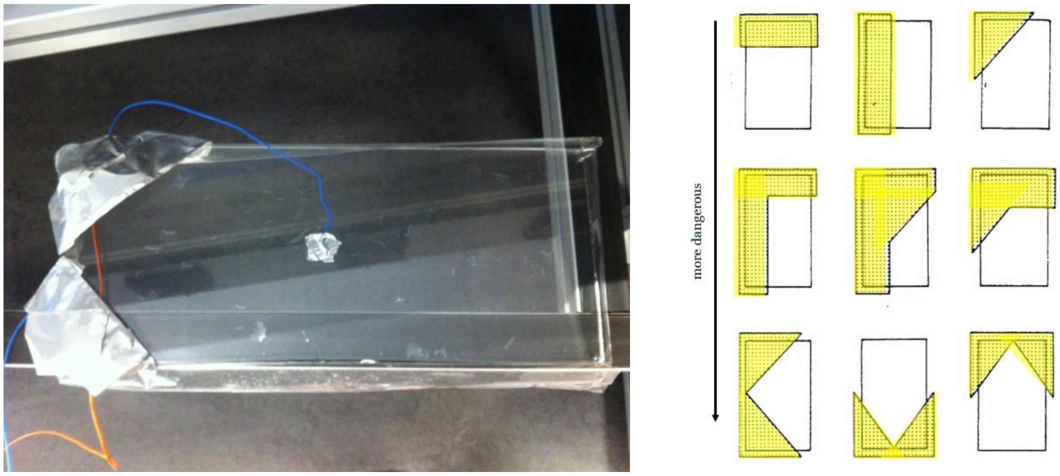

Figure 4.9. 2nd Set-up.

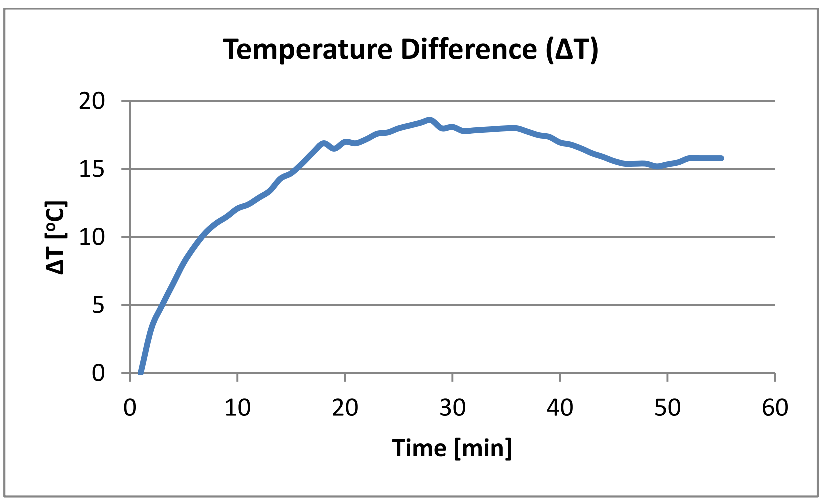

Figure 4.10. 2nd Set-up - Temperature difference diagram.

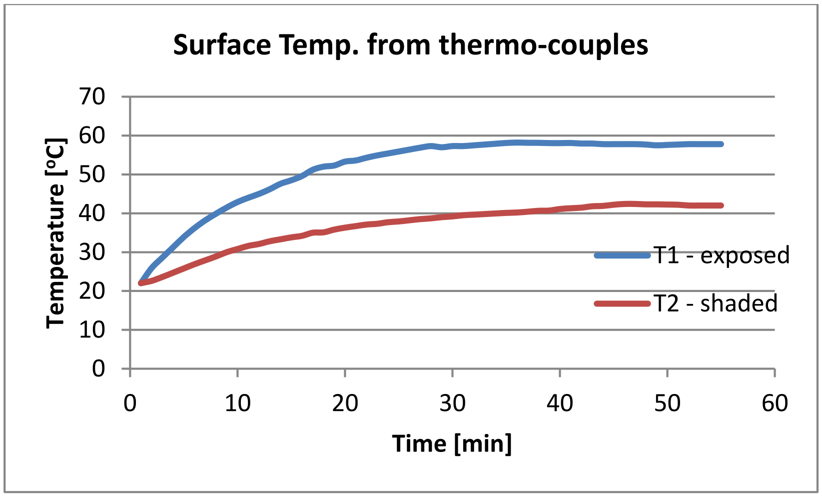

Figure 4.11. 2nd Set-up - Surface temperature diagram.

4.4.4. 3rd Set-up

The third set-up created an additional temperature difference along the thickness of the pane, by half-singing the sample in cold (0º Celcius) water. The results of set-up are summarized below.

Solar simulator:	Large area solar simulator
Glass sample:	6mm thickness, 17x17cm
Shading method:	Critical shading shape with created with reflective tape
Temp. Measurement:	Thermo-couples
ΔT long glass thickness:	Glass half-sang in cool water

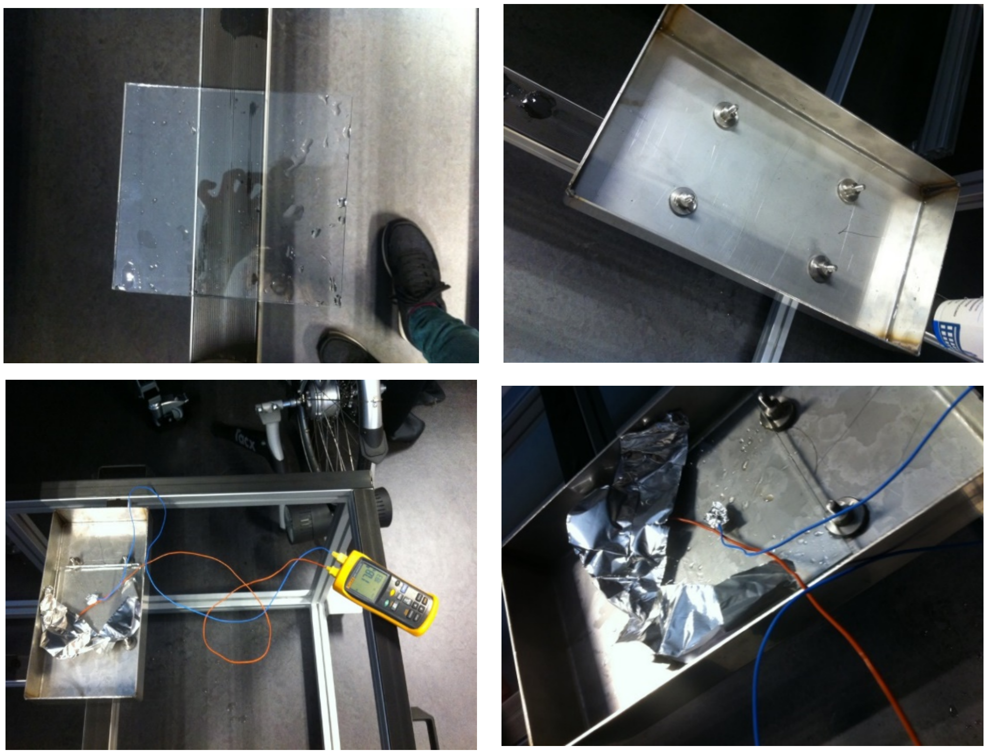

Figure 4.12. 3rd Set-up.

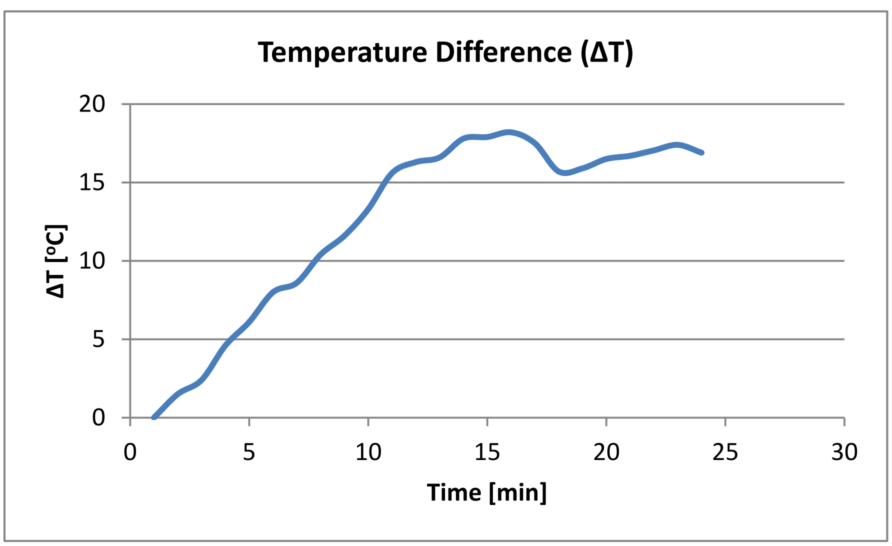

Figure 4.13. 3rd Set-up - Temperature difference diagram.

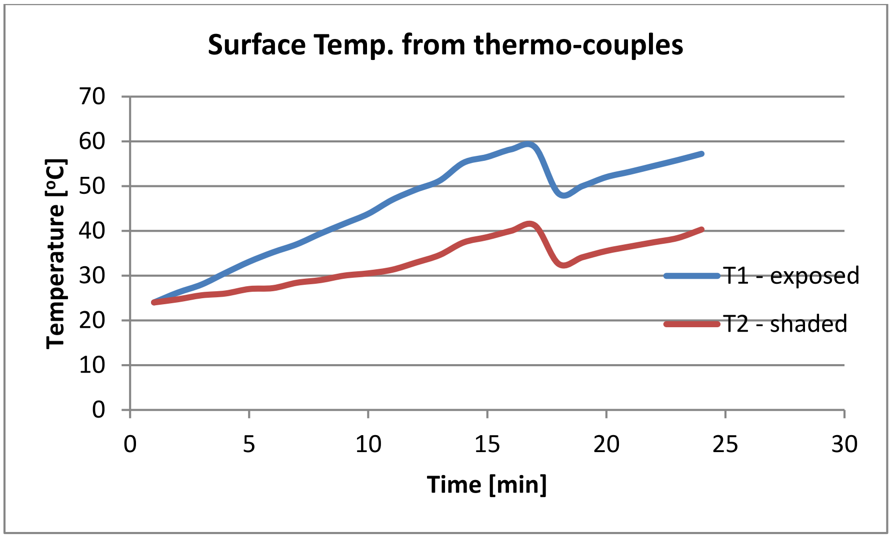

Figure 4.14. 3rd Set-up - Surface temperature diagram.

4.4.5. 4th Set-up

The fourth set-up is making use of the "Super Solar simulator, Wacom" (paragraph 4.3.3). In this case, only a small area of the glass is irradiated with the solar radiation intensity, and thus heated up. The glass edges do remain in room temperature. A cooling plate at the bottom of the sample is keeping the glass surface on the bottom at room temperature (25ºC), in order to crate temperature difference along the thickness of the glass. Because of the small thickness and dimensions of the sample, tough, conduction takes over and the upper surface of the glass does not heat up for more than a couple degrees Celsius. The set-up is repeated with the cooling plate turned off (5th set-up).

Solar simulator:	«Super Solar Simulator»
Glass sample:	6mm thickness, 17x17cm
Shading method:	Edges non-exposed to solar radiation remain in room temp.
Temp. Measurement:	Thermo-couples
ΔT long glass thickness:	Cooling plate 25ºC

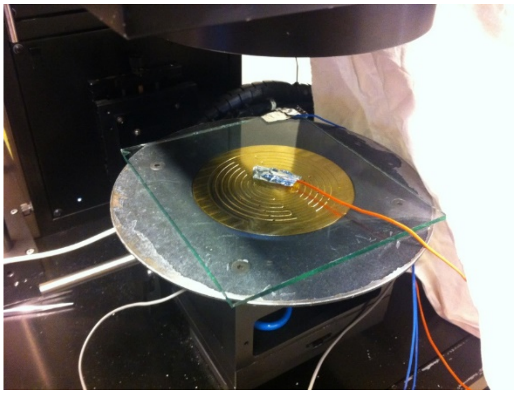

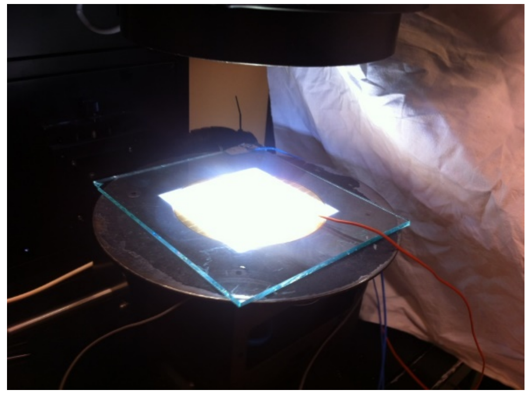

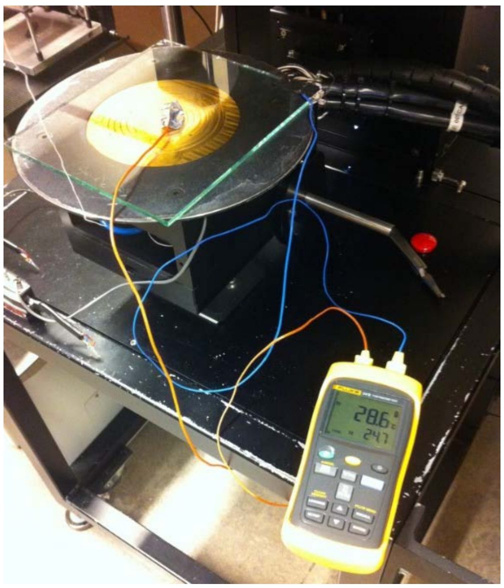

Figure 4.15. 4th Set-up.

4.4.6. 5th Set-up

This experimental set-up is a repetition of the previous with the difference that the cooling plate on the bottom of the glass sample is turned off. This way the temperature in the middle part of the pane is rising a a temperature difference is crated between the center and the edges. The results are presented below.

Solar simulator:	«Super Solar Simulator»
Glass sample:	6mm thickness, 17x17cm
Shading method:	Edges not exposed to solar radiation remain in
Temp. Measurement:	room temperature
Temperature difference	Thermo-couples
long glass thickness:	Cooling plate 25oC: OFF

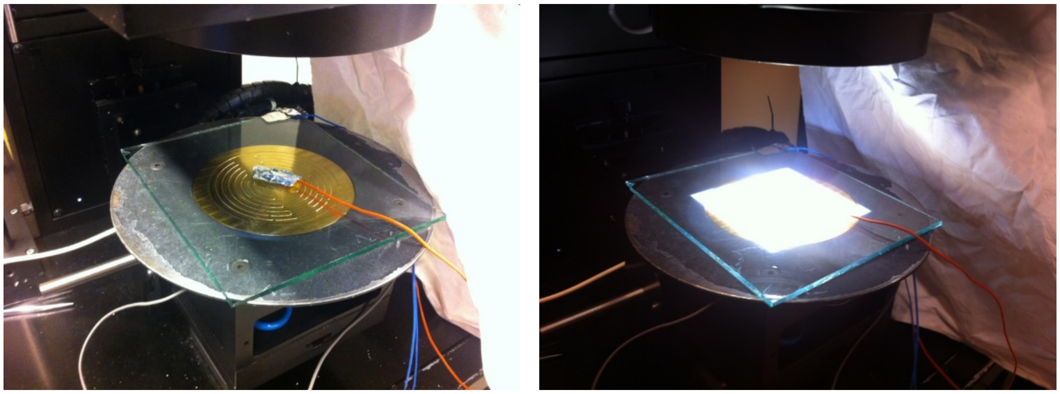

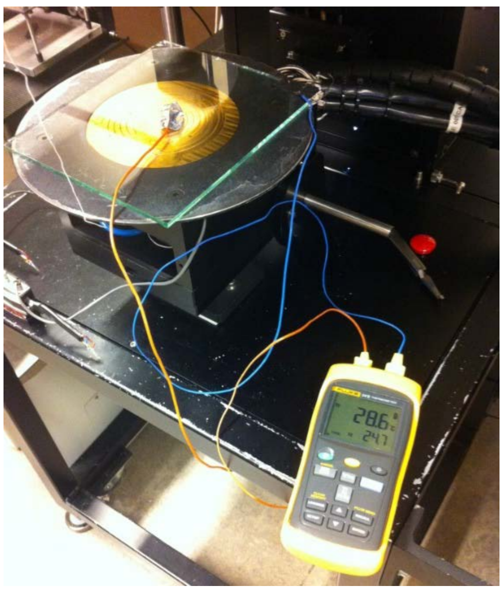

Figure 4.16. 5th Set-up.

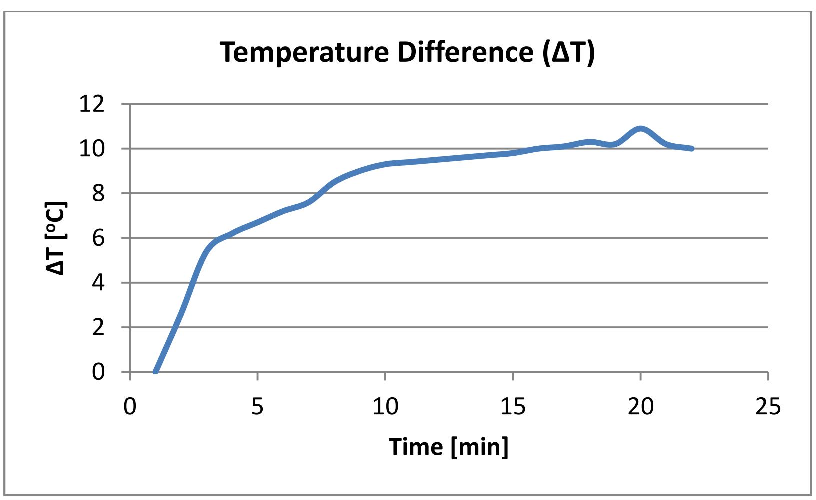

Figure 4.17. 5th Set-up - Temperature difference diagram.

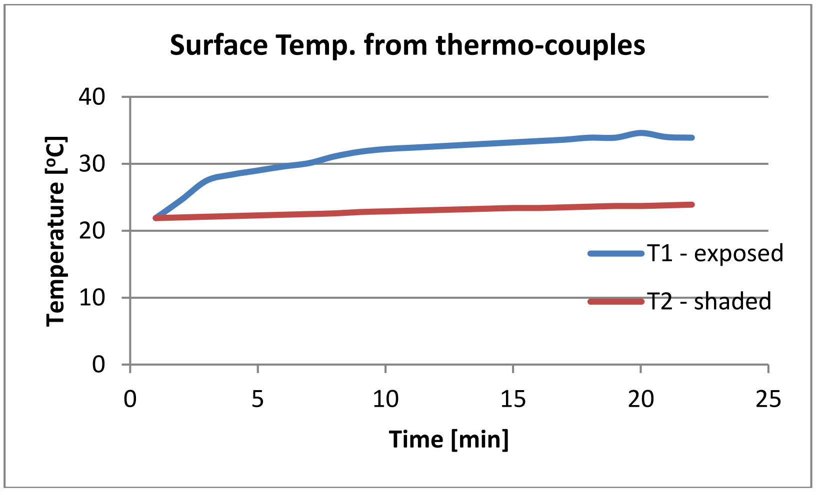

Figure 4.18. 5th Set-up - Surface temperature diagram.

4.4.7. 6th Set-up

For next experiment, a high small, bright beam of intense irradiation is used to test the resistance of a small clear glass specimen to extreme temperature differences. The specimen remained intact even though the radiation intercity this time way stronger than the sun's used in previous experiments (1000W/m^2).

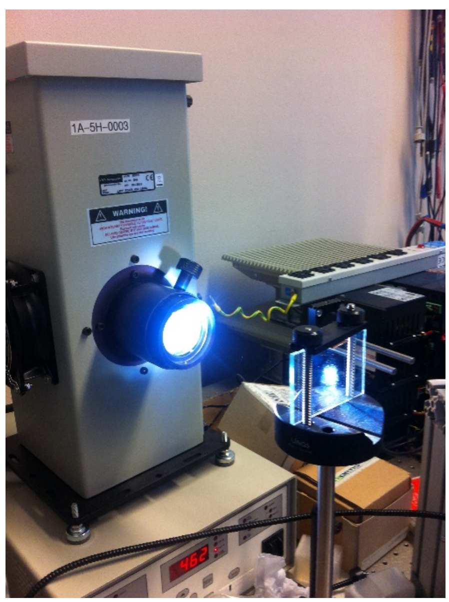

Figure 4.19. 6th Set-up.

Solar simulator:	Research Arc Lamp
Glass sample:	6mm thickness, 5x5cm
Shading method:	Edges not exposed to solar radiation remain in room temperature

4.4.8. 7th Set-up

The coated glass sample with the high solar energy absorption, whose technical characteristics you can see on the table, gave the maximum temperature differences. Tinted and spectrally selective glasses absorb solar radiation and heat up. This makes them more susceptible than clear glass in thermal breakage (PPG Glass Education Center n.d.). Except of the dark coating, the dark cover on its back and the insulation frame contribute to the development of very high temperatures in the middle. That is explained on the parameters of influence for thermal breakage.

Table 4.1. Glass sample for 7th set-up **(Guardian, product Solar Silver 08).**

Colour	Visible light				Solar energy			Solar factor (g) [%]	Shad. coeff.	Uvalue	Selectivity
	Trans-mission [%]	Reflection outside [%]	Reflection inside [%]	Colour Rendering index	Direct Transmission [%]	Reflection outside [%]	Absorption [%]				
Silver	8	43	31	99	6	35	59	9	0.11	1.1	0.89

Figure 4.20. Preparation of glass sample - 7th set-up.

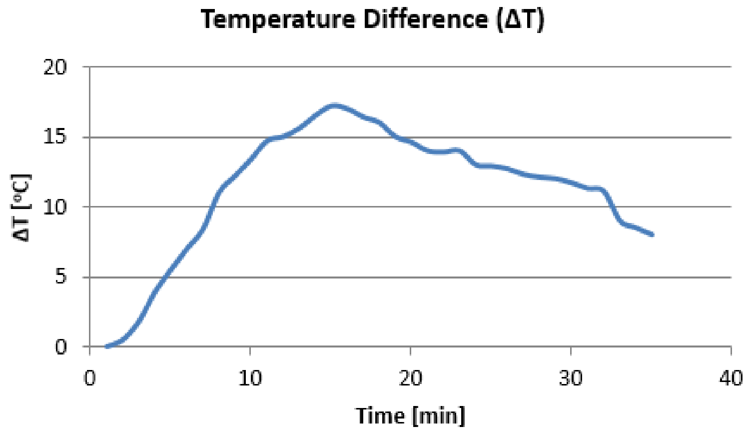

Figure 4.21. 7th Set-up - Temperature difference diagram.

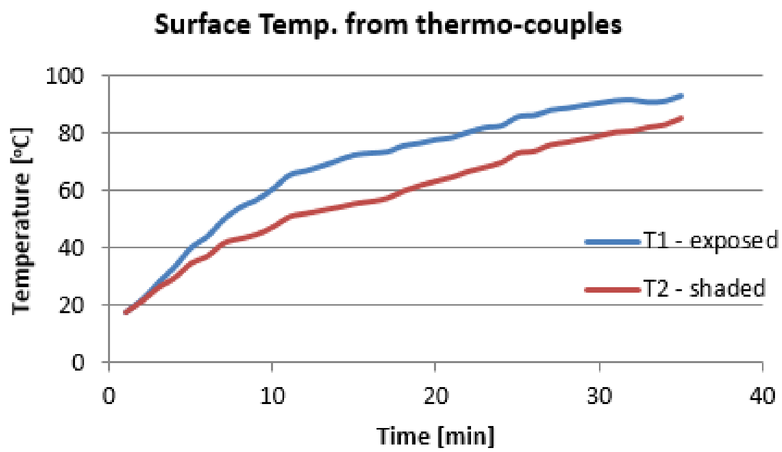

Figure 4.22. 7th Set-up - Surface temperature diagram.

4.4.9. High energy release test Set-up

The experiment presented in this paragraph has been conducted in the context of the PhD research of Dr. ir. Marc Vandebroek, entitled "*Thermal fracture of glass*". The glass specimen does fail using radiation. The type of breakage in this experiment is a high energy release thermal breakage *(q.v. paragraph 3.3)*.

The experiment describes allow for better understanding of the differences between the two types of thermal breakage.

Solar simulator:	Infrared heaters
Shading method:	Fire resistant insulation
Glass sample:	50x50cm

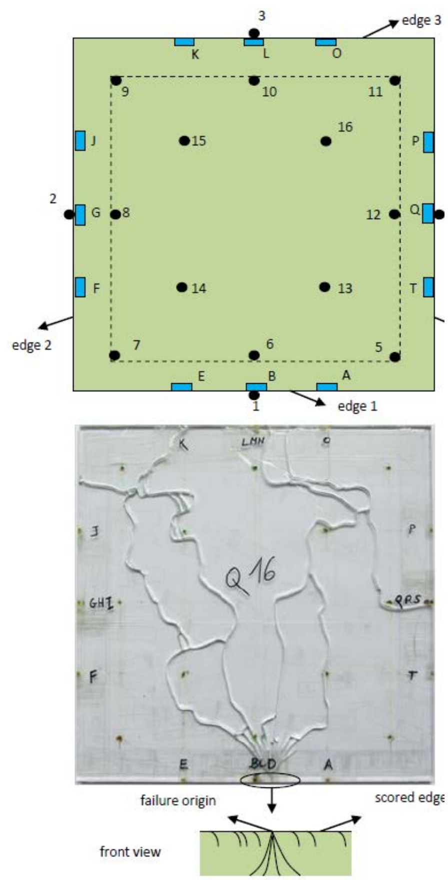

Figure 4.23. Temperature test set-up plan view (above), image of glass pane after failure, failure origin (below) **(Vandebroek 2015)**.

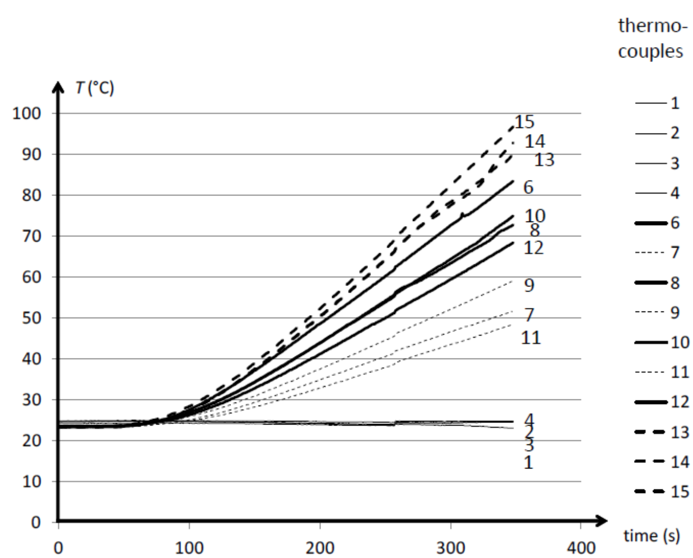

Figure 4.24. Temperature curves **(Vandebroek 2015)**.

As illustrated in the diagram of *Figure 4.24*, the glass breaks after almost 6 minutes following the illustrated pattern (*Figure 4.23*). The recorded temperature difference on the moment of failure was around 73 degrees Celsius with tensile stresses of 38 MPa at fracture moment.

What creates the *high* energy release thermal fracture is the radiation intensity. Five infrared heaters were used, each of them radiating with 500W. This is 7500 W/m², which means 7.5 times more than the maximum incident solar radiation on earth.

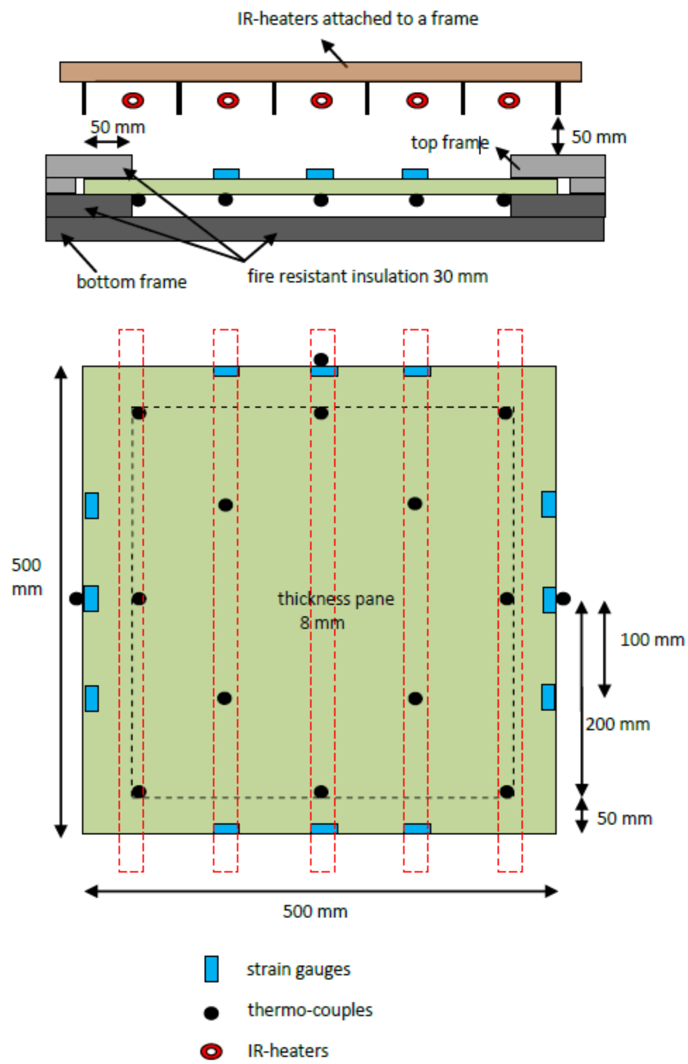

Figure 4.25. Temperature test set-up, vertical view (above) and plan view (below) **(Vandebroek 2015).**

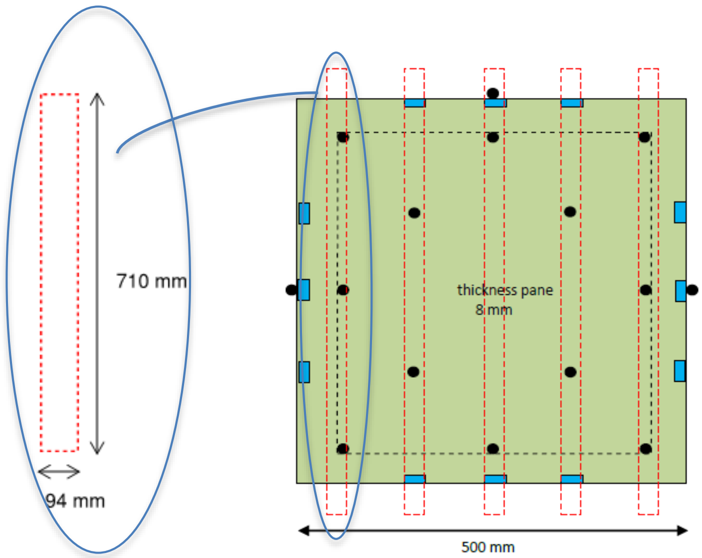

Figure 4.27. Infrared heaters geometrical characteristic
(Vandebroek 2015).

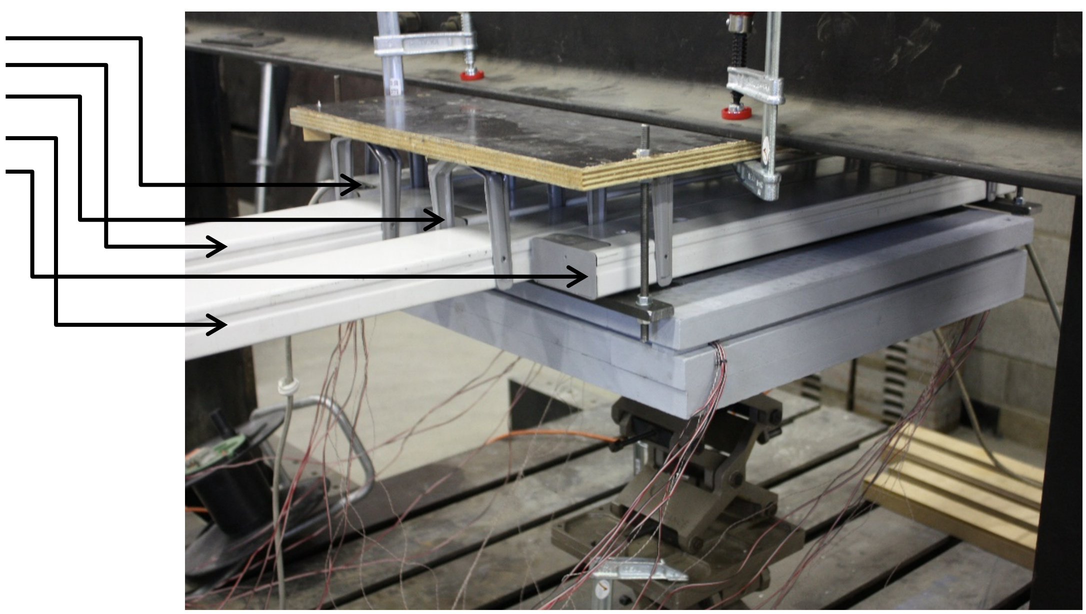

Figure 4.26. Set-up of high energy release experiment **(Vandebroek 2015)**.

Five (5) Infrared heaters

Electric heating: 500 W

$$\frac{500}{0.71 * 0.094} \cong 7500\,\frac{W}{m^2}$$

Total incidence radiation: 7500 W/m^2

Furthermore, an excellent performance insulation material in combination with large dimensions, which allow for a slower distribution of stresses along the whole specimen, make this thermal breakage high energy release.

The dimensions of the pane are important because in a smaller glass sample the temperature becomes quickly uniform –and so do for the stresses- because of conduction.

4.4.10. Comments on results

In order to justify the glass behavior and understand why it remains intact during these experiments, a spectrophotometer is used to measure the absolute reflectance and light transmittance of the samples *(paragraph 4.3.5)*. The diagram illustrated in *Figure 4.29* is a light transmission – wavelength diagram that compares the "clarity" of three clear float glass products (Guardian glass). As the name suggests, clear float glass is transparent, offering high visible light transmittance (VLT). If we compare this diagram with the one resulted from the spectrophotometer test for our tested specimens *(Figure 4.28)*, we come to the conclusion that the glass used in set-ups 1 to 6 was very "clear" (the percentage of the incident radiation transmitted way more than the radiation absorbed). This explains why the temperature difference did not exceed 20°C. •When sunrays reaching a stained glass window occurs reflection, absorption and transmission. Radiation absorbed in the glass caused the temperature of the glass to rise.

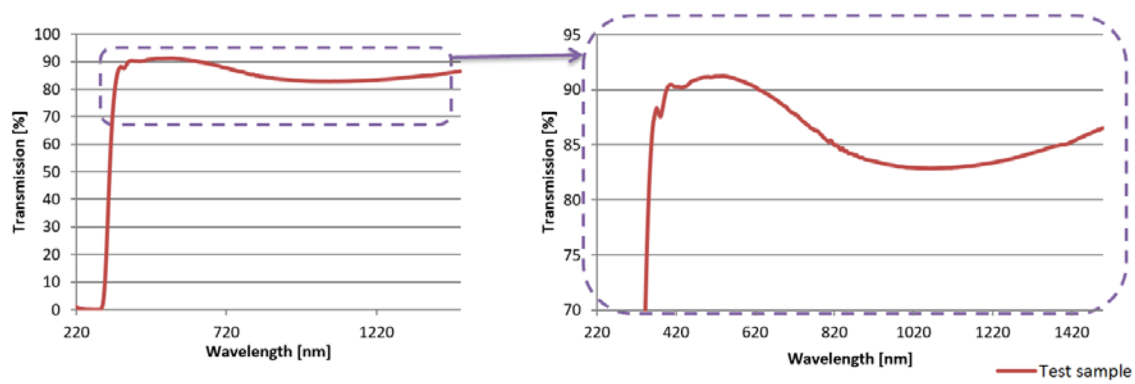

Figure 4.28. Transmission – wavelength diagram, spectrophotometer test

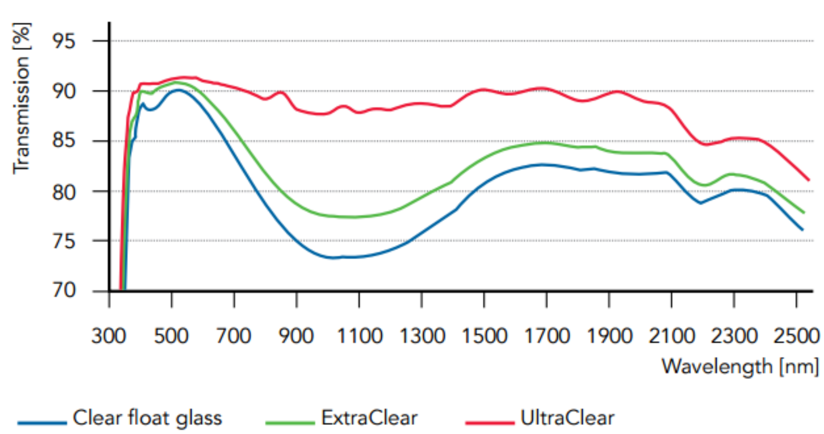

Figure 4.29. Transmission – wavelength diagram **(Guardian).**

The largest temperature difference by radiating with 1000W/m^2 on an annealed glass pane was recorded 17.3^{o}C. This was achieved with the dark coating on a glass spacimen with 59% absorption value.

5. Investigation on Numerical Analysis

5.1. Introduction

With the numerical analysis presented in the hereby chapter we can have a better understanding on the temperature gradients developed in different façade configurations, with more parameters taken into account, like the time of day, that is difficult to simulate on an experimental basis. Many case studies have been collected considering different glass typologies and design solutions. Comparison and validation against each other provides us with a better insight on the effects of parameters of influence and the seasons of the year. Numerical analyses and their findings are going to be described in this chapter, as well as summaries of conclusions.

5.2. Software

The company Physibel has some programs where climate functions and solar radiation can be calculated.

5.2.1. Bisco

Bisco is a thermal analysis program for stationary heat transfer in two dimensional models. Different materials can be assigned, represented with different colors in the simplified bitmap used as an input. Boundary conditions can be set. Bisco associates the materials assigned to the input geometry with their properties. Assigning material the correct properties is very important because the effect of solar radiation depends on a material reflection, transmission etc. The input geometry should be drawn in AutoCad before loading to Bisco through BiscoDxf.

5.2.2. Bistra

Bistra is another Physibel thermal analysis software or transient heat transfer in two dimensions. It is an extension to the time-dependent conditions of the stationary Bisco program. At each time step, the temperature dependent properties are recalculated with a finite element difference method. Most of the numerical simulations are performed with Bistra because of the built-in solar processor and the variable ambient conditions that can approximate reality. Bisco is only used to simplify the geometry of the window models and as a result reduce the calculation time of the models in Bistra. Bistra sees the actual model as an extruded version of the input of Bisco (VandenPoel 2010).

5.2.3. Voltra

Voltra is the three-dimensional equivalent program to Bistra. They both allow for non-stationary heat transfer, while Bisco is only suitable for steady-state heat transfer.

5.2.4. Abaqus

Abaqus is a finite element analysis software that does not allow modeling of variable solar radiation, but is used to convert these data into stresses on the material.

5.3. Single skin façade

In order to investigate the temperature gradients with some transient finite element program, we can start with a single skin façade configuration analyzed in previous studies. VandenPoel 2010, Feryn 2012 and Balcaen 2013 use the model described below *(Figure 5.1)* to investigate with numerical modeling various parameters of influence and behaviour of the glass.

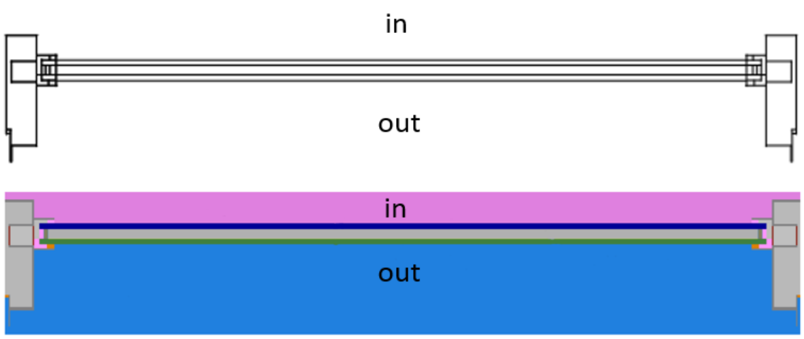

Figure 5.1. (a) Bitmap & (b) BISTRA image of single skin façade
(VandenPoel 2010).

The window examined consists of a double glazing unit (DGU). The boundary conditions at the edges of the model are considered adiabatic: no heat transfer occurs. The simplification of the horizontal section is shown in *Figure 5.2*. The total heat flux from this section is: Q = 39,695 W/m.

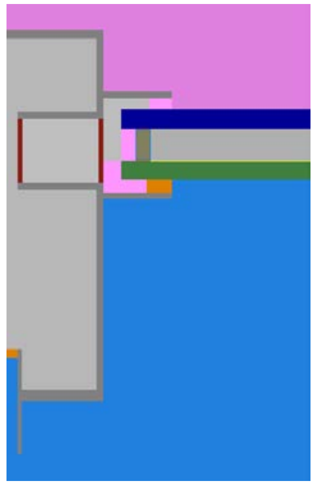

Figure 5.2. Detail of simplified horizontal section of the single skin **(VandenPoel 2010)**.

Climatic conditions

In order to make use of the solar processor of Bistra, the input of horizontal global solar radiation and horizontal diffuse solar radiation are necessary.

5.3.1. French standard climatic data input:

This single skin façade set-up was examined with different climatic data as an input. In the research of VandenPoel 2010, because of the availability of climatic data and the fact that the French standard (NF) are the most widespread method to evaluate thermal fracture, French climatic conditions were used. Because of the large peak value the global solar radiation there, the South facing façade was used.
The input date are summarized below:

Input data	
Indoor temperature:	20 °C
Outside:	max +10 °C, min 10°C
Diffuse solar radiation:	up to 100 W/m^2
Global solar radiation:	1078 max W/m^2
Facade orientation:	South
Calculation	May 1
Geographical position:	Paris (Latitude 48^o 51 ’N Longitude 2^o 21 ’E)

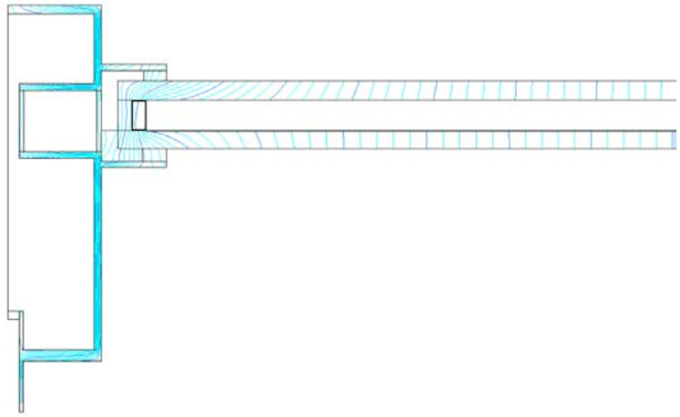

Figure 5.3. Heat flow on the left part of the façade **(VandenPoel 2010)**.

In *Figure 5.3* the heat isocurves reveal the locations of conductive elements (e.g. spacers). Heat flow isocurves in the location of the spacer are closer together than in the central portion and this is because a spacer at the location of the glass edges is a conductive element, while the middle zone the double glazing insulating effect.

The figures below illustrate the minimum and maximum temperatures and the temperature differences of the inner and outer glass plate for a duration of a full day. In the temperature diagrams for the inner and outer pane, we can see that the temperature difference between the center and the edges of the inner panel does not exceed 15°C, and for the outer pane the maximum difference is almost 23°C. At 10:00 and 16:00 we can observe picks on the ΔT curve.

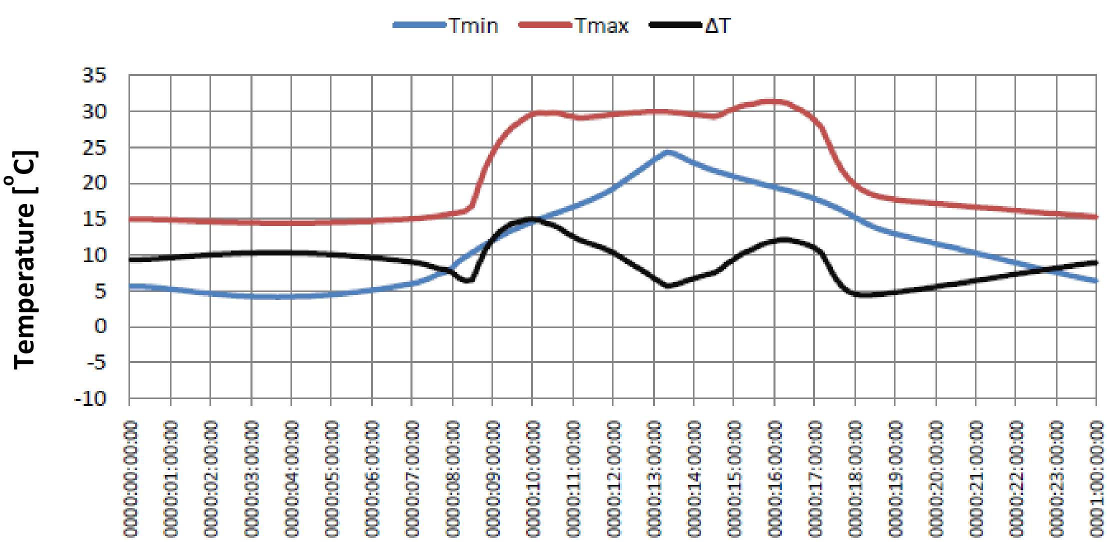

Figure 5.4. Temperature differences for single-skin facade inner panel (VandenPoel 2010).

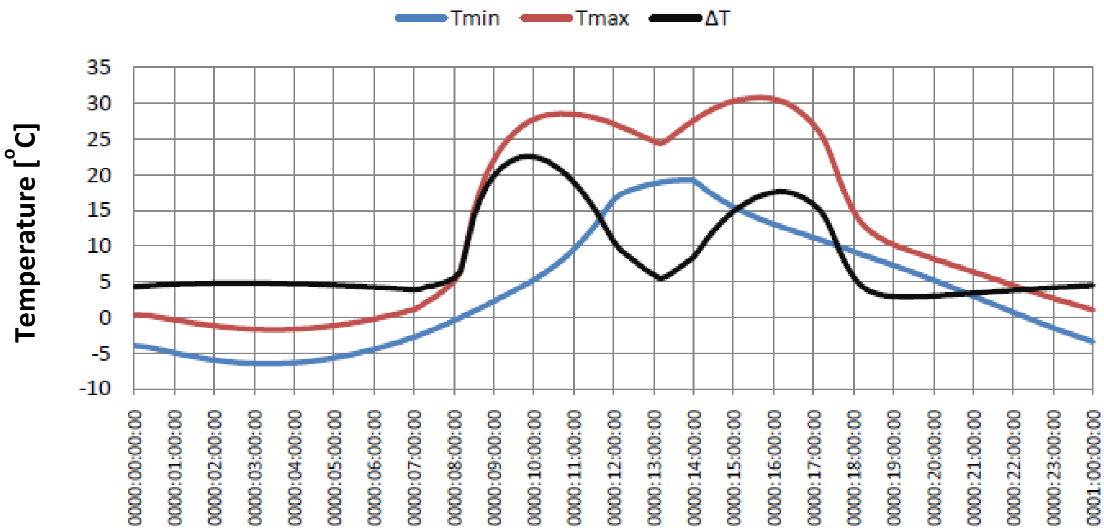

Figure 5.5. Temperature differences for single-skin facade outer panel (VandenPoel 2010).

In *Figure 5.6* and *Figure 5.7* we can see the temperature gradient of the single skin at the two hours with the digger temperature differences, during a spring day with outside temperature at 10ºC. The left side is warmer than the right because of the sun's position. Therefore, the tension in the right edge is smaller than the left and a compressive stress is developed on the left edge. Press tensions, however, do not pose a risk against thermal breakage, since the compressive strength of glass is much greater than its tensile strength.

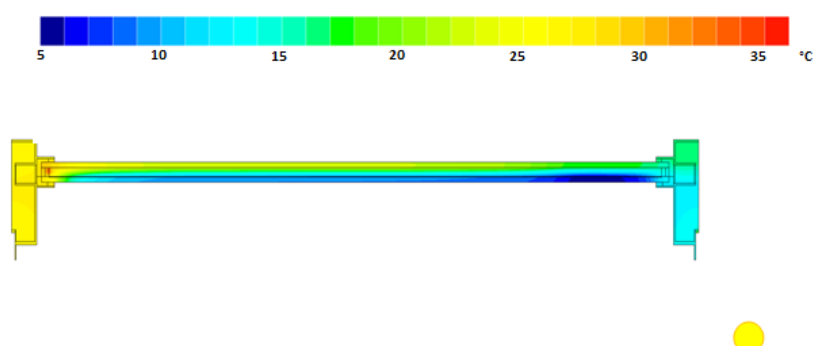

Figure 5.6. Temperature gradient of single skin façade at 10:00 **(VandenPoel 2010)**.

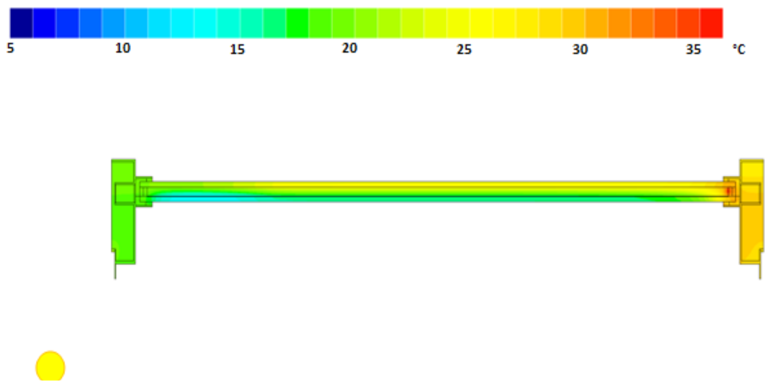

Figure 5.7. Temperature gradient of single skin façade at 16:00 **(VandenPoel 2010)**.

Table 5.1. Maximum temperature differences single-skin facade 10am **(VandenPoel 2010)**.

	Tmin (°C)	Tmax (°C)	ΔT (°C)
Inner pane	5.27	27.77	22.50
Outer pane	14.62	29.60	14.98

According to the analysis of (Feryn 2012), a glass plate fully irradiated with a symmetrical radiation source gives a maximum temperature difference on the glass that is equal to 15 ° C. This is a realistic ΔT value for glazing in buildings verified by my experiments. *Figure 5.8* illustrates this temperature difference for a single skin façade for four different element sizes in Abaqus. As in the same study the influence of the element size in tension results was also investigated, the diagram in *Figure 5.9* shows this influence. The stress is decreasing as the element size in the temperature model increases.

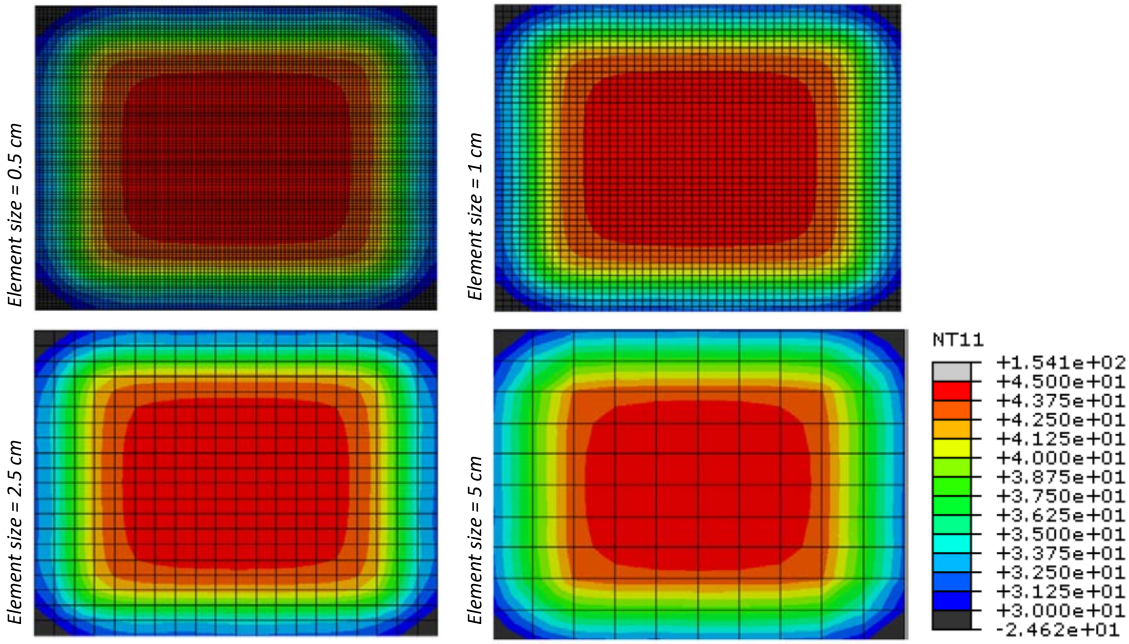

Figure 5.8. Temperature results in fully, symmetrically irradiated pane **(Feryn 2012)**.

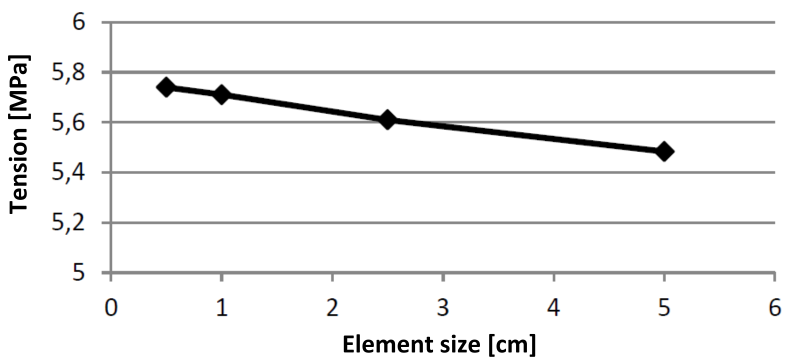

Figure 5.9. Influence of element size on tension results **(Feryn 2012)**.

The peak hours within the day as regard to temperature differences on the glass are confirmed also by the study of (Feryn 2012). In the following figures we can observe that in a diagram of tensions, since the bigger the temperature difference, the greater the tension developed. Furthermore, the diagrams this tension is compared with kt*E*a*DT, the allowable tension according to the French regulations. It becomes obvious that calculated thermal stresses are even in the most critical situations lower than the ones predicted by the French standard.

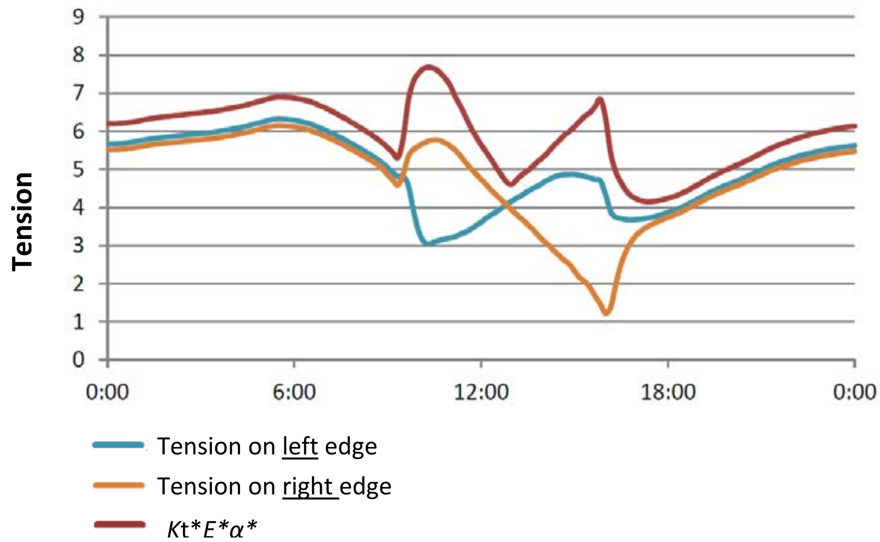

Figure 5.10. Tension in inner pane **(Feryn 2012)**.

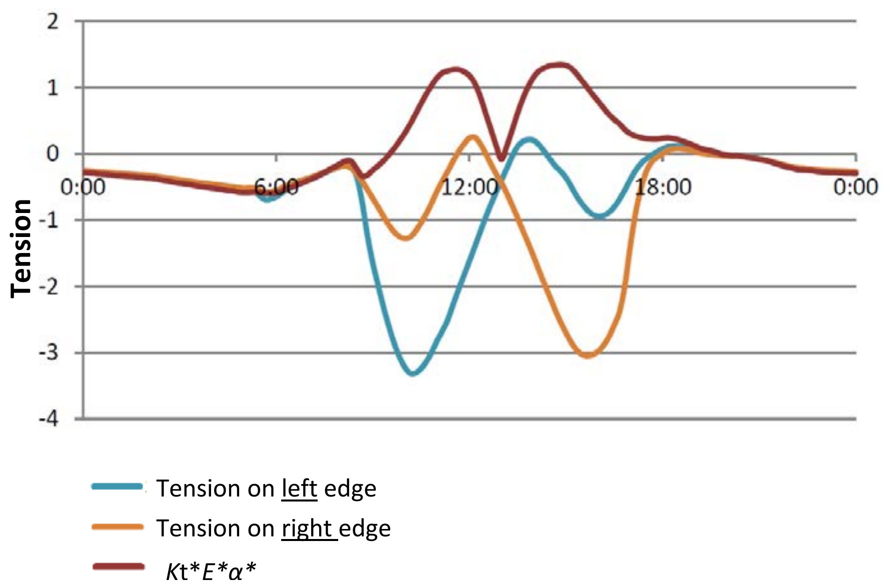

Figure 5.11. Tension in outer pane **(Feryn 2012)**.

Table 5.1 referred to the temperatures and temperature differences of the single skin on a typical spring day. In the following *Table 5.2* and *Table 5.3* we can see for the same window configuration the maximum temperature differences and maximum stresses developed per season. An important observation is that the temperature difference ΔT in the inner pane as almost throughout the year, higher than the outer pane.

Table 5.2. Inner pane max. ΔT and max. stress per season **(Feryn 2012)**.

	Spring	Summer	Autumn	Winter
max. ΔT [°C]	2.39	6.25	9.41	13.55
max. stress [MPa]	1.24	2.95	4.63	6.32

Table 5.3. . Outer pane max. ΔT and max. stress per season **(Feryn 2012)**.

	Spring	Summer	Autumn	Winter
max. ΔT [°C]	2.37	3.15	2.27	-0.3
max. stress [MPa]	0.25	0.09	-0.62	-0.78

5.4. Double skin façade

The double skin facade under consideration consists of a double glazing on the inside, a single glass plate on the outside and a cavity between them. It is interesting to note the position of the minimum and maximum temperatures through the day for the inside and outside pane are the same as these on a single glazing window.

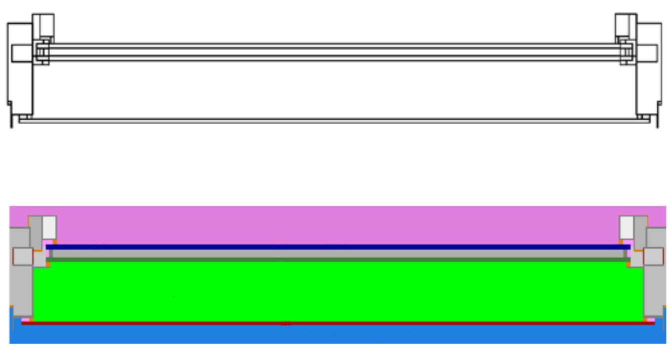

Figure 5.12. (a) Bitmap & (b) BISTRA image of double skin façade **(VandenPoel 2010)**.

The graphs below show the minimum and maximum temperature and the temperature difference function of time for the inner, the middle and the outer glass plate of the double skin facade. From the graphs it follows that the largest temperature difference in the outer and middle panel almost equal and occur at the same time (10am). At this moment the sun in the southeast.

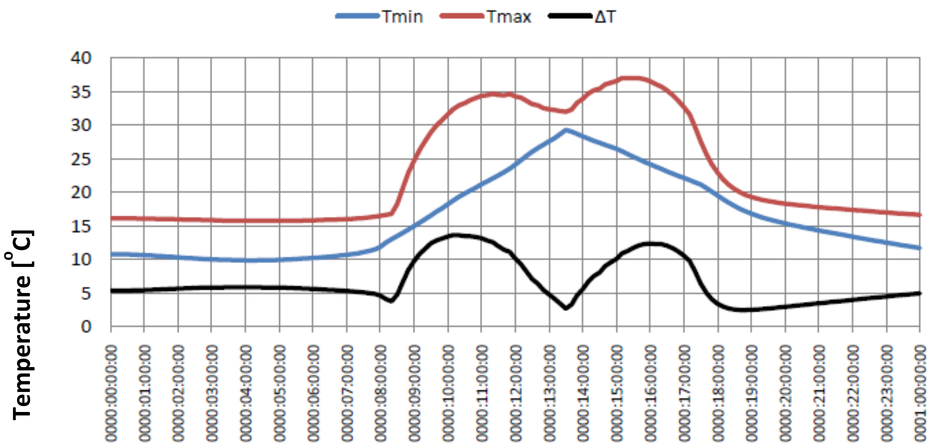

Figure 5.14. Temperature differences for double-skin facade inner panel **(VandenPoel 2010)**.

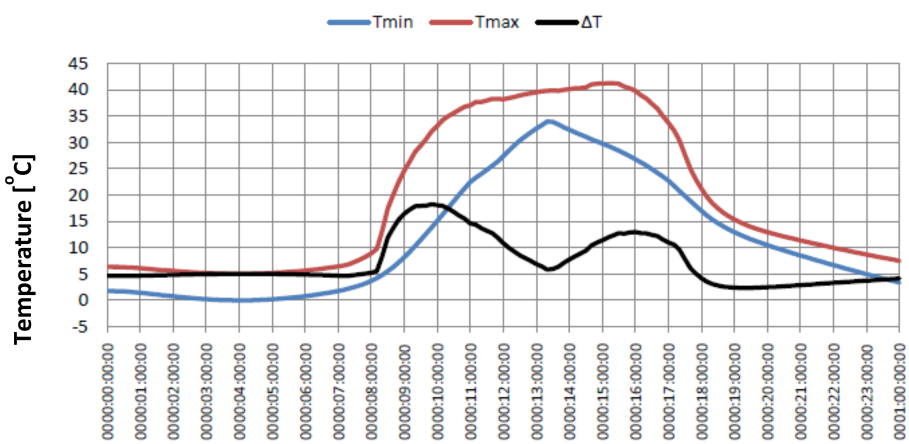

Figure 5.15. Temperature differences for double-skin facade middle panel **(VandenPoel 2010)**.

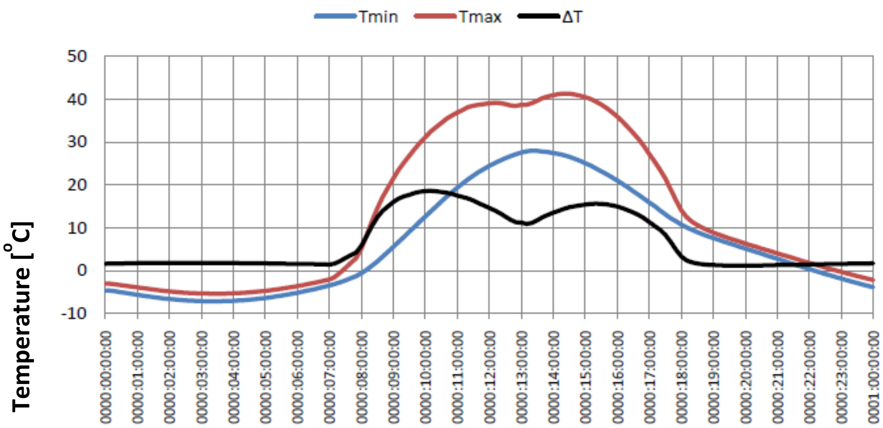

Figure 5.16. Temperature differences for double-skin facade outer panel.

The temperature gradient at 10am when we have the largest temperature difference is shown below, where a comparison with the single and double skin facade is displayed.

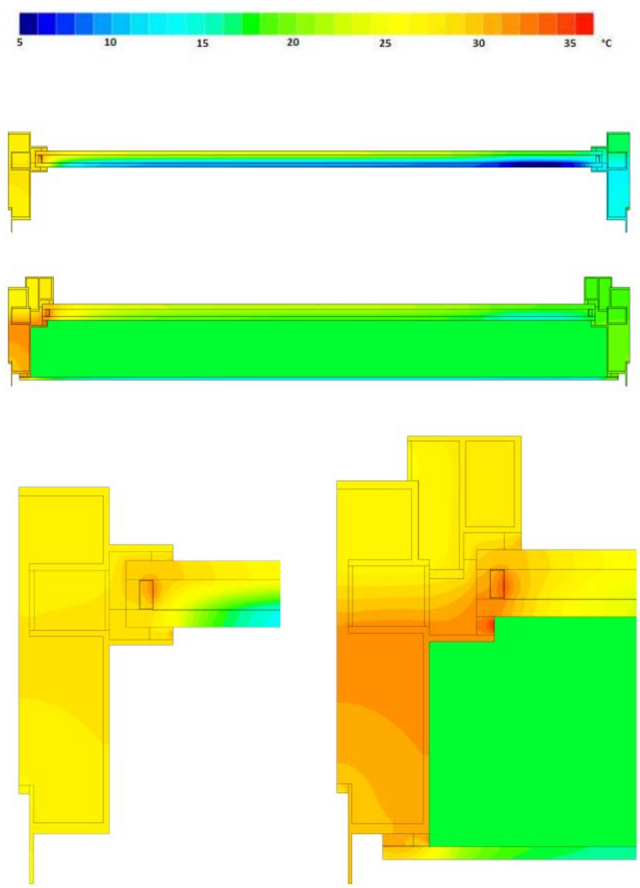

Figure 5.17. Temperature gradient at the maximum temperature differences (10pm) for single and double-skin façade **(VandenPoel 2010)**.

The values of the maximum temperature differences in all the sheets of glass are summarized in the following tables:

Table 5.4. Maximum temperature differences double-skin facade 10am **(VandenPoel 2010)**.

	Tmin (°C)	Tmax (°C)	ΔT (°C)
Inner pane	18.21	31.62	13.41
Middle pane	15.08	33.14	18.06
Outer pane	12.63	31.18	18.55

The same double skin configuration was analyzed by (Feryn 2012) and the middle glass pane was proven to develop larger temperature differences. In *Figure 5.18* the tension diagram for the middle, most critical pane is illustrated and compared to the allowable stresses according to the French standard. The middle glass pane, which is the exterior of the double glazing unit, experiences a maximum temperature difference of 11,22°C during autumn which results in a thermal stress of *5,11 MPa*.

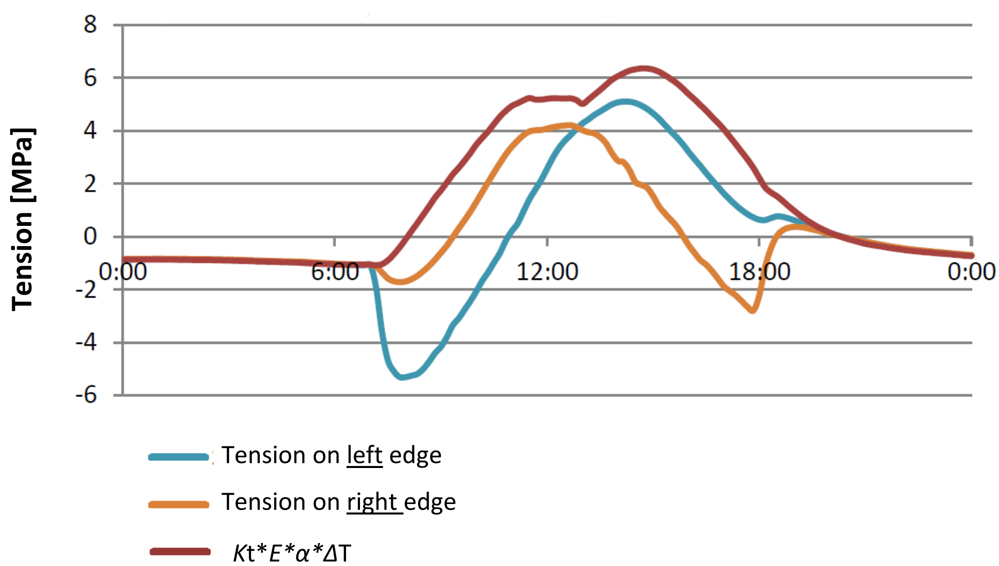

Figure 5.18. Tension in middle pane **(Feryn 2012)**.

The numerical investigation in the context of a research for the impact of climatic stress in glass facades (Vansteenbrugge 2012) supports the previous claim that the middle glass pane d a double skin façade is the most critical one against thermal stress fracture. Selectively, the maximum stresses for the left and right edge per season for the middle glass are presented in the following table.

Table 5.5. Stresses according to the NF for the middle panel **(Vansteenbrugge 2012)**.

Spring	**σ_{max} (MPa)**	**time**
right edge	2.727	14h40
left edge	1.908	12h10
Summer		
right edge	2.432	14h10
left edge	1.799	12h30
Autumn		
right edge	3.329	14h20
left edge	2.381	12h10
Winter		
right edge	2.259	15h
left edge	1.165	12h

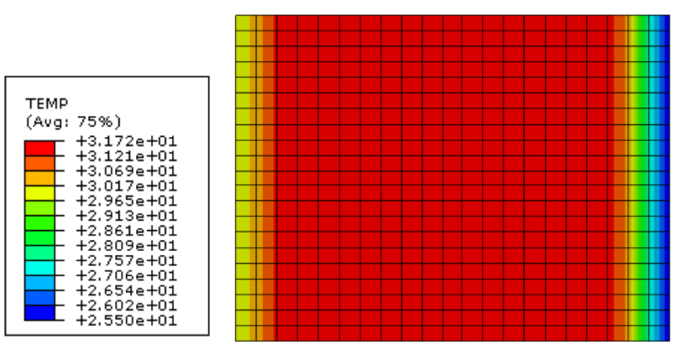

Figure 5.19.Temperature development in the middle glass panel during the typical winter day at 15:10 [°C] (Vansteenbrugge 2012).

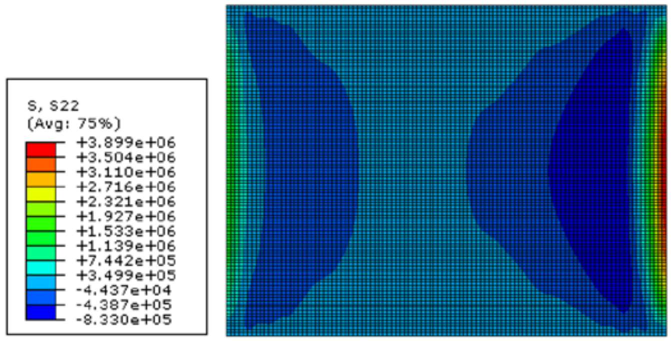

Figure 5.20. Stress plot of the middle glass panel during the typical winter day at 15:10 [N/m²=10⁶MPa] **(Vansteenbrugge 2012).**

For the same, middle pane of the double skin façade, the research also allow for a comparison between 2D and 3D plotted geometries. *Table 5.6* summarizes the maximum stress per season for these two periods.

Table 5.6. Maximum stresses for 2D and 2D analysis **(Vansteenbrugge 2012).**

	2D		**3D**	
	σ_{max} (MPa)	**time**	**σ_{max} (MPa)**	**time**
Spring	2.727	14h40	1.978	15h
Summer	2.432	14h10	2.422	14h20
Autumn	3.329	14h20	2.634	15h
Winter	2.259	15h	1.298	16h

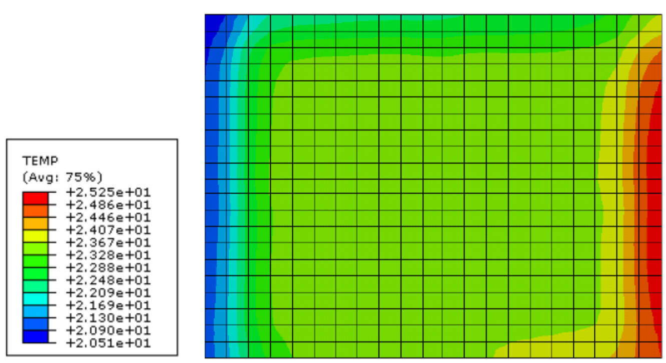

Figure 5.21. Temperature development in the middle glass panel during the typical winter day at 15:10 [oC] in 3D **(Vansteenbrugge 2012).**

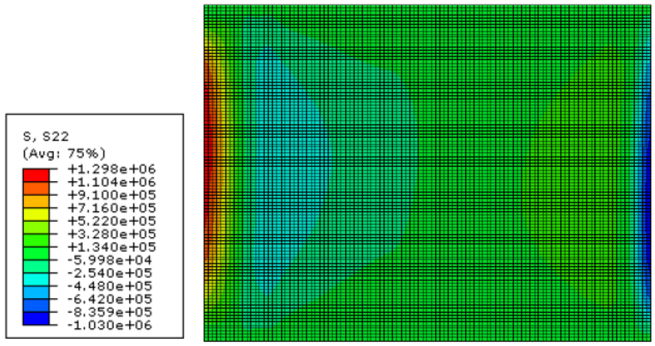

Figure 5.22. Stress plot of the middle glass panel during the typical winter day at 15:10 [N/m2=106MPa] **(Vansteenbrugge 2012).**

For the same double skin configuration Balcaen 2013 provides a table with the maximum stresses throughout the year, for the righe and left edge of the glass (*Figure 5.23*).We can confirm that the most crucial period of the year is autumn, and this time the maximum measures stress was registered: *6.86 MPa*.

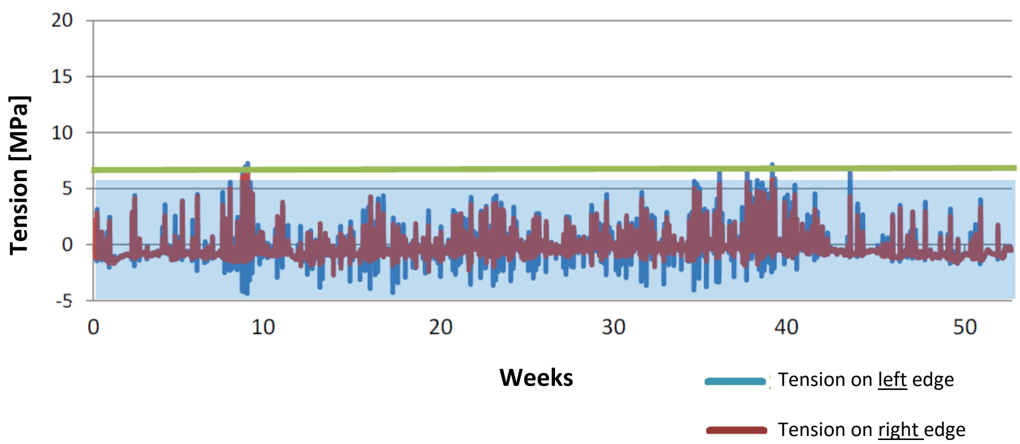

Figure 5.23. Tension results throughout the year **(Balcaen 2013)**.

From the sun's position at the time of maximum thermal stresses. It is obvious that there will be a considerable temperature difference across a distance of only a few cm so the temperature gradient is high.

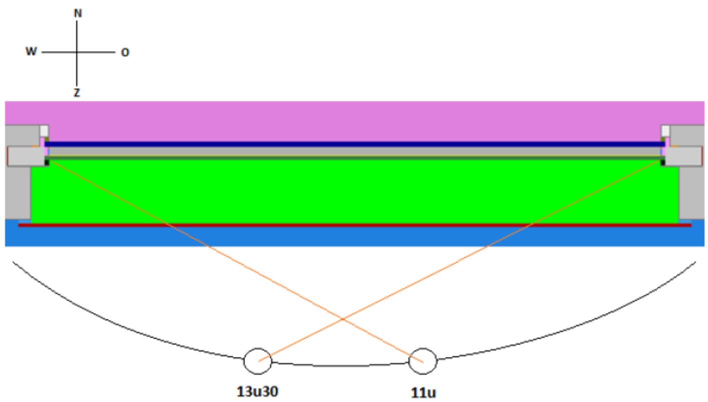

Figure 5.24. Sun position at the hours of the maximum thermal stresses **(VandenPoel 2010).**

Figure 5.7 indicated similar temperatures in the two edges of the single skin window of the façade (VandenPoel 2010). On the other hand *Figure 5.23* (Balcaen 2013) indicates that stress peaks in the left edge are typically larger than in the right edge. This is the result of the orbit of the sun: when southeastern the right edge is shaded, while the left and the middle part of the glass are exposed to sun radiation. When the sun moves so that the left edge is shaded, the center of the glass sheet is already heated by the sun. This will make the temperature difference betweent the center and the left edge higher than with the right edge (Balcaen 2013).

5.4.1. Influence of orientation, climatic data and calculation method

In order to define the climate conditions, French standard use as an input a function of temperature, global radiation and diffuse radiation *(q.v. 3.6.2 French standard)*. In order to compare stress results that result from NF to actual climatic date from Uccle, the input horizontal global a diffuse solar radiation were used:

Table 5.7. Horizontal global radiation and diffuse radiation from Uccle **(Balcaen 2013)**.

Season	**Hor. Global radiation [W/m²]**	**Diffuse radiation [W/m²]**
Spring	653.9	100

Summer	921.5	137.5
Autumn	677.4	100
Winter	266.2	62.5

The following table summarizes the different stress values resulting from calculation with different methods (Abaqus and NF -Norme Francaise) and different climate data as input (Uccle, NF).

According to (Balcaen 2013), façade orientation also has an influence on the maximum stresses developed on the window glass panes. The following table indicated these stresses for East and West orientation, in addition to the South we had so far. When the bitmap is modified to an East orientation and West orientation, the maximum stress peaks reveal that the South orientation is the most critical one.

Table 5.8. Comparison of stress values for different calculation methods and input climatic data for different orientations.

Orientation	**Acting ΔT [°C]**	**Calculation method**	*Bistra - Abaqus*	*NF*	*Bistra - Abaqus*
		Input climatic data	*Uccle*	*NF*	*NF*
			max.stress [MPa]		
South	13.61		11.91	7.94	7.01
East	11.69		10.12	6.82	6.28
West	15.21		10.35	8.87	7.32

*NF = Norme Francaise
** Values for *Table 5.8* obtained by (Balcaen 2013)

According to the table above, the climatic data from French standard are less strict than climatic data using real climatic data (Uccle) by 26.7%. The safest –or more conservative- method of accessing thermal breakage is with Bistra – Abaqus method, using Uccle climatic data.

In addition, the NF calculation method is more strict than the Bistra-Abaqus numerical investigation, since the acting stresses seem to be higher. Based on the table above, Bistra-Abaqus calculation method underestimates the acting temperature stresses by 12.4% in comparison to NF, for input climatic data of NF.

An interesting finding as regard the safety of the French standard came as a result of comparison of stresses generated by real climate data as input to those generated with climatic information from French standard. The maximum stresses of 10 years for the middle glass pane based on real climatic data are listed in *Table 5.9* (for autumn) (Vansteenbrugge 2012).

A cumulative distribution function uses a Gumbel maximum distribution to verify the NF in comparison to actual climatic data. The maximum tensile stress in the middle panel in the calculation according to the NF is obtained (3,329 MPa) and is equal to the 70% value in the drawn cumulative distribution. The possibility that stresses from actual climate data are smaller or equal to those given by NF is only 70%. Thus, the method according to the French norm is not as safe as when using actual climatic input, with regard to the thermal stresses (Vansteenbrugge 2012).

Table 5.9. Maximum stresses in middle glass for middle glass pane **(Vansteenbrugge 2012).**

	σ_{max} (MPa)
autumn 2002	3.052
autumn 2003	3.082
autumn 2004	3.206
autumn 2005	3.393
autumn 2006	3.229
autumn 2007	3.053
autumn 2008	3.003
autumn 2009	3.558
autumn 2010	3.164
autumn 2011	3.321

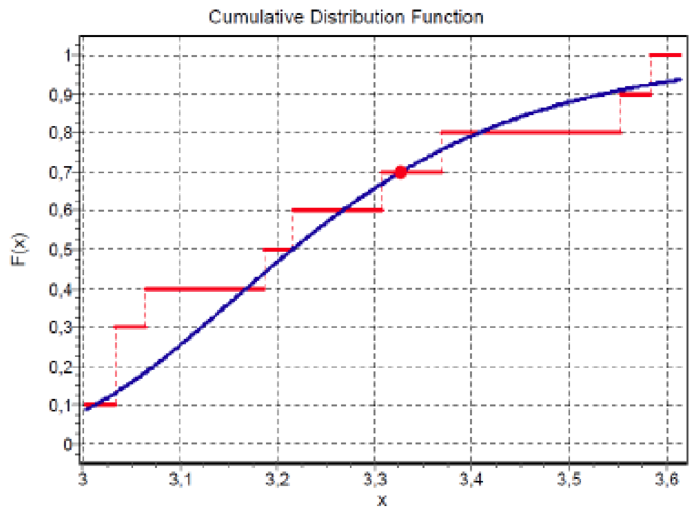

Maximum tensile stresses from calculations based on real climatic data

Maximum tensile stresses according to NF calculations

Figure 5.25. Cumulative distribution function - N.F. and real climatic data **(Vansteenbrugge 2012).**

As part of the numerical investigation of Feryn 2012, a comparison between two calculation mehtods that use as in input NF climatic data, in a base of stresses, is summarized in the following table. This regards the middle glass pane of the fame double skin configuration, in south orientation.

Table 5.10. Comparison of stress values for different calculation methods and input climatic data for different seasons.

Season	**Acting ΔT [°C]**	**Calculation method**	*Bistra - Abaqus*	*NF*
		Input climatic data	*NF*	*NF*
			max.stress [MPa]	
Summer	7.82		3.88	4.34
Autumn	11.22		5.70	6.36

Spring	9.5		4.89	5.39
Winter	8.96		4.36	5.08

*NF = Norme Francaise
** Values for *Table 5.8* obtained by (Feryn 2012)

According to (Feryn 2012), with the same acting temperature for each season, thermal stresses calculated with Bistra-Abaqus method are lower than the ones predicted by French standard. This comparison is done with both calculations using French standard input climatic data.

The difference between the values calculates with numerical methods and the ones resulting from standard is on average 11.5%. In other words, *acting thermal stress values resulting from French standard are on average 11.5% higher than the ones calculated with Bistra-Abaqus method.*

Note: *According to NF, the allowable stress for annealed glass is 20 MPa. Comparing the resulting acting thermal stress values with this, these is no risk against thermal breakage for any situation and annealed glass can be used.*

It is important to point out that these results concern the case study described in the beginning of the paragraph. The application of blind, increase of the window depth and other factors mentioned in … do increase the resulting stresses significantly.

As an example of that, according to (Balcaen 2013), *the application of blinds in a south oriented, double skin window can increase tensile thermal stresses to 28.97 MPa.*

5.5. Chapter highlights

If we combine the information from the analysis mentioned in this chapter, we can conclude that:

The most crucial season of year against thermal fracture is *autumn*.

The most critical glass pane on single skin is the *inner* pane.

The most critical glass pane on double skin, throughout the year: *middle* pane.

The most critical façade orientation: *South*.

Maximum tensile thermal stresses appear between 11h00 and 11h20 for one edge and 13h00 and 14h00 for the other one, depending on the orientation of the window.

The schematic diagram below summarizes the differences in acting thermal stresses per calculation method and input climatic data. The higher thermal stresses are given with real climatic data as input and numerical methods of calculation, then the stresses calculated by French standard are 26.7% lower than these, and finally stresses calculated with numerical methods, with NF input climate data are 11.5% lower than the later:

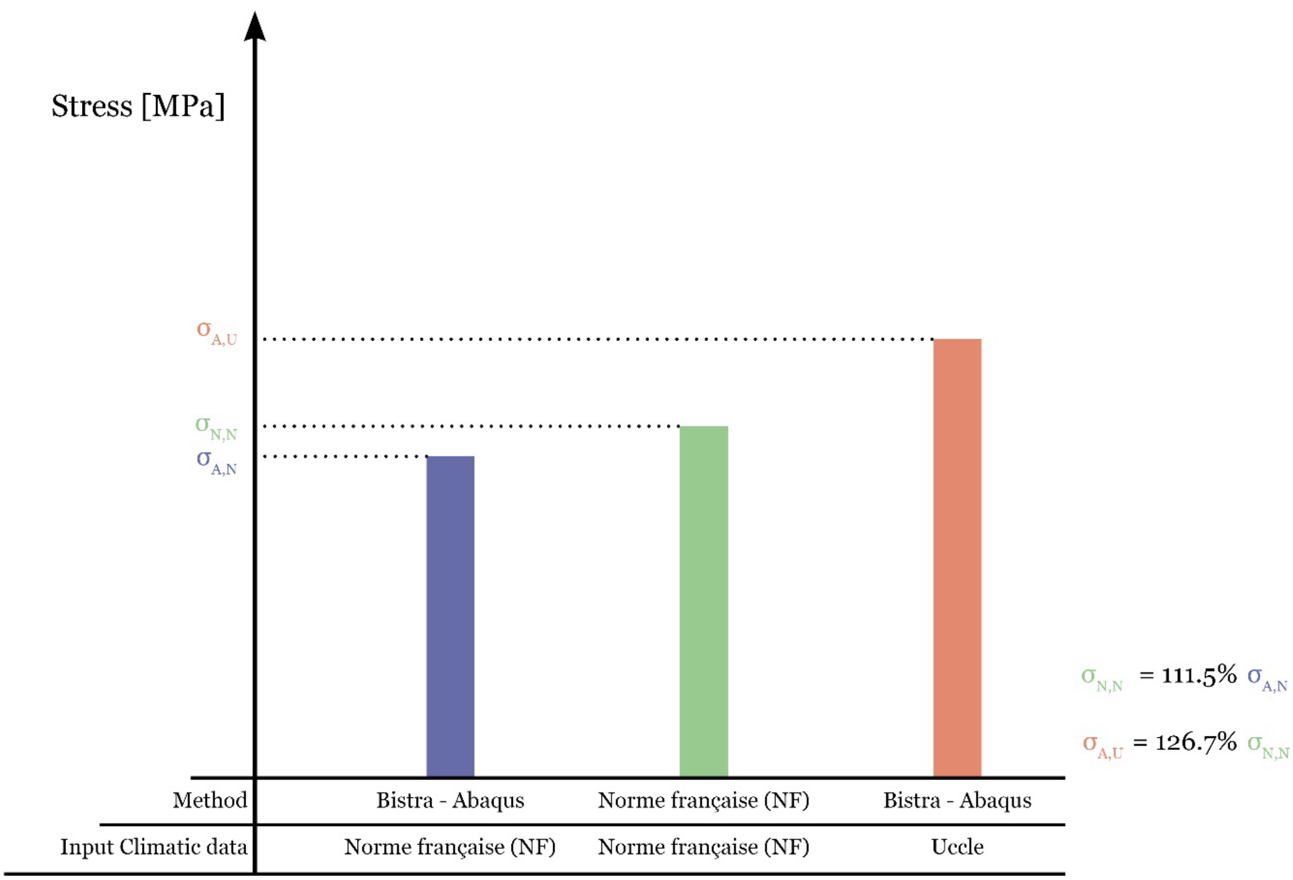

Figure 5.26. Schematic illustration of influence of calculation method and climatic data on stresses **(by author)**.

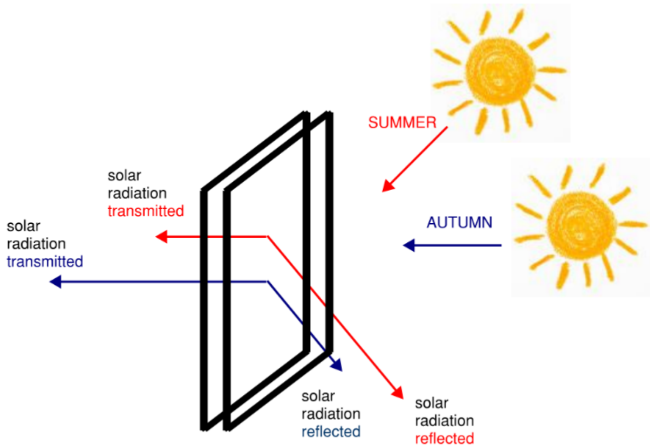

Figure 5.27. Schematic illustration of sun radiation in summer and winter **(by author).**

The temperatures in the glass sheets for the different seasons according to the French standard does not always take the expected proportions. So is the middle glass during *autumn* for example is warmer than during the summer, while both the outdoor temperature and the solar radiation have the largest values in the summer. This phenomenon is probably explained by the fact that the sun position during the autumn is lower than during the summer. This means that the percentage of solar radiation absorbed during the summer is much less that the radiation reflected, while for autumn it is the other way around.

6. Conclusion

6.1. Summary and Result discussion

Thermal breakage of glass occurs as a result of large temperature difference between different areas of the glazing. Under the influence of solar radiation tensile stresses develop that can lead to failure if exceeding a certain value. There are two types of thermal breakage that depend on the magnitude of these stress. Based on the pattern of fracture, a high or low energy release breaking can be recognized.

Current literature on thermal break is not detailed enough and is non-applicable to double skin facades. The deterministic method has limited possibilities to estimate the thermal stresses. Finite element software studies are needed to examine the temperature difference in glass façades and the induced thermal stresses. Thermal actions are simplified in literature and the standards. Only simple façade configurations are taken into account. Fatigue of a glass is not accounted for.

Experiments and numerical methods examined in this thesis indicate no risk against thermal fracture under conditions with no blinds or other incidental shades on a window. Experiments conducted in the context of this research as well as previous numerical investigations, indicate a maximum temperature difference of 15^{o}C on single annealed glass (partially shaded pane in room temperature, subjected to solar radiation). This temperature difference does not lead to breakage, as the developed stresses are not high enough. So what causes these incidental, seemingly random breaks? According to statistic information from IFS glass suppliers, (iFS SGT n.d.), 3% of tempered glass fails due to mishandling on the building site. This is considered a normal, acceptable percentage. A failure of tempered glass in one or more layers is causing irreparable damage to the glass plate because of the breakage pattern of tempered glass. On the other hand, annealed glass plates do not shutter when an edge flaw is created. In this case, the usually invisible edge damage is not taken into account on site, the flawed pane is installed while the damage is cover with sealant. This information implies that 3% of the installed annealed glass do not perform with the designed glass strength and is much more vulnerable to thermal tensile stresses and thermal breakage.

As mentioned, the generated tensile stresses developed on the glass might be sufficient to activate pre-existing micro-cracks and lead to fracture. That does not mean that these tensile stresses are sufficient to cause thermal breakage acting on their own. The majority of thermally fractured glass were not "healthy" before fracturing, meaning that there were pre-existing micro-cracks or even cracks visible with the bear eye.

6.2. Future research

The duration of the MSc thesis and the availability of software set limitations to my research. What I would propose for future researchers is investigate the effects of a pre-existing damage to annealed glass on breakage resistance. That could happen with artificial damage of the annealed glass pane edges on laboratory, controlled conditions. Afterward, exposure of the damaged glass to solar radiation, with the use of solar simulators, like the ones used on my experiment, could cause thermal breakage to the pane. It would be very interesting to examine the form of this breakage and its association with the type and location of the pre-existing damage.

The comparison of the numerical set-up results described in the hereby thesis with results from another multiphysics software, like Comsol, could also be an interesting addition to the research. Until now, all the temperature gradient results in regard to thermal fracture investigation are done using Physibel software.

Furthermore, additional parameters of influence could be investigated and their impact could be quantified by finite element software simulations.

Bibliography

n.d. *AGC.* Accessed Feb 11, 2016. http://www.agc-group.com/en/about/flatglass_03.html.

AGC, Technical Advisory Service. 2008. "Evaluation of risk of breakage by thermal shock."

Agtmaal, Bianca Cornelia Maria van. 2012. *A user-centred re-design of indoor comfort.* MSc Thesis, Delft University of Technology.

Antonine, education. n.d. Accessed Feb 23, 2016. http://www.antonine-education.co.uk/Pages/Physics_2/Solid_Materials/MAT_03/Materials_Page_3.htm.

ASTM E2431-12. 2012. *Standard practice for determining the resistance of single glazed annealed architectural flat glass to thermal loadings.* American standard.

Baldini, A., P. Lenk, and L. Rammig. 2015. *Temperature effects on curved annealed glass.* GPD Glass Performance Days.

2011. *Bohlin Cywinski Jackson.* Accessed Feb 05, 2016. http://bcj.com/projects/apple-store-fifth-avenue/.

Buch Polak, A. 1975. *Glass: its tradition and its makers.* Putnam.

Cable, Michael. 2008. *Bontemps on Glassmaking: the Guide du Verrier of Georges Bontemps.* Society of Glass Technology.

CEN/TC129/WG8-N180E. 2004.

n.d. *Chance Brothers and Co.* Accessed Feb 11, 2016. http://www.gracesguide.co.uk/Chance_Brothers_and_Co.

Colvin, J. 2005. "Thermal Stress Breakage in Building Glass." *Workshop, Glass Processing Days.* Tampere, Finland.

CWCT. 2010. *Technical Note No. 65 Thermal fracture of glass.* University of Bath.

DIN 1249-11. 1986. *Glass in building; glass edges; concept, characteristics of edge types and finishes.* Deutsche Norm.

Dutch National Weather Institute. n.d. *Weather data Rotterdam.*

n.d. *EEB Hub Simulation Platform.* Accessed March 16, 2016. http://tools.buildsci.us/comprehensive.

EN 12150-1. 2000. *Glass in building - Thermally toughened soda lime silicate safety glass.* European Norm.

EN 572-1. 2004. *Glass in building - Basic soda lime silicate glass products. Part 1: Definitions and general physical and mechanical properties.* European Norm.

n.d. *Eternal Sun.* Accessed Feb 12, 2016. http://www.eternalsun.com/products/solar-simulator/.

Feryn, Dries. 2012. *Spanningsopbouw in beglazing onder invloed van een thermische belasting.* Universiteit Ghent.

FEVE. n.d. *FEVE The European container Glass federation.* Accessed Feb 10, 2016. http://www.feve.org/index.php?option=com_content&view=article&id=86:glass-is-inert-and-impermeable&catid=9&Itemid=29.

FIV (Fédération de l’Industrie du Verre), Belgian Glass 01. 1997. Brussel.

n.d. *Fluke.* Accessed Mar 23, 2016. http://en-us.fluke.com/products/thermometers/fluke-54-ii-thermometer.html#features.
n.d. *Glass Alliance Europe.* Accessed Feb 12, 2016. http://www.glassallianceeurope.eu/en/environment.
Glazette. n.d. "www.glazette.com." Accessed Jun 15, 2016. http://www.glazette.com/Glass-Knowledge-Bank-25/tempered-glass.html.
Griffith, A. 1920. *The phenomena of rupture and flow in solids.* Royal Society of London.
Haldimann, M. 2006. *Fracture strength of structural glass elements – Analytical and numerical modelling, testing and design.* École polytechnique federalel de Lausanne.
Haldimann, M., A. Luible, and M. Overend. 2008. *Structural Engineering Document 10: Structural use of glass.* Zürich, Zürich, Switserland: IABSE / ETH.
Hertzberg. 1996. *Deformation and fracture mechanics of engineering materials* . 4th ed. Wiley and Sons.
2015. *Ian Weekes - Nickel Sulphide Inclusions.* Sept. Accessed Jun 25, 2016. http://ianweekes.weebly.com/nis.html.
n.d. *iFS SGT.* Accessed Jul 09, 2016. http://ifs-sgt.com/.
n.d. *Instrumentation Toolbox.* Accessed Mar 23, 2016. http://www.instrumentationtoolbox.com/2011/01/sensors-used-in-industrial.html#axzz43X4NoPFQ.
Irwin, G. 1957. "Analysis of stresses and strains near the end of a crack traversing a plate." *Journal of Applied Mechanics* 24:361–364.
Jacob, L. 1999. "A new model for the design of window glass plates using fracture mechanics concepts." In *Glass Processing Days*, 196–199.
Kim, J.-H. 1996. " The influence of cutting edge radius on the machined surface of brittle materials in simulated orthogonal machining." *International Journal of Machine Tools and Manufacture* 36(9):971–983.
Kondrashov, L., and V. Shitova. 1999. "Dependence of the crack depth on glass cutting speed." *Glass and Ceramics* 56(7-8):238–240.
Lawn, B.R. 1993. *Fracture of brittle solids, 2nd edition.* Cambridge University Press.
Lindqvist, M. 2013. *Structural glass strength prediction based on edge flaw characterization.* École polytechnique federale de Lausanne.
Lindqvist, M., M. Vandebroek, C. Louter, and J. Belis. 2011. *Influence of edge flaws on failure strength of glass.* Glass Perform Days.
Metro, performance glass. n.d. "www.metroglass.co." Accessed Jun 14, 2016. http://www.metroglass.co.nz/catalogue/076.aspx.
Mognato, E., and A. Barbieri. 2013. *The breakage of glass – Thermal shock and nickel sulfide.* COST Action TU0905, Mid-term Conference on Structural Glass – Belis, Louter & Mocibob (Eds).
2013. *National Trust Filming Locations.* Accessed Feb 05, 2016. http://www.nationaltrustimages.org.uk/filming-locations/properties/midlands/hardwick-hall.
NF P 78-201-1/A1(DTU39). 1998. *Travaux de miroiterie-vitrerie – Partie 1 : Cahier des clauses techniques – Amendement 1.* France: CEBTP.
NF P 78-201-3/(DTU 39). 2006. *Glazing works – part 3: Memorandum for thermal stress calculation.* France: CEBTP.

Niels, Balcaen. 2013. *Thermische breuk van dubbele glazen gevels: parameterstudie*. Ghent University.

Ovchinnikova, E., V. Litvinov, and T. Khazova. 1984. *The optimal parameters for cutting glass using a cutting-alloy roller*. Steklo Keram.

Papathanasiou, Ifigeneia. 2014. *Smart window integraton into the building envelope*. TU Delft.

Pella. n.d. "pressroom.pella.com/." Accessed Jun 02, 2016. http://pressroom.pella.com/photo_library/preview/726/.

Pilkington. n.d. *Pilkington*. Accessed Feb 23, 2016. https://www.pilkington.com/en-gb/uk/architects/glass-information/functions-of-glass/mechanicalfunctionsofglass/glass-and-thermal-stress.

Porter, M. n.d. *Aspect of structural design with glass*. 2001: The University of Oxford.

n.d. *PPG Glass Education Center*. Accessed Feb 11, 2016. http://educationcenter.ppg.com/glasstopics/heated_glass.aspx.

prEN thstr. 2004. *Glass in building – Thermal Stress Calculation Method. Draft European standard*. CEN.

Schipper, Roel. 2011. In *CIE4215-Facade Design Plus - Large Transparent Glass Surfaces*. Delft University of Technology, faculty of Civil Engineering and Geosciences.

Schittich, C., G. Staib, D. Balkow, M. Schuler, and W. Sobek. 1999. *Glass construction manual*. Birkhäuser Publishers.

Stevens, Will. 2013. *Interface facade engineering*. May 23. Accessed Mar 20, 2016. http://www.interface-facades.com/operable-smoke-vents/.

2013. *The Telegraph*. Accessed Feb 05, 2016. http://www.telegraph.co.uk/culture/art/architecture/10353277/Crystal-Palace-exhibition-hall-to-rise-again.html.

n.d. *US Lighthouse Society - The Fresnel Lens Makers*. Accessed Feb 11, 2016. http://uslhs.org/fresnel-lens-makers.

Vandebroek, M. 2015. *Thermal Fracture of Glass*. Ghent University; University of Antwerp.

VandenPoel, Margot. 2010. *Thermische belasting en breuk bij glazen gevels*. Universiteit Ghent.

Vanderbroek, M., J. Belis, and C. Louter. 2013. "Thermal breakage of glass." *Cost Action TU0905 Midterm Conference on Structural Glass, Belis, Louter & Mocibob (Eds) Taylor & Francis Group* 563-569.

Vansteenbrugge, Dries. 2012. *Klimaatbelasting en breuk bij glazen gevels*. Ghent Univirsity.

Viracon, Tech Talk. n.d. "Viracon architectural glass." *http://www.viracon.com*. Accessed Jun 26, 2016. http://www.viracon.com/images/pdf/TTThermalStress.pdf.

Viwinco. 2012 . "Visual Distortion Observed in Low-E Tempered Glass ."

Vuolio, A. 2003. "Structural behaviour of glass structures in facades." *Teknillisen korkeakoulun terasrakennetekniikan laboratorion julkaisuja 27.*

n.d. *Weather Online*. Accessed Mar 18, 2016. http://www.weatheronline.co.uk/reports/climate/The-Netherlands.htm.

n.d. *Wikipedia*. Accessed Feb 11, 2016. https://en.wikipedia.org/wiki/Float_glass.

Worner, J.-D., J. Schneider, and A. Fink. 2001. *Glasbau: Grundlagen, Berechnung, Konstruktion*. Springer.

Zammit, Kenneth, interview by Chrysanthi Anastasiou. 2015. *Thermal Fracture of Glass* (November 26).